Recent advances in hydrogen production via autothermal reforming process (ATR): A review of patents and research articles.

Full reference: Nahar, G. and Dupont, V. *Recent Patents on Chemical Engineering*, 2013, 6(1):8-42

Gaurav Nahar [*] and Valerie Dupont

[*] Energy Research Institute, The University of Leeds, Leeds LS2 9JT, UK, email- g.nahar05@leeds.ac.uk

Keywords- hydrogen, fuel cells, autothermal

Abstract:

This review examines recent patents and research articles in autothermal reforming (ATR) of fossil fuels like gasoline, diesel, JP-8 along with renewable fuels such as methanol, ethanol, glycerol, butanol, bio-oils and biodiesel into H_2 gas. The focus of the research was the recent developments in terms of ATR reformer design, ATR fuel processors, reformer start up, and reforming catalysts to determine the opportunities for R&D in this area. The production of H_2 by ATR of fossil fuels has been widely investigated; several catalytic studies based on various noble and non-precious metals like Rh and Ni are available, restricting new investigations. In contrast, H_2 production from bio feedstock like bio-oils, biodiesel, ethanol, and butanol are very recent and offer considerable room for further investigation.

.

1. Introduction:

Production and distribution of energy affects all sectors of the global economy. The increasing industrialization of the world requires sustainable and highly efficient energy production. Without major technology advances, energy demand will impact the quality of life on earth. The majority of current energy needs are supplied by combustion of non-renewable energy sources such as fossil fuels, which are associated with release of large quantities of greenhouse gases [GHG], in particular carbon dioxide [CO_2]. These growing environmental concerns and the increasing frequency of energy crises have fuelled research in alternative means of energy generation. This requirement of energy can be fulfilled by developing alternative energy sources like wind energy, solar energy, H_2 energy, geothermal energy, tidal energy, biomass energy [1],[2-6]. Biomass includes use of biofuels like biodiesel, bio-ethanol, bio-glycerol and bio-butanol which are derived from biomass. These

fuels can be utilized for generating green energy in the form of electricity for utilization in propulsion and domestic applications.

Fuel cells are considered as one of the cleaner energy devices for power generation for domestic and propulsion applications. The two most promising fuel cells, Proton exchange membrane fuel cells (PEMFC) and solid oxide fuel cells (SOFCs) are widely researched. PEMFC are promising option for mobile auxiliary power units (APU) for propulsion applications, while SOFCs are considered mainly for stationary combined heat and power generation (CHPs) [7, 8]. Biomass derived fuels can be utilized in fuels cells and thereby help in reducing the cost of operation [1-6] .

PEMFC's utilize high purity H_2 gas as fuel, while H_2-rich syngas is preferred by SOFCs. However H_2 does not occur freely in nature. It occurs in combination with carbon, nitrogen and/or oxygen. Since the last 6 to 7 decades, H_2 on an industrial scale has been mainly produced by steam methane reforming (SMR) process [9]. The H_2 produced by SMR is mainly utilized in refineries and fertilizer plants. It is used in hydrotreating, hydro-desulfurization, and many other refinery processes for the production of fuels like gasoline, diesel, and other products. In fertilizer plants it is used for the manufacture of ammonia, methanol and other derived chemicals like urea, nitric acid, and ammonium nitrate. Most industrial steam reformers use Ni catalysts supported on a ceramic support, operating in the temperatures ranging from 700 to 950 ^{o}C, with pressures ranging from of 15 to 30 atm [10, 11]. The high temperatures thermodynamically favour the steam reforming (SR) reaction as opposed to high pressures. In industry, operating at 15 to 30 atm is necessary due economies of scale, by allowing larger production flows in smaller plants. The reaction mechanism of H_2 production via steam reforming of hydrocarbons and oxygenated hydrocarbons is given by the R-1 and R-2.

$$\text{Steam Reforming } (\text{SR}): C_nH_m + nH_2O \xrightleftharpoons{\Delta H\square\ 0} nCO + (n+0.5m)H_2 \qquad [1]$$

$$\text{Steam Reforming } (\text{SR}): C_nH_mO_k + (n-k)\,H_2O \xrightleftharpoons{\Delta H\square\ 0} nCO + (n+0.5m-k)\,H_2 \qquad [2]$$

The main disadvantage of SR process is its endothermicity, which means a significant source of heat -which varies with the nature of the fuel, needs to be provided for it to proceed.

In contrast to SR, H_2 production via partial oxidation (PO) is exothermic, meaning that it is energetically self-sufficient. But since it involves the use of an oxidant like oxygen or air, the yield of H_2 is lower as compared to SR, as it lacks the contribution of the H_2 produced from steam.

$$\text{Partial Oxidation } (\text{PO}): C_nH_m + 0.5nO_2 \longrightarrow nCO + 0.5mH_2 \qquad [3]$$

$$\text{Partial Oxidation } (\text{PO}): C_nH_mO_k + 0.5(n-k)O_2 \xrightleftharpoons{\Delta H<0} nCO + 0.5mH_2 \quad [4]$$

In contrast to SR, PO does not require an external heat source to shift the equilibrium to the right of R-3 and R-4 as result of exothermic heat of reaction. The use of air or oxygen, results in oxidation of fuel to produce the necessary heat by reactions (R-9) and (R-10), thereby lowering the H_2 yield.

To resolve the problem of lower H_2 yield in case of PO and endothermic heat of reaction in SR, a combination of both the processes SR and PO, called autothermal reforming (ATR) has been developed. This combination is considered as one of the most attractive options for on-board reforming of complex hydrocarbons like kerosene and diesel for H_2 delivery for fuel cells [12, 13]. On-board reforming refers to H_2 production in a fuel cell powered vehicle. Its main characteristics are: low energy requirement (due to the complementary SR and PO reactions), low energy consumption, high Gas Space Velocity (GSV), at least one order of magnitude larger than traditional SR, and preset H_2/CO ratio easily regulated by inlet reactant ratios and CO_2 recycling [14].

In addition to the above reactions, the exothermic water gas shift (WGS) reaction ideally converts the entire CO generated by SR and PO into CO_2, while producing the maximum H_2 yield from the steam co-reactant. Because of the exothermicity of WGS reaction, the high temperatures of SR and PO limit the extent of WGS reaction, and typically, equilibrium between and its reverse reaction (RWGS) is established, leaving unreacted CO in the products.

$$\text{Water Gas Shift } (\text{WGS}): n\times(\text{CO} + \text{H}_2\text{O} \xrightleftharpoons{\Delta\text{H}<0} \text{CO}_2 + \text{H}_2) \quad [5]$$

Conversely, low temperatures favour WGS reaction along with unwanted side reactions, such as methanation (the reverse of SMR, (6)), fuel thermal decomposition (7) and the Boudouard reaction (8). Fuel decomposition (7) and the Boudouard reaction (8) both favour carbon deposition resulting in catalyst coking and deactivation.

$$\text{Methanation } (MTH): n(CO + 3H_2 \xrightleftharpoons{\Delta\text{H}<0} CH_4 + H_2O) \quad [6]$$

$$\text{Thermal decomposition}: C_nH_mO_k \xrightleftharpoons{\Delta H>0} (n-k)C_{(S)} + 0.5mH_2 + kCO \quad [7]$$

$$\text{Boudouard reaction}: 2CO \xrightleftharpoons{\Delta H>0} CO_2 + C_{(S)} \quad [8]$$

To avoid the unwanted side reactions while maximizing H_2 production, SR and PO are executed in a ATR reformer at high temperature (800 to 1200°C), and WGS reaction is

carried out downstream at lower temperature (<350 °C), often in two stages termed ‘high’ and ‘low’ temperature shift (HTS-LTS). WGS reaction can proceed to completion alongside SR and PO when special features that shift simultaneously the thermodynamic equilibrium of all three reactions are used, such as when carrying out in-situ removal of one of the WGS reaction products: CO_2 by ‘sorption enhancement’, or H_2 by membrane separation.

The reaction mechanism involved in ATR is ideally a combination of (R-1 to R-5), however in practice, local excesses of oxygen in the reformer may lead to complete oxidation, as expressed by (R-9) and (R-10).

$$\text{Oxidation } (Ox)\ C_nH_m + (n+0.25m)O_2 \rightarrow nCO_2 + 0.5mH_2O \quad [9]$$

$$\text{Oxidation } (Ox):\ C_nH_mO_k + (n+0.25m-0.5k)O_2 \rightarrow nCO_2 + 0.5mH_2O \quad [10]$$

ATR has theoretically higher reforming efficiencies as compared to PO. [15]. Investigations by Argonne National laboratory (ANL) have suggested that ATR could have a simple design and fast response [16-18]. But an ATR plant carries higher risks of explosion which is why its uptake in world H_2 production has been less successful than SMR. ATR reactor systems have extremely short startup times (< 5 s) and wide flow ranges, presuming that it is possible to manufacture small portable fuel reformers. Among its benefits are: reduction of the internal heat generation, increased efficiency, high purity H_2, fuel flexibility (sulfur tolerance) and coke burnt off during catalyst regeneration.

The process can be applied in the ATR of various fuels including natural gas, diesel, coal and renewable feedstock. Autothermal cyclic reforming (ACR) process, also termed as chemical looping reforming (CLR), and unmixed steam reforming (USR), operates in a three-step cycle that involves SR of fuel on Ni catalyst (reforming), heating the reactor through the oxidation Ni catalyst (air regeneration) and the reduction of the catalyst to its original state (fuel regeneration). In addition, developed experiments with ATR have reported that plants based on oxygen-blown ATR at low H_2O/C ratios are the preferred option for large-scale and economic production of synthetic gas for Gas to Liquids (GTL) plants [19]. Finally, (ANL) has favored catalytic ATR developing new catalysts for the reforming and shift reactors. Researchers have suggested that ATR systems can be very productive, fast starting and compact and was successfully applied for reforming of alcohols, bio-fuels, gasoline and methane [20-22].

The aim of this review is to examine and analyze recent developments in ATR of various fuels covering patents and research articles. This review focuses on the ATR of liquid fuels as compared to gaseous fuels. Since liquid fuels are easy to reform because they dissociate at lower temperatures, however their H_2 yield is lower according to the stoichiometry of the SR, (R-1) and (R-2), and as a result of equilibrium of the methanation

reaction. Liquid fuels have high energy density; they can be stored and transported easily making them ideal for remote, distributed and mobile applications.

There are mainly two types of patents awarded firstly for processes design or modification and secondly for newer or modified catalyst. The processes patents address new designs or arrangements made to improve the performance of the reformers, while the catalyst patents describe the fabrication or manufacture of catalysts.

2. Process Patents:

2.1 Reformer design:

An ATR process is a combination of SR and PO and does not require an external source of heat to shift the reaction equilibrium reaction towards higher conversion. But the major disadvantage of the process is the dissipation of the exothermic heat of reaction and the effects of temperature on the catalyst and the reformer. Of course size reduction is also one of the important aspects investigated for smaller applications for e.g. automotive and distributed power generation using fuel cells.

Ahmed et al., 2010 [23] investigated a three segmented ATR configuration system for generating H_2 for fuel cell applications. Authors patented a porous catalyst support structure based reformer to improve the heat fluid transfer through the catalyst zones. Metal foam was positioned over the first catalyst structure to facilitate the distribution of the reactants radially and also to transfer the exothermic heat of reaction over the first catalyst towards the incoming feed in the reformer. The second structure consisted of a support loaded with a hexa-aluminate oxidation catalyst, capable of withstanding temperatures higher than 900^oC. Finally the last unit comprised of noble metal based catalyst operating at relative lower temperature than 900^oC. The salient feature of this system is a special high surface area oxidation catalyst support, capable of withstanding 1400^oC and reducing the peak temperature in the noble metal catalyst. The design facilitated the dissipation of the heat from the exothermic catalyst towards the cooler feed and the endothermic SR reaction.

Figure 1 shows the ATR reformer patented by Ahmed at al., 2010 [23]. In the figure, part **(11)** represents the housing of the reformer which resembles like a reminiscent of a sleeve. It encloses the peripheral regions of the support **(12)** and extends longitudinally (i.e., axially) substantially to the entire length of the configuration, so as to encircle peripheral regions of all the catalysts utilized. Various configurations of the housing **(A)** used to accommodate the catalyst were devised. The upstream portion **(14)** of the housing supports a hexa-alumiate based oxidation catalyst capable of withstanding a temperature of 1400^oC. The downstream portion **(16)** of the system supports a reforming catalyst providing optimal performances at temperatures not exceeding 850° C. A rhodium based reforming catalyst has

been preferred due to its high reforming activity and coke tolerance. The leading edge **(19)** of the catalyst support is placed over the uncoated part of the catalyst **(18).** This comprises of blank foam, having larger diameter at this part of the system compared to further downstream, providing a means to ensure that heat generated upstream be blown downstream as result of the velocity of the reaction mixture. A palladium based catalyst is applied near the leading edge **(19)** of the support to initialize combustion anchor the flame front at the end of the system. This arrangement also isolated the reforming catalyst from heat spikes.

A 1 kW reformer was designed by the authors using monolith based catalyst to investigate production of H_2 via ATR of dodecane and hexadecane as model components of diesel fuel under oxygen-carbon rich and steam-carbon rich environments [21]. The O_2/C ratio was determined to be the most significant operating parameter that influenced the reforming efficiency which increased with increasing oxygen-to-carbon ratio up to certain value. The increased fuel flowrate was shown to decrease the H_2 selectivity. Since pellets or conventional honeycomb catalysts, used for the reforming process are mass-transport limited, a microchannel based reformer was developed by the authors to reduce the diffusion resistance and thereby achieve the same production rate within a smaller reformer bed **[24]**. A 10 kW reformer was tested for ATR of natural gas and gasoline at space velocities of up to 250 000 h^{-1} with very little deactivation.

A different kind of approach was adopted by Robb et al., 2007 [25] to mitigate the heat associated problem within ATR reformers. A segmented ATR reformer was designed by the inventors, where the oxidant was introduced under each segment or stage **[25]**. Figure 2 shows an ATR reformer designed by Robb et al., 2007 [25]. In the figure the reformer **(48)** is provide with a casing **(80)** placed between an upstream side **(82)** and a downstream side **(84)**. The reformer has different catalyst stages between the upstream side **(82)** and downstream side **(84)**. In the figure, the first stage is denoted by **(82)** while the second stage by **(84).** The reformer can also have n^{th} stage **(86)**, where n represents any whole integer greater than two. The stages can employ PO and SR catalyst. A part from these two stages of catalyst, more stages which can comprise of WGS and CO oxidation catalyst combinations can also be integrated in the reformer. Each stage of the reformer will have different portion of the catalyst bed.

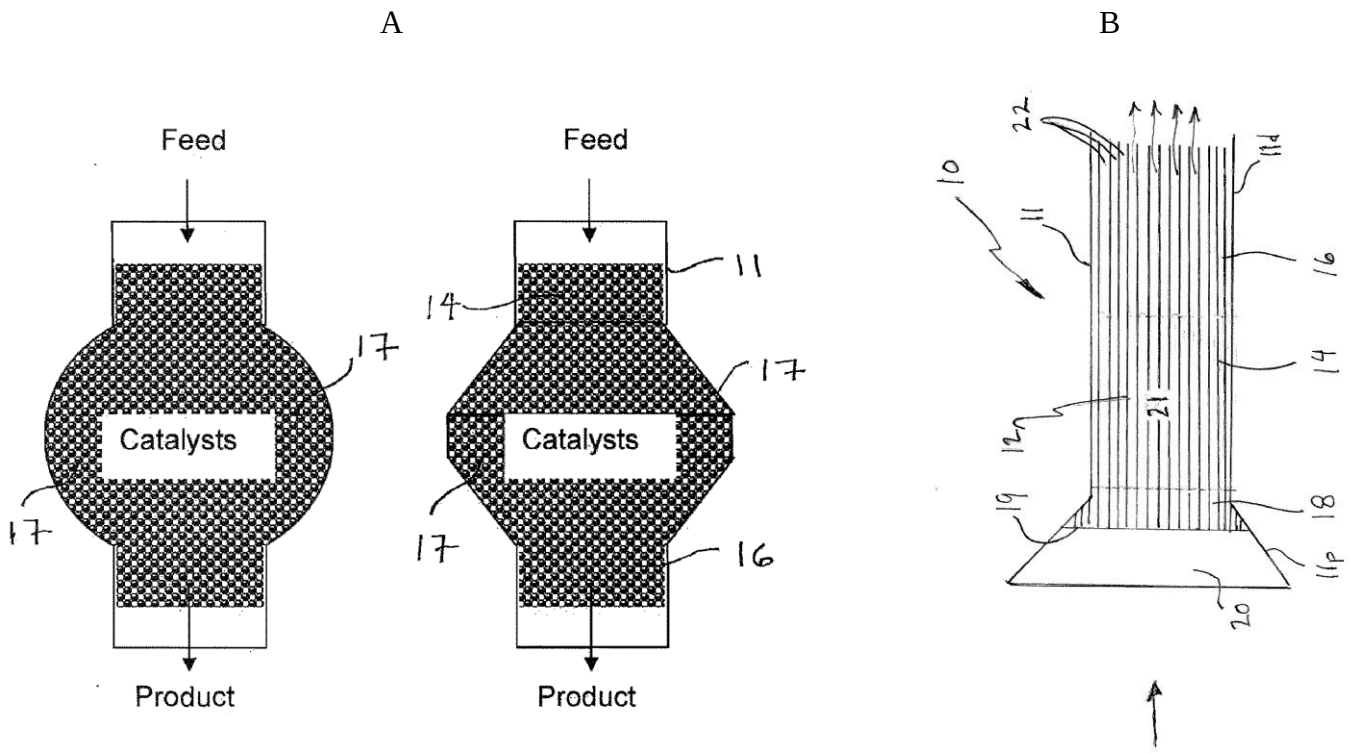

Figure 1: Catalyst configuration comprised of housings (A) and the structure (B) patented by Ahmed et al., 2010 [23]. In the figure B (11) represents the reminiscent of a sleeve which encapsulates peripheral region of the support (12).

The superheated steam/oxidant flow **(52)** and the fuel flow **(24)** flow into the first stage **(50)** of the reformer. Alternatively, fuel, steam, and first oxidant flows **[(24), (26),** and **(28)]** can mix together in a mixing chamber **(90)** to form the first stage flow **(74)** before flowing in to the first portion **(72)** of the catalyst bed **(70)**. The second stage **(62)** is placed above the first one and receives the fluid flow **(72)** routed though the first bed; it has a separate source of oxidant flow **(64)** introduced from the bottom of the bed. The fluids flowing through the second portion **(76)** of the catalyst bed **(70)** are referred as a second stage flow **(78).** The second stage flow **(78)** leaves the reformer**s (**48) in the form of reformate flow **(30).** If required more stages can be added to the reformer. Single or both the stages can comprise of a single catalyst or a combination of catalysts**.** The control valves **(66), (68)** regulate the amount of oxidant received by each stage of the reformer.

A start up method for the ATR reformer was also invented. Since the reformer has two separate oxidant supply sources. It is not necessary to supply all the oxidant through the first stage to attain the corresponding O/C ratio of 1.1 to prevent carbon formation, the second oxidant flow can also be used to prevent carbon formation.

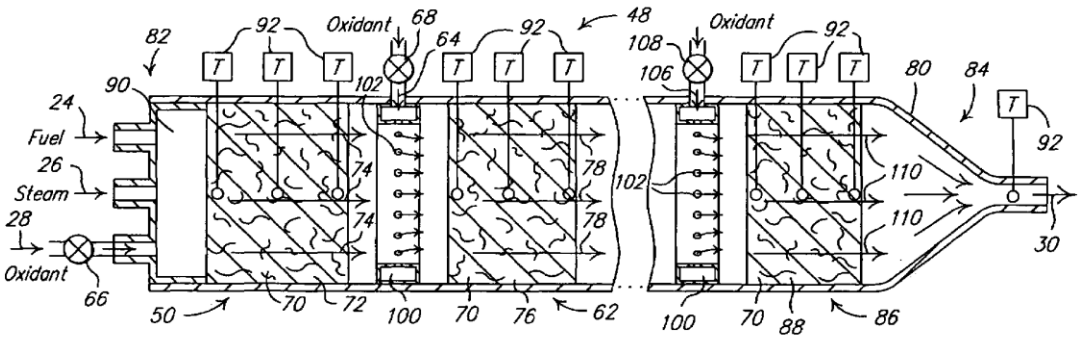

Figure 2: An ATR reformer designed by Robb et al., 2007 [25].

Instead of supplying the oxidant at two different ports, Kaeding et al., 2007 [26] devised a common oxidation inlet but provided two separate fuel ports. A concentric double pipe reformer arrangement connected to a rectangular injection and mixture forming zone at the bottom of the pipes was devised. Three separate oxidant inlets were provided. The first inlet is provided on the inner pipe with second and third inlets on the outer pipe and the rectangular mixture forming zone respectively.

A fuel and oxidant is passed through the inner pipe by fuel supply (1) and oxidant supply (1) respectively. Just enough amount of oxidant is supplied to cause PO of the fuel to

release exothermic heat; this mixture is then realized through the inner pipe which opens in the rectangular reforming zone. This PO mixture is further mixed with more fuel from the second fuel inlet port provided on the injection and mixture forming zone. The thermal energy of the PO fuel will help in the vaporization of the fuel from the second inlet. Thus the formed mixture from the vaporized fuel and partially oxidised fuel is transferred to the reforming zone and converted to H_2 rich gas by SR. Some partially oxidized gas mixture can also be supplied to the reforming zone by bypassing the injection and mixture forming zones. The formed reformate via SR and PO leaves the assembly via outlet ports provided on the concentric outer pipe. The supply port for providing the steam for the SR reaction is not mentioned in the patent.

Instead of oxidizing a part of fuel to provide the necessary heat in ATR reformer Yamazaki et al., 2011[27] developed a reformer that combusts part of the reformate formed by the SR reaction. The reformer designed by Yamazaki et al., 2011 [27] is shown below in Figure 3. The reformer consists of triple circular tube structure**.** Two cylindrical tubes are separated by the inner cylinder **(4).** The radially inner partition wall **(6A),** the radially outer partition wall **(6B)** and the outer cylinder **(5)** are placed annularly and concentrically to form a fourfold circular tube structure**.** The reforming catalyst layer **(2A)** is placed between the walls of tube **(4)** and (**6 (6 A**)**.** Similarly the second reforming catalyst layer is placed in the annular space between the outer tube **(5)** and the tube **(6 (6 B).** The reforming catalyst layer is placed on the upstream side of oxidation catalyst**.** Thermally conductive material layer **(3B)** is placed below the oxidation catalyst **(3A)**. Fuel and steam in vaporized state are introduced through port **(7)** while the oxidant is introduced from port **(12).**

The vaporized fuel and steam is passed through the reforming catalyst compartment supports **(9A)** and **(9C) respectively.** It flows uniformly upward through the reforming layers **(2A)** and **(2 B).** The supports prevent the catalyst from falling down and provides passage to fuel, steam, and the reformate gas. The reformate formed by SR of fuel travels upwards over the oxidation catalyst and mixes with the oxidant introduced from port **(12),** to generate the necessary heat required for the SR reaction. The heat released from the oxidation catalyst is transferred to the thermally conductive materials and finally to the reforming catalyst layers. A tubular ring is provided on the oxidant inlet for adequate mixing and blowing of the oxidant over the oxidation catalyst. The amount of the oxidant can be adjusted to generate the necessary heat for the SR reactions. The reformed gas after passing over the oxidation catalyst passes over the compartment **s**upport **(9B),** and is guided to a reformed gas channel **(17)** and is discharged from the reformed gas-outlet **(8).**

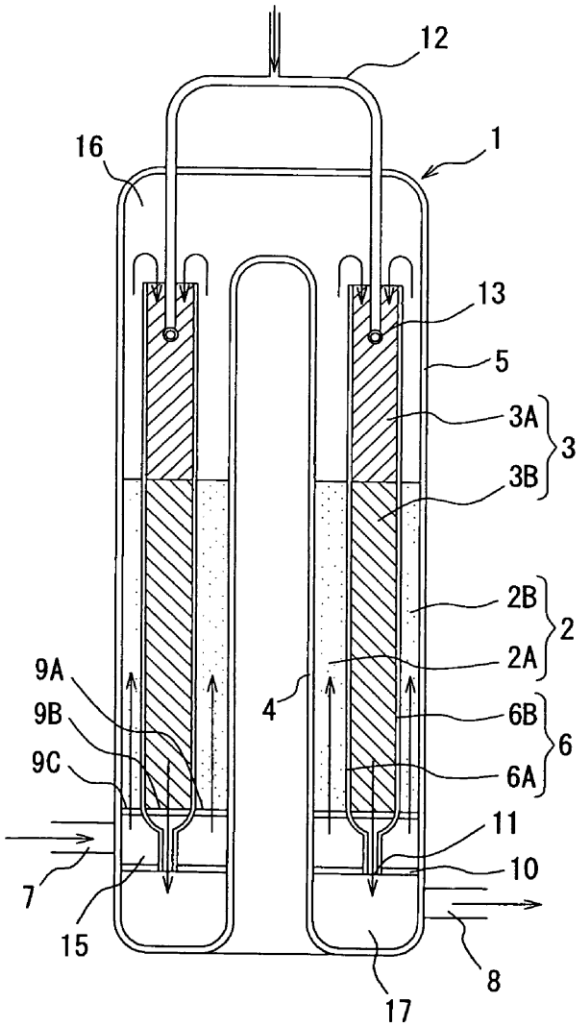

Figure 3: ATR reformer designed by Yamazaki et al., 2011 [27].

A different kind of approach for heat management was investigated by Docter et al., 2009 [28]. As a result of faster reaction kinetics, the exothermic oxidation reactions take place to a greater extent in the entry zone of the ATR reformer, resulting in a marked increase in temperature in this region. While the endothermic SR reactions take place predominantly in the downstream reaction zone in which the temperature consequently decreases, which result in the lower conversion of the fuel by SR. To tackle this problem, a hybrid concept was proposed in which an ATR reformer of hydrocarbons is combined with an external heating device. Figure 4 shows the ATR reformer designed by Docter et al., 2009 [28] for reforming of hydrocarbons.

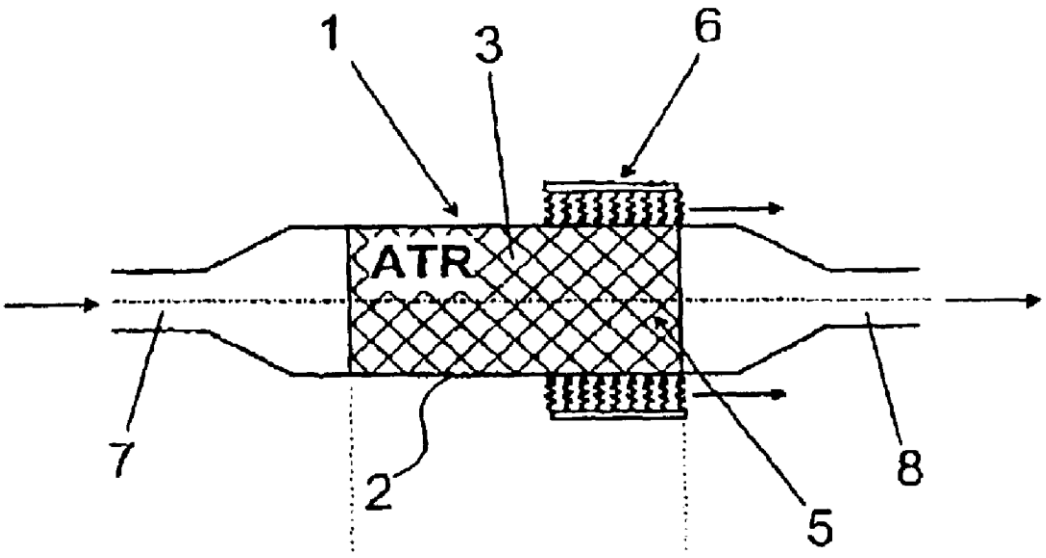

Figure 4: A schematic of ATR reformer designed by Docter et al [28]. In the figure, 1 and 3 represent the catalyst structure in the reaction zone 1 with the inlet and outlet zones shown by 7 and 8 and external heater 6.

Unlike the autothermally generated heat, the heat released by the external heating device is not generated directly in the reaction zone at the location of the reforming reactions but has to be transferred to the reaction zone through heat-conductive walls. According to the invention, heat supply takes place in the end region of the reaction zone, especially in the lower end region of the reaction zone. The fuel conversion and the autothermally generated heat are not sufficient for complete conversion of the hydrocarbons. This can be remedied by use of excess air to supply the thermal energy. But this will result in lower H_2 yield.

This design claims to favor the complete conversion of the residual hydrocarbons in the end region of the reaction zone resulting in a high H_2-yield. Since the reactor according to the present invention can be operated at a relatively small excess-air factor, a comparatively small amount of nitrogen is introduced in the product gas, which altogether results in higher H_2 concentrations. Finally the expenditure of electric energy for a possible air compression can be reduced as result of this invention.

The first variation of invention shown in Figure 5 A, consists of a reaction zone 1 which includes a first partial zone **(12)** and a second partial zone **(13)** connected downstream. Upstream of the second partial zone **(13),** a heating device is arranged for intermediate heating of the reformate stream**.** The heating device includes a catalytic radiant burner **(6)** and a gas/gas heat exchanger **(14)** which is arranged between first partial zone **(12)** and second partial zone **(13)** and is fed with the exhaust gas of catalytic radiant burner **(6).**

In a second version of the invention, heat transfer tubes **(10)** in the form of a tube bundle are integrated in the catalyst structure **(4)** arranged in the end region **(5)** of reaction zone 1 as shown in Figure 5B. The heat transfer tubes can also act as catalytic radiant burners **(6)** themselves if a suitable catalyst is arranged in the interior.

Finally in the third version of the invention is shown in Figure 5C, the outlet cross-section of reaction zone 1 is heated by a correspondingly arranged radiator plate **(11)**. The radiator plate is in thermal contact with exit zone **(8**) and is maintained at the required temperature by the exhaust gases of a catalytic radiant burner **(6)**. This burner is located outside the reaction zone (1).

Keading et al., 2007 [26] adopted a different approach to mitigate heat transfer problems associate with ATR reformer. According to the proposed design, fuel may additionally be supplied to the reforming zone, and heat may be supplied to the reforming zone. The additionally supplied fuel along with the exhaust gas from the oxidation zone forms the starting gas mixture for the reforming process. The heat from the exothermic oxidation within the oxidation zone may be supplied to the reforming zone. The heat resulted from the oxidation zone is converted in the course of the reforming reaction such that the net heat generation of the entire process can prevent the problems associated with temperature management of the reformer.

Figure 6 shows a schematic of a ATR reformer designed by Keading et al., 2007 [26]**.** Fuel **(12)** and oxidant **(16)** are supplied to the reformer **(10)** through respective ports. The heat generated by combustion of the fuel is partially discharged in an optionally provided cooling zone **(36).** This mixture then proceeds further into the oxidation zon**e (24)** which is further discharged in the reforming zone **(26)** through a pipe arranged within the zone. In alternative arrangements, the oxidation zone is released by multiple pipes or a specific pipe arrangement within the reforming zone **(26).** Within the oxidation zone, a definite conversion of fuel and oxidant within an exothermic reaction takes place, with $\lambda \approx 1$ (fuel/oxidant ratio). The gas mixture **(32)** produced then enters an injection and mixture forming zone **(30)** where fresh fuel (**14)** is injected. The thermal energy of the gas mixture **(32)** helps in evaporation of the fuel **(14).**

Additional oxidant can be supplied to this zone by inlet **(20).** The mixture then enters the reforming zone **(26)** where it is converted by an endothermic reaction**,** with $\lambda \approx 0.4$**.** The heat **(28)** needed for the endothermic reaction is discharged from the oxidation zone **(24).** For optimizing the reforming process, oxidant **(18)** may be supplied additionally into the reforming zone **(26)**. The reforming zone **(26)** can be supplied directly with a part of the gas mixture (34) produced in the oxidation zone **(24)** bypassing the injection and mixture forming zone **(30).** The reformate gas **(22**) then flows out of the reforming zone **(26)** available for utilization**.**

Instead of modifying the design of the reformer, Lesiuer et al., 2005 [29, 30] designed an ATR reformer utilizing end cell foam to provide high surface area and heat transfer paths. The foam contributes to increase turbulence in gas flow to enhance heat

transfer rates in reactive systems. The foam is also utilized as a catalyst bed. Figure 7 shows a foam based ATR reformer designed by Lesiuer et al., 2005 [29]. In the figure the reformer assembly is denoted by **(3)** which include the catalyst bed **(2).** The catalyst is placed in an inner cylindrical housing **(12),** the bottom of which contains a porous mesh screen **(14).** The mesh screen supports the catalyst bed **(2)** and allows the reformed gas stream to exit from the inner housing **(12).**

An intermediate cylindrical housing **(16)** surrounds housing (channels) and forms an inner annular gas flow path **(18)** for the gas exiting the catalyst bed **(2).** The outer most cylindrical housing **(20)** forms the outermost wall of the reformer assembly **(3).** The housing **(20)** combines with the intermediate cylindrical housing **(16)** to form an outer annular gas flow path chamber **(22)** of the reformer assembly **(3).** The annular wall **(24)** and lower annular wall **(26)** with manifold **(28)** are used to seal the reformer from the upper and the lower ends.

The manifold **(28)** comprises of an upper fuel/stream-inlet chamber **(30)** and a lower air-inlet chamber **(32).** The chambers **(30)** and **(32)** are separated by a plate **(34)** resulting in the formation of plurality of passages **(36).** A similar plate **(38)** forms the lower wall of the air-inlet chamber **(32).** Fuel passages tube **(40**) interconnects the two plates **(34)** and **(38)**; the tubes **(40)** along with perforations **(42)** which admit air from the chamber **(32)** into the gas stream flowing through the tubes **(40).** The air and fuel/steam stream mixes in the tubes **(40)** before it enters the inlet end **(8)** of the catalyst bed **(2).**

The fuel/steam mixture enters the reformer assembly **(3)** at a temperature of ~235^{o}C via a heat exchange tube **(44),** shown by the arrow **(A),** while the air stream enters the reformer assembly **(3)** via a heat exchange tube **(46),** indicated by the arrow **(B)**. The heat exchange tubes **(44)** and **(46)** are wound coaxially around the cylindrical housing **(16)** through the chamber **(22)** to transfer the heat from the exhaust stream to fuel/steam mixture and air stream. Thus, the proper mixture of air, steam is formed in the tubes **(40)** which flows into the inlet end **(8)** of the catalyst bed **(2)**. The temperature of the mixture ranges between ~430 to 595^{o}C**.** The reformed fuel stream exits from the catalyst bed **(2)** through the screen **(14)** at a temperature of ~595 to 760^{o}C, and then passes upwardly through the annulus **(18)** shown by **arrow (C).** The reformed gas continues to supply heat to these tubes as it travels through the chamber **(22)** to the exit **(52).**

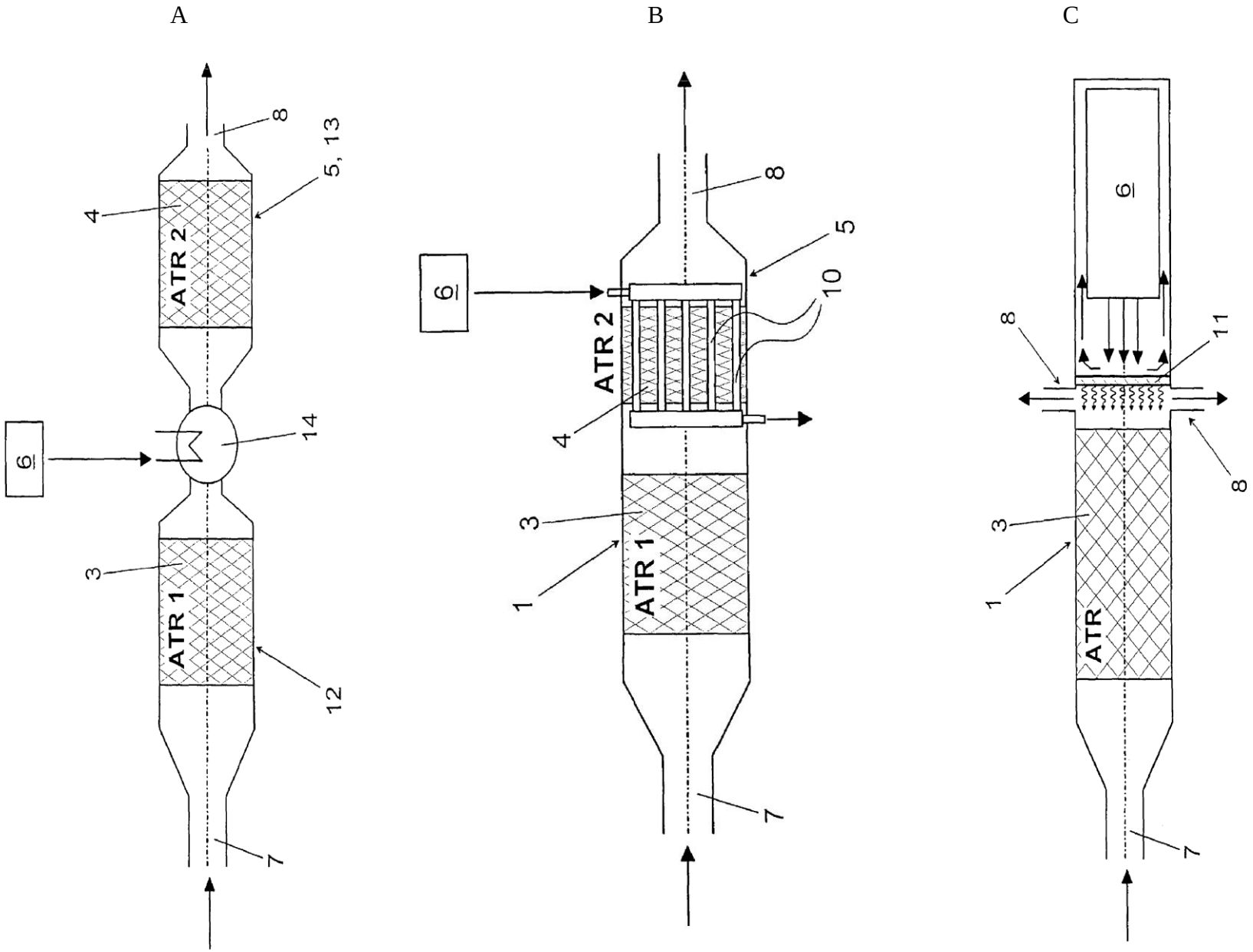

Figure 5: Configurations of ATR reformer with external heat source designed by Doctor et al., 2009 [28]

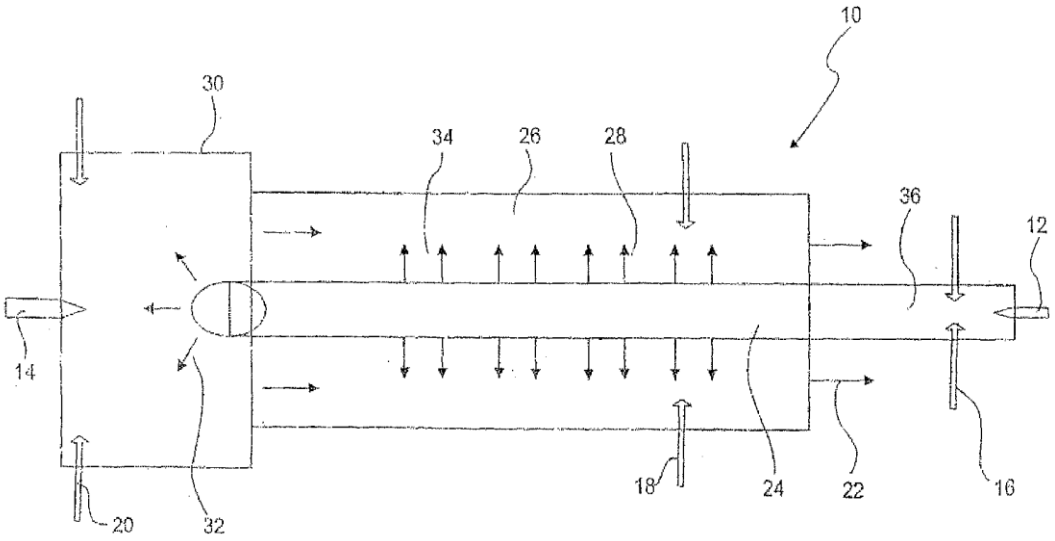

Figure 6: Reformer configuration of ATR reformer designed Keading et al., 2007 [26].

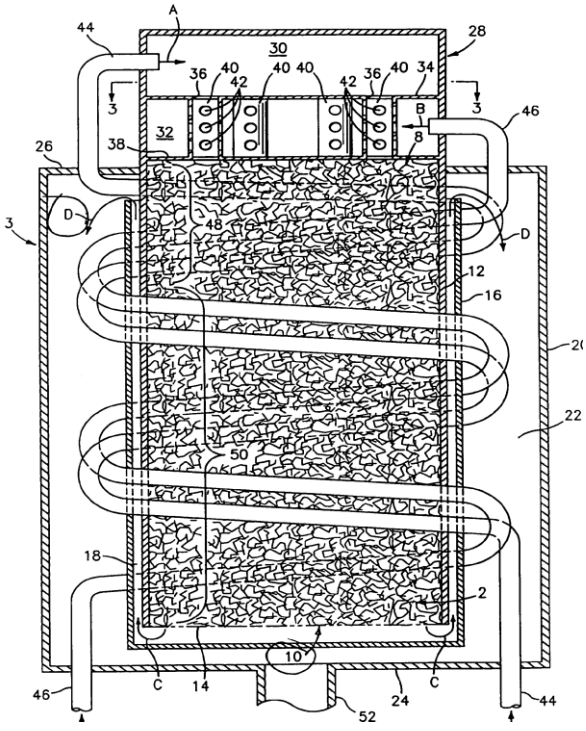

Figure 7: Reformer configuration of ATR reformer designed Lesiuer et al.,2005 [29].

The use of multiple reforming zones to increase the surface area of the supported catalyst in order to allow faster reaction rate to take place and decrease the size of the ATR reformer, was patented by Papavassiliou et al., 2007 [31].

In the current invention the rapid formation of the reactant stream allows the reactor to be compact yet have a production rate of syngas that is sufficient for small on-site production.

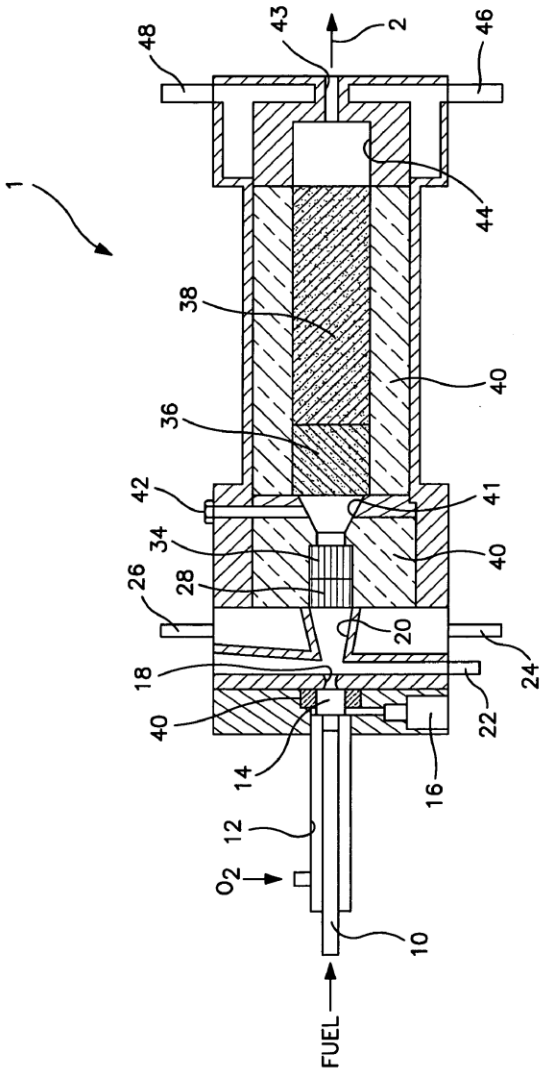

Figure 8: Reformer designed by Papavassiliou et al., 2007[31].

The reformer designed by Papavassiliou et al., 2007 [31] is shown in the Figure 8. The reformer is provided with a fuel injector tube **(10)** and concentric oxygen passage **(12)** which is in contact with a thermal mixing chamber **(14)**. The fuel is ignited in the mixing chamber and it burns in the presence of the oxygen, where the ignition is initiated by means of an oxygen mixture, which mainly comprising of oxygen. Heated oxygen containing stream

is introduced into mixing chamber **(20)** where it meets with the hydrocarbon containing stream to form a high temperature reactant mixture. The rapid mixing in the mixing chamber **(20)** is accomplished by expelling the heated oxygen containing stream from the thermal mixing chamber **(14)** via an orifice **(18**) expanding the heated the stream. The hydrocarbon containing stream is introduced into mixing chamber **(20)** through a tangential inlet **(22)** located in adjacent to the orifice **(18).**

Water cooling is also provided to draw off heat from the surface to avoid overheating of the surface of mixing chamber **(20).** Water is circulated through the reformer to remove the heat from the mixing chamber **(20)** through a water passage surrounding the chamber. The passage is provided with water inlet **(24)** and outlet **(26).** The reactant stream flows from mixing chamber **(20)** into a honeycomb monolith **(28)** prepared from Al_2O_3. The reactant stream from mixing chamber **(20)** expands radially to the honeycomb monolith **(28)** and flows straight through it for another millisecond. Following the mixing chamber **(20)** the reactant stream then enters a PO zone **(34).** The oxidation zone is coated with a PO catalyst operating at 800 to 1400° C with pressure ranging between 1.5 to about 30 bars.

An endothermic reforming zone **(36)** follows the PO zone using Al_2O_3 doped platinum catalyst operating between 1000 and 1200°C**.** A second endothermic reforming zone **(38)** follows the first one which operates at lower temperature, since some of the heat released from the PO is utilized for the reforming reaction. The endothermic reforming reaction zone **(38)** is operated at 700° C with pressure between 1.5 to 30 bars. The reactant stream, prior to entering the endothermic reforming reaction zone **(36)** can also be mixed with a recycle stream introduced into a secondary mixing chamber **(41)** through an inlet **(42),** with recycle ratio not greater than **3.** The crude synthetic gas obtained from the reforming reactions is quenched by expanding in expansion nozzle **(43)** in conjunction with a water cooled chamber **(44)** surrounded by a water passage having a water inlet **(46)** and a water outlet **(48).**

Peters et al., 2009 [32] designed a reformer heat exchanger assembly, in contrast to Papavassiliou et al., 2007 [31] who used an expansion nozzle to cool the reformate gas obtained from the reforming of fuel. Peters et al., 2009 [32] designed a reformer heat exchanger assembly as shown in Figure 9. The invention couples the reformation and the post-combustion of the anode exhaust gases obtained from a fuel cell reformate, in the same reformer in order to operate the unit autonomously.

The invention addresses the heat demand of the water evaporation by using the heat from the burner exhaust gases and the reformate heat. Further this also helps in lowering the reformate temperature at the purification stage or high temperature shift **(HTS)** reaction zone. The apparatus has a reformer part **(RT)** and a combustion part **(BT).** The reformer is provided with a first mixing chamber **(MK-1)** which has a first inlet which feeds fuel and oxidizing agent via a nozzle, and a second inlet feeding in water vapour and carrier gas mixture via a supply line**.** During ATR operation, the oxidizing agent mixes with the vaporized fuel, water vapor, and carrier gas. In order to convert this mixture to reformate gas, the mixture is then passed over a catalytically active surface in a reaction chamber **(RR).**

The heat released during this process is absorbed by a first and a second heat exchanger, cooling the reformate gas. At the same time, residual anode gas from the fuel cell is supplied to the combustion part **(BT)**. These residual gases along with the required oxidizing agent are fed to the catalytic surface, where they react exothermically. The heat released during this process is absorbed by a third heat exchanger. The cooled exhaust gas is then removed from the apparatus. The water/carrier gas mixture required in the reformer part is added to the apparatus via a feed line and conducted via a first **(WT-1)** and a second **(WT-2)** heat exchangers, where water is completely evaporated and the mixture is superheated. The water vapor/carrier gas mixture is fed via feed line to reforming part where it is mixed with the vaporized fuel/oxidizing agent mixture.

This inventive method couples the chemical conversions of the reformer to that of the post-combustion in such a way the water vapor required for the reformation can be produced without the addition of external heat. It reduces the reformate temperature to that required for the subsequent gas purification, and also advantageously cools the residual anode gases from fuel cell that are converted to exhaust gas in the burner.

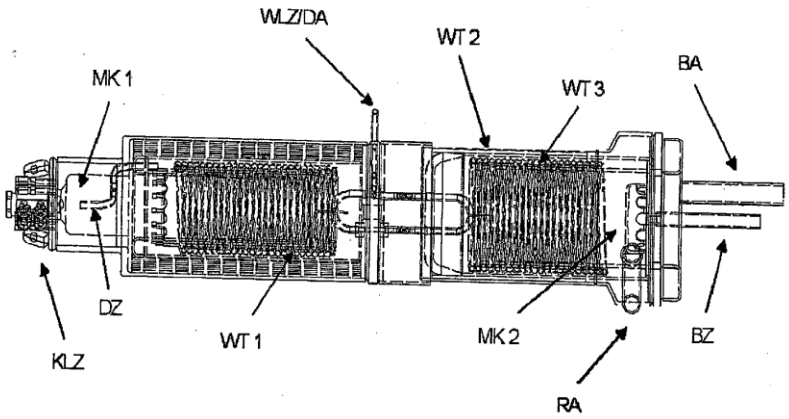

Figure 9: A reformer/ heat exchanger designed by Peters et al., 2009 [32]

Although ATR reforming is an energy neutral process, the major drawback of the process in comparison to SR is lower H_2 yield. Hence several investigators have tried to work on methods to obtain higher H_2 yield by various different approaches. In one such approach Retallick et al. ,2007 [33] designed an autothermal SR reformer. Figure 10 shows an autothermal SR reformer invented by Retallick et al., 2007 [33].

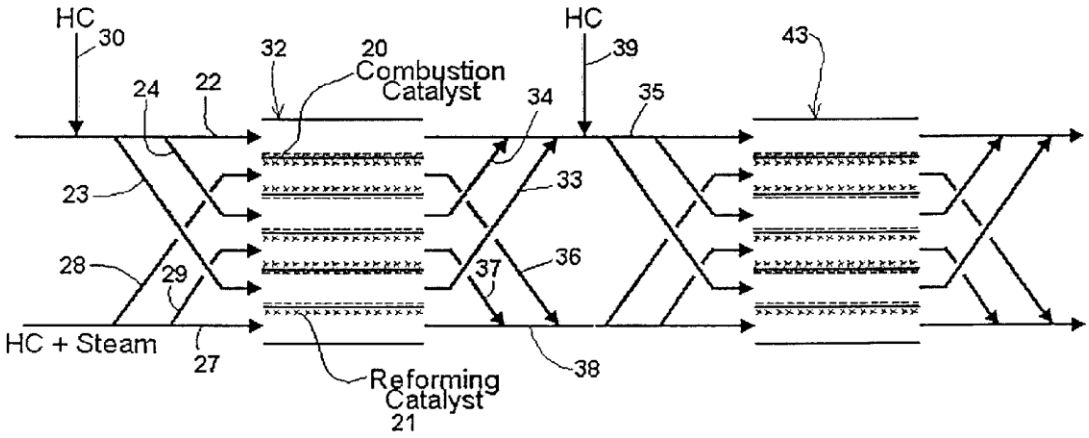

Figure 10: An autothermal SR reformer designed by Retallick et al., 2007 [33].

The reformer comprises of three strips which define two adjacent channels. The channel configurations are as shown in Figure **(11A-B).** The first channel **(2)** is a reforming channel, i.e. it houses the SR reaction. The second channel **(3)** is a combustion channel. The middle strip **(7) i**s partially coated one side with a reforming catalyst **(4),** and partially on the other side with a combustion catalyst **(5).**

A mixture of a hydrocarbon and steam is injected as shown at the left-hand side of the reforming channel, while an air-hydrocarbon mixture is injected on the right-hand side of the combustion channel. Additional hydrocarbon fuel can be injected into the combustion channel, at various positions along the channel, as indicated by arrows **(6).** Heat from the combustion reaction is transferred to the endothermic SR reaction via heat transfer through the common walls. Each reactor **(32)** and **(43),** comprise of stacks of strips which are alternatively coated with combustion catalyst **(20), and** reforming catalyst **(21).** Conduits **(23)** and **(24)** branch off from the conduit **(22)** supplying other combustion channels with fuel-air mixture. While conduit **(27)** supplies the various channels with a mixture of hydrocarbon fuel and steam for SR. Conduits **(28)** and **(29)** branch off from conduit **(27)**, and supply other reforming channels with the fuel-steam mixture. The fuel in the fuel-air mixture in conduit **(22)** is supplied from an inlet source. Additional fuel without air can be injected before each stage at the inlet via conduit **(30).** The fuel entering through conduit **(30)** comes directly from the source. This source supplies fuel to all other fuel to the system. The additional fuel injected via conduit **(30)** into the fuel-air mixture is automatically distributed among the individual combustion channels.

The conduits **(33)** and **(34**) are merged into conduit **(35),** to carry combustion products out of the system or into the next reactor stage. Likewise conduits **(36)** and **(37)** merge with conduit **(38)** to transfer the reforming products out of the system or into the next reactor stag**e.** Similarly new fuel injection for combustion, is made through point **(39)**, similar to that made at **(30).**

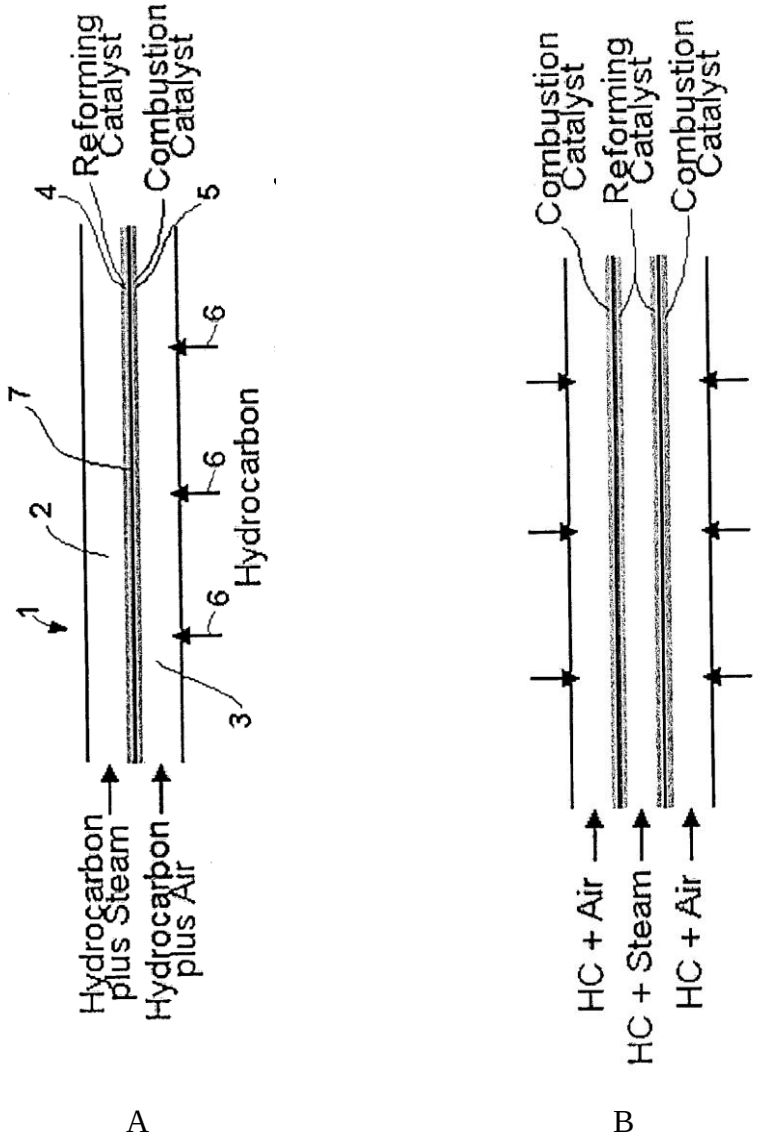

Figure 11:Schematic arrangement of single stage (A) and multiple stacks (B) [33].

The reactor has two valves, at the inlet and outlet. In the first valve position, stream comprising of fuel and air and second stream comprising fuel and steam is directed, into reforming channels and combustion channels respectively. In second valve position the streams are reversed, stream one is directed to channel **(2)** and stream **(2)** is directed to channel **(1)**.

At the first valve position, the outlet valve directs gas from the first channel into the combustion conduit, and from second channel into conduit for reformed products. At the second position the valve directs gas from first channel into the conduit for reformed products and from the second channel into the combustion products conduit.

In another illustration, similar use of indirect method for supplying heat to carry out SR reaction in an exchanger type reformer was developed by Fillipi at al., 2008 [34] as shown in Figure 12.

The process steps related to the reforming of hydrocarbon have been indicated by the blocks **(10), (11)** and **(12)** and by the flows **[(1, 2, 2*a*), (3) and (4)].** Blocks **(10)** represent the water supply source while **(11)** and **(12)** represent a compression and reforming block. The flow **(1)** indicates a gas flow comprising of water vapour and flows **(2, 2*a*)** indicate hydrocarbon fuel. The mix feed of water vapour and hydrocarbon is represented by **(flow 3)** and finally the outlet gas mixture containing H_2 is shown by **(flow 4).** The reformate gas obtained from the reforming step can undergo further processing in **(block 30)** to get the final reformate **(flow 31).**

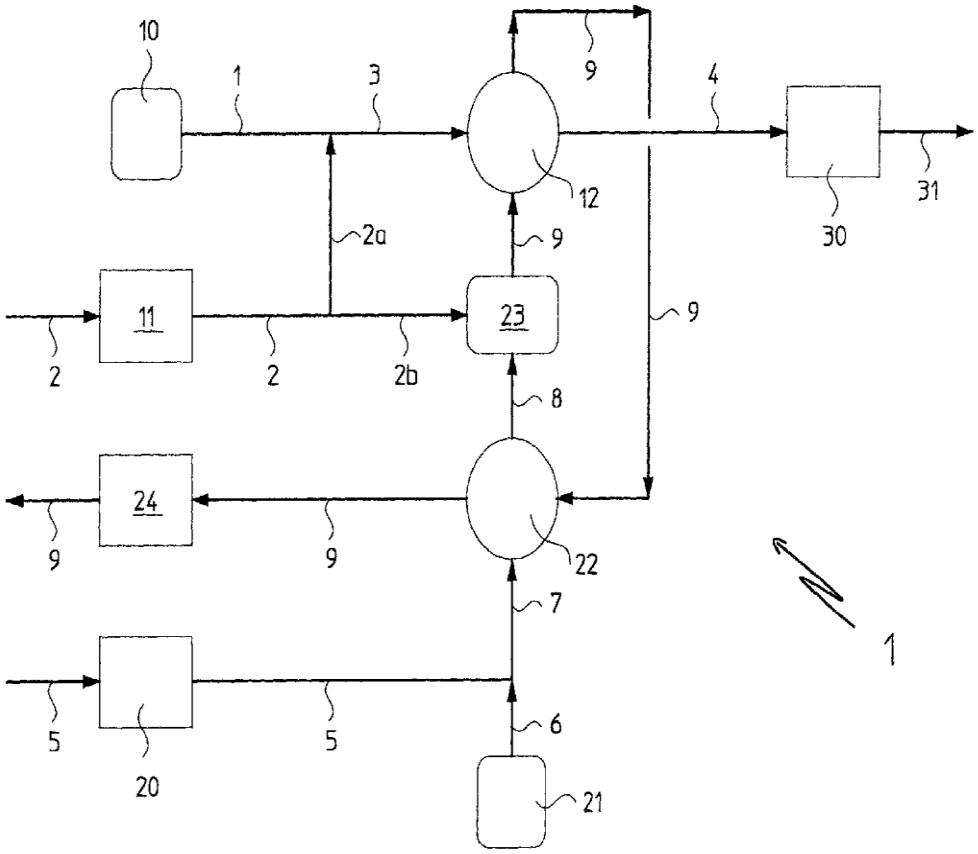

Figure 12: An autothermal SR process invented by Fillipi at al., 2008 [34].

The process water vapour source **(block 10)** generates water vapour between 2 and 100 bars at temperature comprised between 120 and 600°C. Similarly the fuel flow comprising of hydrocarbons is compressed in a compression step represented by block **(11)** to the same pressure range of water vapour. The mix feed is preheated before it is reformed. The hydrocarbon fuel undergoes reforming and shift reactions to produce H_2, CO, and CO_2. The reforming block comprises of an exchanger type reformer. The gas flow exiting the reforming block (**12) (flow 4),** is cooled to effectively recover the heat and to allow the condensation of the water vapour.

The steps for obtaining the heating fluid are indicated by the blocks **(11)**, (**20-24**) and by the flows **(2, 2*b*, 5 to 9).** Block **(20 to 24)** indicates a compression step of a gas flow comprising of oxygen block **(20)** and water source block **(21),** with a heating step of a flow comprising oxygen and water block **(22**), a mixing and combustion step block **(23).** The combustion block comprises of a gas mixture comprising of fuel flow along with a flow consisting of oxygen and water vapour and an expansion step of a heating fluid block **(24).** The flows **(2 and 2b*)*** indicate hydrocarbon gas flow, a gas flow of oxygen **(flow 5),** a flow of water **(flow 6**), a flow of both oxygen and water **(flow 7),** a gas flow of oxygen and water vapour (**flow 8**) and a heating fluid **(flow 9),** respectively**.**

A portion of **flow 2 (flow 2*a*)** from the compression step block **(11)** is mixed with a water vapour flow **(flow 1).** This mixed flow is fed to the reforming step i.e. block **(12) (flow 3).** The remaining portion of the hydrocarbons (**flow 2b**) is used as fuel in the combustion step block **(23).** The gas flow similar in composition to reforming step block (12) feed is fed to the combustion step block **(23)** through flows **(2)** and **(2b).** The ratio of the forming flow to combustion is maintained to 2:1. The air required for the combustion block **(23)** is supplied from compressed block **(20).**

The water flow coming from block **(21)** is fed at a predetermined pressure to the air **(flow 5). (Flow7)** comprising of air and water which is obtained by mixing (flows **(5)** and **(6),** is sent to a heating step **block (22)** for partial evaporation of the water to obtain a mixture of air and water vapour **(flow 8).** This mixed flow of air and water vapour is then directed to the combustor block **(23),** or even downstream of it, in the high temperature fluid of burnt gases **(flow 9).** The combustion **block (23)** comprises of a combustor inside which one or more burners for the combustion of the hydrocarbons/air mixture are provided. The heating fluid **(flow 9)** from the block (**23)** is employed for the reforming step i.e. block **(12)**, as indirect heat source for the reforming of hydrocarbons. The advantage of the process is that the heating fluid vented will have a particularly low content of pollutants, such as nitrogen oxide, as the presence of water in the combustor reduces the formation of these compounds.

2.2 Fuel processor design:

In addition to the various ATR reformer deign inventions, reported by the various authors as above, several inventions in design of the process for producing H_2 are also been reported. The process for generating H_2 for fuel cell application is known as a fuel processor. Pettit et al., 2007 [35] developed a fuel processor based on ATR and SR reactor. Figure 13 shows a fuel processor based on ATR and SR processes.

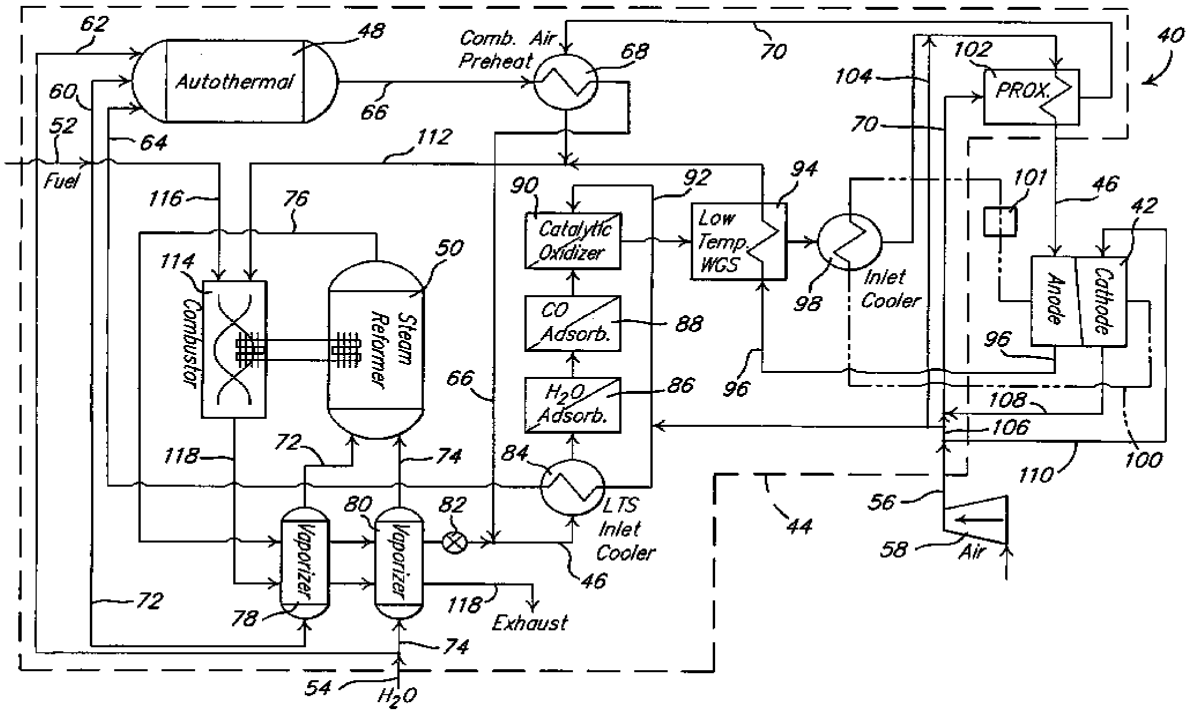

Figure 13: Fuel processor designed by Pettit et al., 2007 [35].

The incorporation of ATR and SR reformers in the fuel processor makes possible for the fuel processor to respond quickly to transient changes in the demand for the H_2-containing reformates, while it produces more efficiently H_2-containing reformate during nontransient operation. Further during cold-start up, the ATR reactor **(48)** can be used for starting the processes. Fuel stream **(60)** and air stream **(64)** are supplied to the ATR reactor and it is operated as PO reactor.

The fuel cell system **(40)** comprises a fuel cell stack. The processor consists of an ATR reformer **(48)** and a SR **(50)** reformer which provide a reformate stream **(46)** to the anode flow channel **(28)**. The ATR reactor **(48)** receives a fuel stream **(60)** from the fuel

supply **(52),** a water stream **(62)** from the water supply **(54)** and an air stream **(64)** from the air supply **(56).**

The ATR and SR reformers operate at are different pressures. The ATR reformer is operated at 1.5 to 3 bars while the SR is operated at 5 to 7 bars**.** The ATR reformer produces the first reformate stream **(66)** that contain H_2 as well as CO and CO_2. The ATR reformate exits the ATR reformer **(48)** and flows through a combustor air preheater **(68)** where the thermal energy of the reformate gas is used to preheat the oxidant stream **(70)**. The SR reformer **(50)** receives a fuel stream **(72)** from the fuel supply **(52)** and a water stream **(74)** from water supply **(54).**

The fuel stream **(72)** is vaporized in vaporizer **(78)** prior to entering the SR reformer (**50).** Similarly the water stream **(74)** prior to injection in SR reformer **(50)** is passed through a water vaporizer **(80)** where the thermal energy of the second reformate stream **(76)** is utilized for evaporation**.** The second reformate i.e. from SR reformer then passes through a pressure let down valve **(82)** which lowers the pressure of the second reformate stream **(76)** to the fuel cell system pressure. The first and second reformate streams **(66)** and **(76)** then combine together to form reformate stream **(46).**

The fuel stream **(72) is** vaporized in vaporizer **(78) p**rior to entering the SR reformer **(50).** Similarly the water stream **(74)** is passed through a water vaporizer **(80)** prior to injection in the SR reformer **(50)**, by utilizing the thermal energy of the second reformate stream **(76).** The second reformate i.e. from SR reformer then passes through a pressure let down valve **(82)** which lowers the pressure of the second reformate stream **(76)** to the fuel cell system pressure. The first and second reformate **s**treams **(66)** and **(76)** then combine together to form reformate stream **(46).**

The reformate stream **(46)** exchanges heat with the air stream **(64)** in a low **te**mperature **s**hift inlet cooler **(84**). The reformate stream **(46)** then pauses through a water adsorber **(86).** The gases leaving water adsorber enter CO adsorber followed by a catalytic oxidizer **(90).** The catalytic oxidizer also receives air stream **(92)** from air supply **(56).**

The heat generated in the catalytic oxidizer **(90)** is used to heat a low temperature WGS reactor **(94)** via radiation and/or reformate stream **(46)** which flows from the catalytic oxidizer **(90)** and through the WGS reactor **(94).** The heat generated by the WGS reactor **(94**) is utilized to heat an anode effluent **(96)** that leaves the fuel cell stack **(42).**

The reformate stream **(46)** leaving the WGS reactor **(94)** passes through a preferential oxidation reactor inlet cooler **(98)** extracting heat from the reformate stream **(46)** and transferring it to the coolant stream **(100).** The treated reformate **(46)** from the cooler is fed to a partial oxidizer reactor **(102)** which receives air stream **(104). The** treated stream from the partial oxidizer **(102)** then enters the anode flow channels **(28)** of the fuel cell stack **(42).**

Air stream (**110)** from air supply **(56)** is fed to the cathode flow channels **(26)** of the fuel cell stack **(42**). This air stream **(110)** and the reformate stream **(46)** are reacted within the fuel cell stack **(42)** to produce electricity, cathode effluent **(108),** and anode effluent **(96).** The unreacted anode effluent **(96)** exits the fuel cell stack **(42)** and passes through the WGS reactor **(94)** for heat exchange**.** The cathode effluent **(108)** containing unused oxidant combines with air stream **(106)** to form oxidant stream **(70)**. Oxidant stream **(70)** after

passing through the combustor air preheater **(68)** combines with the anode effluent **(96)** to form effluent stream **(112).**

Figure 14 shows a reformer heat exchanger arrangement based fuel processor designed by Malhothra and Gosnell, 2009 [36].

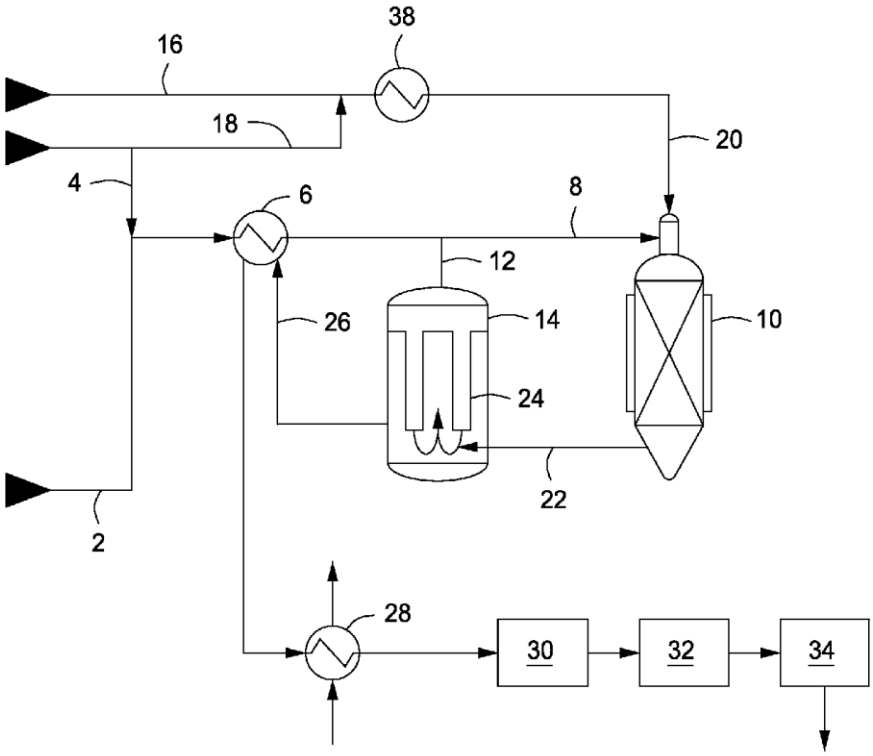

Figure 14: A reformer/heat exchanger based fuel processor designed by Malhothra and Gosnell, 2009 [36].

According to the invention hydrocarbon stream is supplied from line **(2)** is mixed with process steam from line **(4)** and the feed is preheated in a preheat exchanger **(6)**. A first portion of the preheated mixture is feed to the burner of autothermal reformer (ATR) via line **(8)** and a second portion is supplied via line **(12)** to the tube-side inlet of reforming exchanger **(14)**.

Air is supplied via line **(16)** and mixed with steam from line (**18)**, and the steam-air mixture is preheated in preheater **(38)** to a temperature range from 200° C to 650°C, and feed to the burner via line **(20)**, taking care that the flame temperature in the burner is maintained below 1500°C. The molar ratio of steam/O_2 ratio in the air-steam mixture maintained about 1 to 1.6 and O_2/C in the hydrocarbon stream is maintained in 0.6 to 0.7.

The split of the hydrocarbon feed to the ATR **(10)** via line **(8)** relative to the total hydrocarbon feed to the ATR **(10)** and the reforming exchanger **(14)** via line **(2).** The flow is maintained between 65 to 75 percent of the flow to the ATR.

The syngas effluent in line **(22)** from the ATR **(10)** is supplied to the shell-side inlet of the reforming exchanger **(14)**. The reformed gas from the outlet ends of the catalyst tubes **(24)** mixes with the ATR effluent and the mixture then passes on the outside of the catalyst tubes **(24)** to the shell-side outlet where it is collected in line **(26)**. This combined syngas is cooled within a cross exchanger **(6)** waste heat boiler **(28)** to generate steam. The mixture is further supplied to downstream processing which would include a CO-shift section **(30),** heat recovery **(32),** and mixed gas separation **(34)** unit i.e. a pressure swing adsorber**.**

The heat requirement for the reforming exchanger **(14)** is met by the quantity and temperature of the ATR effluent. The temperature of the ATR effluent in line **(22)** should be from 650 to 1000 or 1050° C, and is limited by the material of construction**.** The operating pressure of the reformer is between 25 to 30 bars.

As mentioned previously, ATR reforming has a disadvantage of lower H_2 yield as compared to SR. In order to mitigate this problem a process called Autothermal cyclic reforming (ACR) has been developed by GE [37, 38]. Chemical looping SR is processes where the catalyst also works as an oxygen transfer material (OTM). This type of SR uses both steam and oxygen to react with fuel without mixing the two, using the OTM as intermediate. In this process an oxygen transfer material (OTM) that also a SR catalyst is cycled through alternating fuel feed and air steps. During the fuel step, The OTM is reduced due to unmixed combustion which occurs before the SR reactions begin. The OTM is then oxidized during the subsequent air feed cycle which is an exothermic reaction. This release of heat that can be used to support the SR reaction for the next fuel feed cycle. The advantage of ACR process is that, the overall process is autothermal. Further since the flows of air and fuel /steam are separate, the obtained reformate is not diluted with the N_2 from the air. It avoids the need for an air separation unit and it allows for better heat transfer in the reformer.

Figure 15 shows a fuel processor based on ATR cyclic reforming process designed by Kumar et al., 2005 [37]. The fuel processor uses a packed bed reactor system, which uses two SR reformer reactors **(204)** and **(206)**. When the reforming reactor **(204)** cycles in regeneration step the second reactor **(206)** switches to reforming mode. The cycling process of the reformer reactors **(204)** and **(206)** are similar to the cycling of reactors **(132)** and **(108).** Each of the reformer reactors **(204), (206)** are loaded with catalyst, and they include an integrated heat exchanger in which the product gas from a respective reactor transfer heat to the feed gas to the same reactor.

Steam generated from HRSG **(202)** and fuel from fuel supply (**201)** are mixed and fed to the reactor **(204)** when operated in reforming mode. In a reforming step, fuel and steam are reacted to produce a reformate gas, while in a regeneration step, unreacted recycled fuel flows through the reactor. Reactor **(206)** processes a portion of anode and cathode vent streams from fuel cell **(214)** to produce a vent gas during regeneration mode. The remaining anode and cathode vent streams are sent to the auxiliary burner **(216)** on the HRSG **(202)** via loop **(222).**

The remaining portion of the vent gases is then fed to auxiliary burner **(216)** for heat recovery, by means of steam generation. Fresh fuel can also be used instead of the anode vent stream, and fresh air instead of cathode vent stream. The reformate gas obtained from reforming reactor **(204)** is fed to a shift reactor **(208)** to reduce the CO to less than 2 % (on a dry basis). The shift reactor receives steam from HSRG **(202).** The treated reformate from the WGS reactor **(208)** is fed to a condenser/heat-exchange **(210)** to the heat anode and cathode vent streams and is then fed to CO oxidizer **(212)** along with air. The product gas from CO oxidizer **(212)** is fed to the anode side of the fuel cell **(214).** Anode vent gas and cathode vent gases from the fuel cell **(214)** are passed through the cold side of the condenser **(210)**. These gases are then sent to the heat recovery as mentioned before**.**

In an alternative arrangement, the product gas from the reformer reactor **(206)** can be used to preheat the feed gas to the reformer reactor **(206)** in the regeneration step using extra heat exchanger. Further in another alternative arrangement a pressure swing adsorber can be added after the condenser/heat-exchange **(210).**

A compact fuel processor was designed by Ahmed et al., 2009 [39] based on the ACR concept. The advantage of this fuel processor over that designed by Kumar et al., 2005 [37] is its compact nature where most of the steps are included in one housing. A cross-sectional view of a fuel processor is shown in Figure 16. The fuel processor **(10)** is comprised of an exterior housing **(20),** inner reforming zone **(30),** an outer reforming zone **(40),** a cooling zone **(50),** a sulfur removal zone **(60),** and a WGS zone **(70).** It also includes a steam heating zone **(80)**, an air heating zone **(90)**, and an ignition source **(100).** The catalyst zone is loaded with a PO catalyst and a SR catalyst or a catalyst that can catalyze both PO and SR reactions**.**

PO and SR are performed in the inner reforming zone. A sulfur removal material effective in removal of compounds like H_2S or COS, from the reformate gas stream is provided in sulfur removal zone **(60).** Two zones for WGS reaction are provided with two different catalysts. Zone 1 contains Gd-CeO_2 or platinum on CeO_2 supported on aluminum based catalyst, while second WGS zone **(480)** comprises of CuZnO based WGS catalyst. A top cover plate encloses the fuel processor **(510)** and is secured with bolts **(520)** with a graphite based gasket **(540).**

Pipes **(530)** are provided for supplying sulfur containing fuel to the removal zone **(460**). Inlet pipe allows the heated steam and fuel to enter mixing nozzle **(436)**, the mixer is supplied with air before entering inner reforming zone **(430).** This pipe is inserted through the insulation **(545).** The top plate **(510)** also includes steam outlet pipe **(570)** which allows steam to flow out fuel processor **(410)** into pipe **(580)** to juncture **(590)** where it mixes with fuel and enters pipe **(595)** prior to entering pipe **(560).**

A bottom plate **(600)** is provided to close the fuel processor **(410).** The plate is provided with a perforated outer portion **(602)** below second WGS zone **(480)** and is secured with bolts **(610)** to lower exterior section **(612).** The plate provides an exit for the reformate gas from the fuel processor (410). It flows through the perforations from outer portion (602) and enter into lower exterior section (612)**.** The reformate gas from lower exterior section **(612),** enters the reformate gas exit pipe **(630)** attached to lower exterior section **(612)** by flanges **(614)** and **(616)** secured with bolts **(618).**

Air enters through the inlet **(650)** and is heated as it passes through coils **(660)** in outer reforming zone **(440)** before reaching air pipe **(435)** where it is further heated before entering mixing nozzle **(436).** Steam or water enters through steam inlet **(670)** and then passes through steam coils **(680)** where it used to cool the reformate gas in the zones **(450), (460),** and **(470).** The produced heated steam flows out through the steam outlet pipe **(570).**

Similarly fuel enters fuel inlet **(690)** and circulates through fuel heating coils **(695)** around the exterior of exterior housing **(420)** before exiting fuel outlet **(700).** The heated fuel enters fuel pipe **(710)** before reaching juncture **(590)** where it is combined with heated steam**.**

A further cooling of second WGS zone **(480)** is accomplished by supplying cooling water into secondary water inlet **(720),** which then circulates through secondary water coils **(725)** before exiting secondary water outlet **(730)**. This allows the temperatures of second WGS zone **(480)** to be maintained at a different temperature from first WGS zone **(470)** since different catalyst are used in both the zones**.**

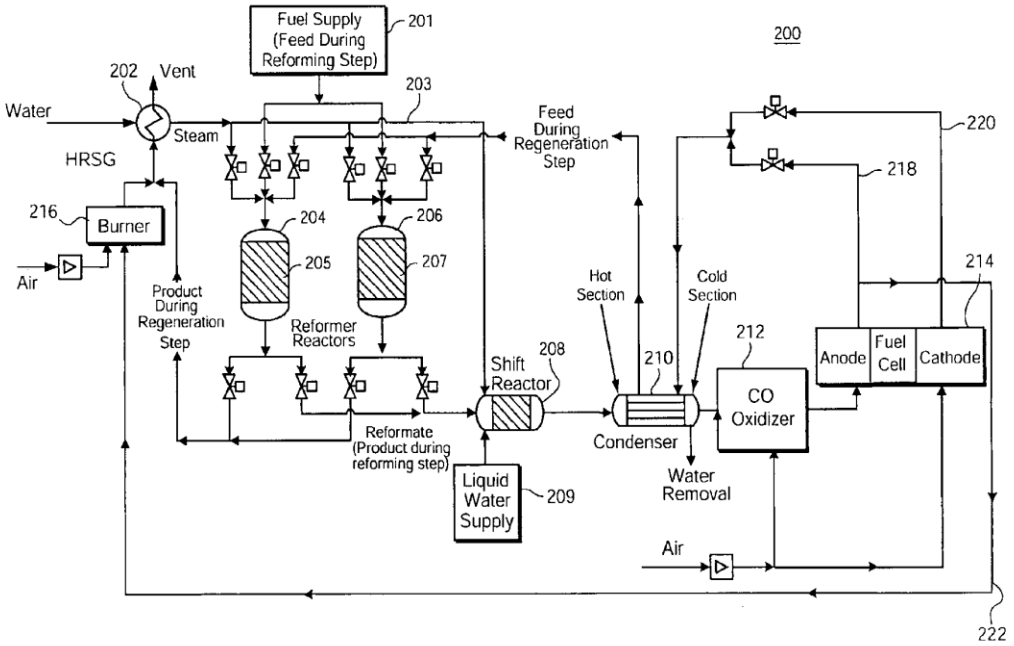

Figure 15: Fuel processor designed by Kumar et al., 2005 [37].

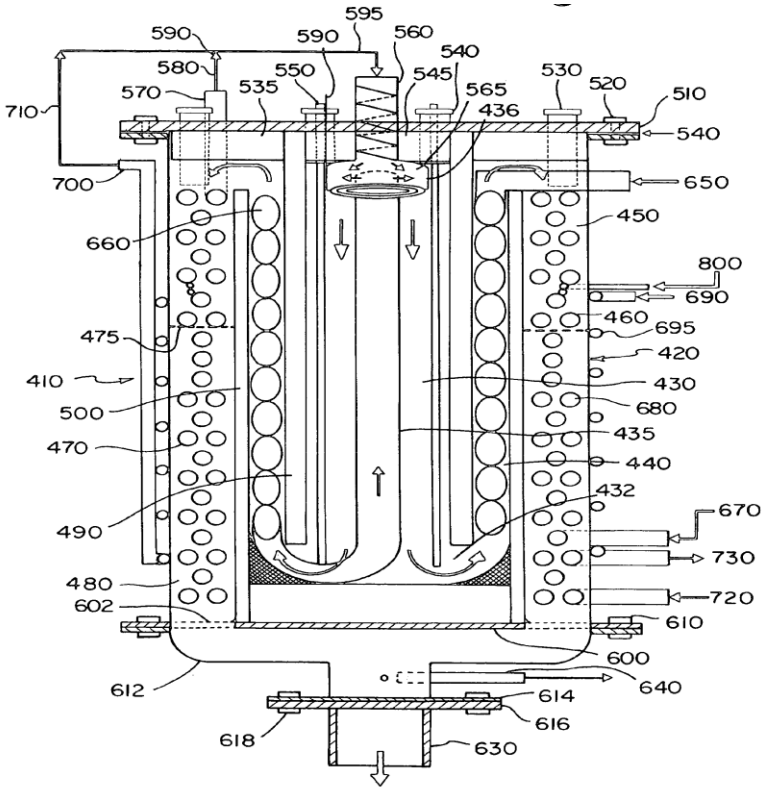

Figure 16: Fuel processor designed by Ahmed et al., 2009 [39].

2.3 Reformers start up:

One of the major areas of developments in an ATR technology is start up of the reformer. The start up of the reformer is very crucial for an ATR reformer since it needs to have short start up period giving the user better control over the system. The transition period of a cold reactor to the operating temperature is a key factor, as it requires synchronization with the rest of the fuel processing processes and close control over the reaction parameters.

The start up of ATR reformer is performed by initiating PO reaction over the catalyst bed, by reacting fuel and the oxidant and making use of the exothermic heat to increase the temperature of it, the reaction is switched to the ATR mode by introducing steam. The main aim of these investigations is to reduce the start up time.

Yukihiro and Mizuno,2009 [40] used pre heating means placed upstream of the ATR catalyst to preheat the catalyst to the desired temperature. Figure 17 shows an ATR start up method developed by Yukihiro and Mizuno, 2009 [40].

After the predetermined catalyst temperature is reached heating is stopped, and vaporized fuel and is fed allowing it to be oxidized by the reforming catalyst and heating the reforming catalyst simultaneously.

The shift from the first preheating step to the second preheating step is achieved at 250^{o}C or higher temperature, while the shift from the second preheating step to the steady state ATR is performed with catalyst bed temperature reaching at 600°C.

In the invention the first preheating step is achieved by means of burner, by introducing the vaporized liquid and air into the burner and igniting them. The air-fuel ratio prefferd is in the range of 1 to 2 (volume ratio). In the second preheating step the burner is turned OFF and combustion is allowed to take place over the catalyst. The burner operation is stopped by increasing the air flowrate to extinguish the burner flame. By use of catalytic combustion the catalyst bed outlet temperature is raised to sufficient value without the catalyst bed inlet alone being heated. The preferable air-fuel ratio in the second preheating step is in the range of 2.5 to 5 (volume ratio).

After the second preheating step, steam is fed to the preheated reforming catalyst; the amount of liquid fuel fed is varied in the predetermined amount to achieve a steady state ATR reaction.

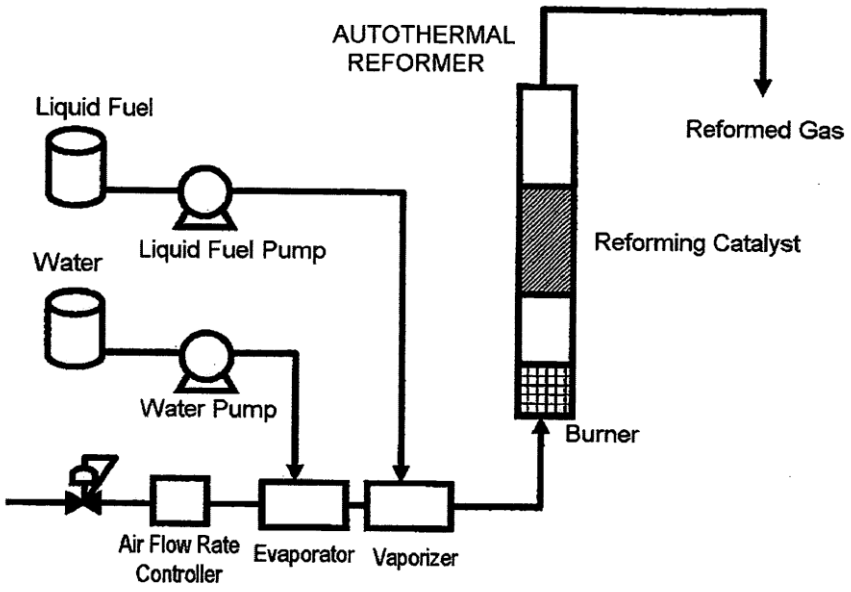

Figure 17: ATR reformer start up developed by Yukihiro and Mizuno, 2009 [40]

Arcuri et al., 2008 [41] devised an ignition free approach for ATR reformer start up. The invention describes a flameless method using a feed composition which is outside of the flammability envelop to allow the catalyst to initiate the PO reaction without the risk of introducing a flammable mixture to process volumes downstream of the ATR reformer.

In the inventive process, a gas mixture comprising of about 5 to 10 % steam, 20 to 30 % natural gas and about 2 % H_2 of natural gas flow (or less than about 0.6% of the total flow) with air is fed to the reformer. To obtain this mixture a feed gas with an air/NG and

steam/NG ratio well above the upper flammability limit is introduced to the reformer. Upon introduction of these non-flammable mixtures, the onset of pre-reforming can be observed through a decrease in the catalyst bed and downstream process temperatures or analysis of gas composition. According to the invention a relatively very high gas flow rates having Reynolds number flow, >about 100,000, is employed. According to the invention the gas velocity should be sufficient to ensure that the feed gas residence time prior to contacting the catalyst is less than the time required for auto-ignition i.e. the feed gas should reach the ATR catalyst prior to the onset of auto-ignition. According to the method the catalyst employed in the processes should possess high activity for PO. The steam content of the mixture can also be varied to avoid any soot formation over the catalyst.

Likewise another flameless method was devised by Wheat et al., 2006 [42] who introduced an oxidizer before the ATR reformer for start up of the reformer. According to the inventors the process involves bringing the oxidizer to the operating conditions by lighting off the oxidizer and the ATR reformer. The oxidizer light off involves a reaction of fuel and air over the catalyst in a desired temperature range. Similarly, the ATR the light off is considered when the catalyzed reaction occurs between the process stream and a stream received from the oxidizer. Few different methods of stat up, for both the oxidizer and ATR reformer were reported. In one such method the oxidizer is purged with air at an initial temperature to generate a part of the heat, by producing ignition heat in at least one portion of the purged oxidizer. This achieved by heating a portion of a catalyst bed to least light off temperature or actuating a spark source. The ignition heat in the catalyst bed is generated by heating it to 280° C by use of heat exchangers. Fuel is then introduced to the heated region of the oxidizer reactor in such a way that fuel and air mixture stays below the lower explosive limit of the fuel, followed by heating the oxidizer to the operating temperature. The operating temperature is high enough to start and sustain a catalyst reaction of the fuel air mixture. The oxidizer temperature is maintained between ~400°C and 800°C showing that the oxidizer is lighted off.

Similarly for the ATR reformer light off begins with purging the reformer with fuel to the upper explosive limit of the fuel. In the invention a non-pyrophoric shift catalyst is placed after the reformer. The light off continuous by maintaining the WGS catalyst at a temperature between approximately 150° C and 200° C, sufficient to prevent condensation of water therein. The purged ATR reformer is then heated to the light off temperature of the WGS catalyst with fuel flowing through the reformer. Finally air is introduced to produce an air and fuel mixture and heating the reformer to 600 to 900°C, and maintaining the non-pyrophoric shift catalyst to approximately 250°C.

A different approach was examined by Pettit et al., 2007 [43] where they devised an separate chamber in the ATR reformer for startup purposes. Figure 18 shows a schematic of the reformer designed by Pettit et al., 2007 [35].

According to the invention a multi port ATR reformer **(10)** was developed with fuel inlet system **(12),** a start-up system **(16)** and a normal operation system **(18),** both in fluid contact with the common volume **(22).** A start-up air inlet **(24)** and a fuel inlet **(20)**, makes up as a part of start-up system **(16).** The start-up air inlet **(24)** includes a port **(25)** embedded in housing (510), which is in fluid contact with an annular volume **(26)**. This port is also in fluid contact with the porous material **(28)** through which air flows. Porous material **(28**) is

placed within the annular volume **(26)**, radially inward from port **(25),** and is in further contact with a swirler or vanes **(30)** which are symmetric with respect to centerline**.**

Air passes from the porous material **(28)** and then into the swirler **(30).** Swirler **(30)** is further connected to the common volume **(22)** and is utilized to induce a desired flat tangential air velocity profile before it enters the volume **(22).** The common volume **(22)** is used for both the mixing volume for normal operation and the site for thermal combustion during start-up operation.

Common volume **(22)** is placed in a conical housing positioned upstream from the reforming section **(14).** The common volume is provided with an ignition source **(32),** heat shield **(50),** and a temperature sensor **(34).** The heat shield provides a boundary between the common volume **(22)** and the reforming section **(16).** The temperature sensor **(34)** is a thermocouple mounted on the heat shield **(50).**

The fuel inlet **(20)** introduces metered fuel into the start-up system **(16)**, via metering device **(21)** embedded in the housing **(500),** allowing the housing to be in contact with the common volume **(22).** Air and the introduced fuel form a mixture is ignited using the ignition source **(32)**. Once the light off temperature in the reforming section **(14) is** achieved sensed by the thermocouple normal operation of the ATR reformer is started.

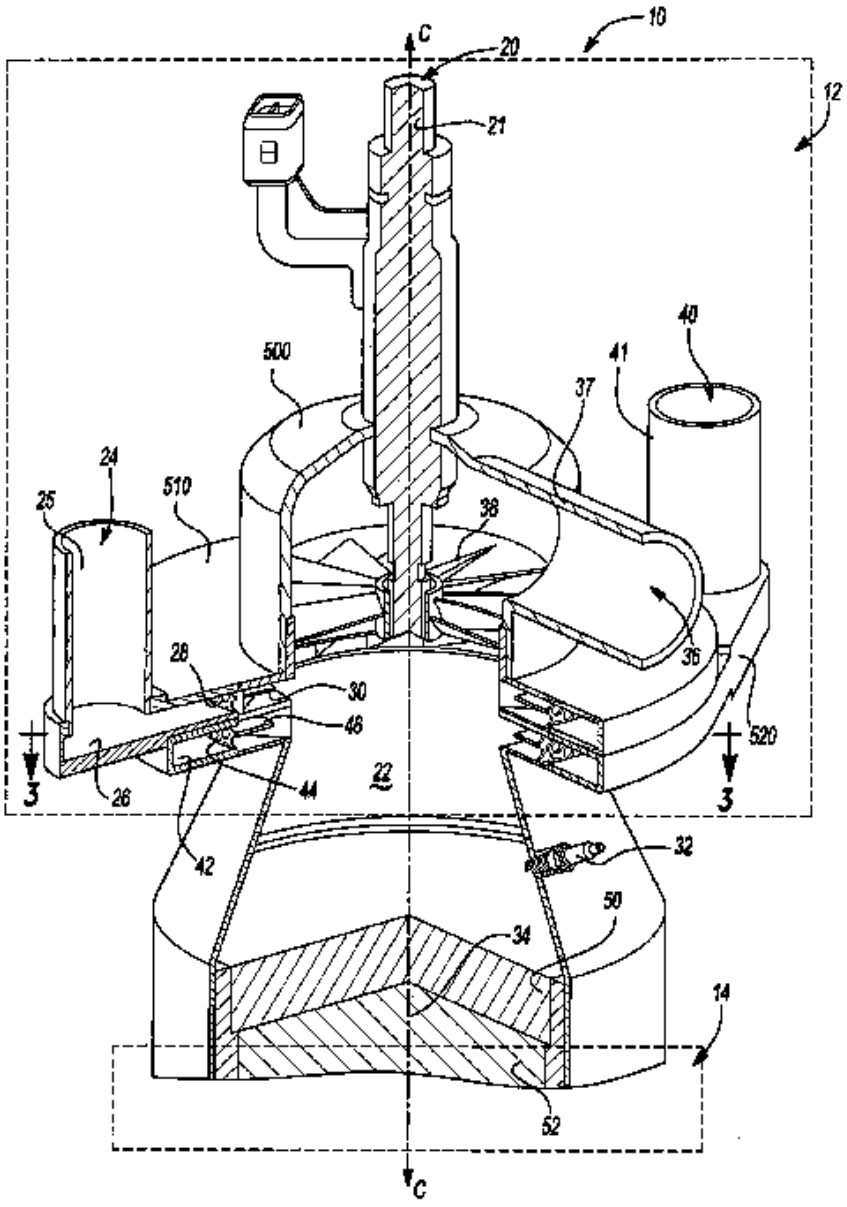

Figure 18: Schematic of the ATR reformer designed by Pettit et al., 2007 [43].

Unlike the previous inventions, Yanlong and Zhao, 2005 [44] developed a catalytic method for start up of an ATR reformer**.** A schematic of the ATR reformer is shown in Figure 19. Two catalyst portions are placed in the reformer one in the upstream side **(14)** and one on the downstream portion **(16)** enclosed in a common housing **(18).** The upstream catalyst **(14)** has a comparatively low light-off temperature, while the downstream catalyst has a higher light-off temperature. The catalysts form the major part of both the housings**.**

During ATR operation, fuel **(20),** steam **(22)** and a controlled amount of air **(24)** are optionally premixed and then injected into the upstream end **(10)** of the housing **(12).** Fuel and air react over the catalyst to produce heat**.** The heat is absorbed by the endothermic reforming reaction of fuel and steam, which occurs at the same time over the catalyst beds. On reaching the operating temperature, the amount of heat required for the reforming reaction can be generated by controlling the ratio of the inlet air to the amount of fuel being reformed.

During system startup, the system must initially be heated by preheat mechanism **(18)** which can be hot gas, electrically heating the beds, or by heat transfer from a combustion reaction, such as from an external burner, so that the catalysts reach their effective operating temperatures**.** As the reactor is heated with the external source the light-off temperature for the catalyst in the first portion **(14)** is reached sooner as compared to the catalyst with the high light-off temperature. The heat generated by the oxidation over the first catalyst is enough to maintain or increase the catalytic activity. Further this heat is also enough to heat the second catalyst to its light off temperature. Thus the reformer can reach the operating temperature much faster than the normal ATR reformers.

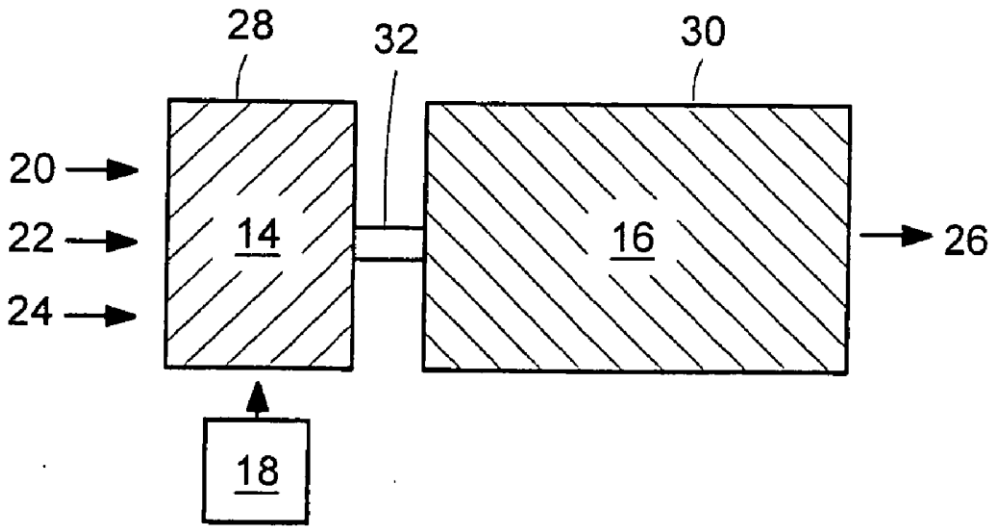

Figure 19: Fast start up ATR reformer designed by Yanlong and Zhao, 2005 [44].

Table 1 summarizes the various inventions patented by various authors. The table provides the objectives of various authors and the nature of the invention.

Table 1: An overview of patents based on the nature of the invention.

		Table 1
Author	**Investigation**	**Research Objective**
Ahmed et al., 2010 [23]	Patent	Reformer design for heat management based on porous catalyst support was invented.
Doctor et al., 2009 [28]	Patent	Reformer design by providing an external heater was invented.
Fillipi et al, 2008[34]	Patent	Autothermal SR reformer to avoid the problems of lower H_2 yield and selectivity, in ATR reformer as a result of fuel oxidation was invented.
Lesiuer et al.,2005 [29]	Patent	This invented ATR reformer assembly provides an enhanced catalyst and heat transfer surface area with compact and light weight and enhanced gas mixing and distribution flow path was invented.
Kaeding et al., 2007 [26]	Patent	Reformer design and heat management by modification of fuel inlet was invented.
Papavassiliou et al., 2007 [31]	Patent	Reformer design to avoid fuel oxidation during mixing of oxidant and fuel. Better heat management and size reduction with higher H_2 production rate was invented.
Peters et al., 2009 [32]	Patent	Heat management and utilization of the heat from burner exhaust gases for generating steam for the reforming reaction was invented.
Retallick et al., 2007[33]	Patent	Design on an autothermal SR to eliminate the problems of lower H_2 yield as a result of fuel oxidation in an ATR reformer was invented.
Robb et al., 2007 [25]	Patent	Reformer design by modification of oxidant supply and reformer startup was invented.
Ahmed et al.,2009[39]	Patent	ACR fuel processor based fuel processor was invented.

Kumar et al.,2005[37]	Patent	ACR based fuel processor involving two reactors for alternating between reforming and regeneration steps was invented.
Malhothra and Gosnell [36]	Patent	Design ATR reformer/exchanger based fuel processor for heat utilization and steam generation for the reforming reaction was invented.
Pettit et al., 2007 [43]	Patent	Fuel processor based on ATR and SR reformers for quick start up and transient capability providing high overall efficiency during normal operation was invented.
Pettit et al., 2007 [43]	Patent	A multiport reformer with fuel inlet system for quick reformer start up was invented.
Wheat et al., 2006 [42]	Patent	An oxidizer was introduced before the ATR reformer for quick reformer start up was invented.
Yanlong and Zhao [44]	Patent	A dual bed catalytic system was designed for the reformer start up was invented.
Yukihiro and Mizuno [40]	Patent	Start up of the reformer by combusting a specific amount of fuel in the burner in first step and allowing the combustion to take place over the catalyst by switching off the burner; to increase the catalyst temperature for fast reformer start up was invented.

2.4 Catalysts:

One of the integral parts of an ATR reformer is the catalyst. As seem previously, several catalysts can also be employed in ATR. The catalysts are responsible for the conversion of the fuel to H_2 rich gas. The requirements of ATR catalysts are as below.

- ATR catalysts have to be active for SR and PO.
- High surface area
- Higher selectivity for H_2 production
- Resistance to coke formation
- Higher WGS activity
- Oxidation stability
- Lower H_2 oxidation activity
- Robust at high temperature and resistant to sulfur and coke formation, especially in the catalytic zone that runs with limited O_2.

Various supports and active metals can be used in the preparation of the catalysts. Noble metals and particularly Rh and Pt are active for the reforming of hydrocarbons [17, 45]. These metals can also work under sulfurous environment [46]. Noble metals are also very active in C-C bond breaking resulting high reforming activity. But due to economic reasons the use of these metals is limited. Similarly uses of various kinds of supports like Al_2O_3, mix oxides, and perovskite have been researched.

2.4.1 Al_2O_3 supported catalyst:

Mawdsley and Krause, 2006 [47] studied the use of a 2 wt% Rh/La–Al_2O_3 catalyst in the ATR of sulfur-free and 34 ppm-S containing gasoline in the temperature range of 700 to 800^{o}C with molar S/C of 1.5 and molar O/C of 0.45. The authors reported that the activity of the catalyst is affected by the S content in the fuel. The positive effect on the activity was reported to be more pronounced at 700 °C than at 800 °C. A 50 % catalyst activity recovery at 700^{o}C and complete recovery at 800^{o}C were reported when S containing gasoline was switched with S free gasoline. Sulfur increased Rh sintering due to an increase in the catalyst temperature caused by a greater inhibition of SR than PO. Further addition of K to the Rh catalyst significantly enhanced the S tolerance of the catalysts. In comparison to Rh, Al_2O_3 supported Pt catalysts have shown higher tendency to coke formation. Shamsi et al, 2005 [48] examined the use of Pt/Al_2O_3 catalyst in ATR of tetradecane, decalin, and methylnaphthalene as model hydrocarbons. They reported that type of hydrocarbons affects the amount of coke deposited on the catalyst, with decalin showing the least amount in comparison to the other two. They also reported that the coke deposited on the metal support was easily oxidized in comparison to that on the support.

In contrast to Shamsi et al., 2005[48], Xue et al., 2009 [49] reported that doping of Al_2O_3 helps to improve the performance of Pt based catalyst in terms coke resistance. A 1.2 wt %-Pt/1.6%-Gd_2O_3-15%-CeO_2–Al_2O_3 catalyst was examined for the reforming of gasoline containing 158 to 500 ppm S with S/C of 5 and O/C of 0.35. Authors reported that Gd_2O_3 addition provided significant improvement and stabilization of Pt–CeO_2 interaction, great attenuation of Pt-sintering and enhancement of oxygen ion conductivity of bulk CeO_2 resulting in higher conversion, H_2 selectivity, and coke resistance. They also reported that the catalyst was stable for 300 h with CH_4 and C_2 hydrocarbons content 1ess than 1.9 %.

Likewise Galvan et al., 2008 [50] utilized 0.75 wt% Pt/ 10%-CeO_2–Al_2O_3 catalyst in ATR of diesel surrogate with H_2O/C of 3, O_2/C of 0.5 at 800^{o}C. The catalyst exhibited high activity and the performance was attributed to the Pt–Ce interaction that may have changed the electronic properties and/or the dispersion of active metal phase. Further the formation of Ce^{III} form of Ce^{IV}/Ce^{III} redox pair was reported to enhance the adsorption of oxygen and water molecules on the catalyst thus increasing the catalytic activity and decreasing coke deposition over surface active Pt phases. In contrast, Navarro et al., 2006 [51] reported different results in ATR of hexadecane at the same conditions examined by Galvan et al., 2008 [50]. Authors reported lower catalytic activity over 0.7 wt% Pt/ 8.1% CeO_2–Al_2O_3 in comparison to 8.2 wt% Ni/ 8.1% CeO_2–Al_2O_3. Authors reported that the catalytic activity strongly depends on metal, Pt showing lower specific activities per atom of metal introduced and higher selectivity to combustion products resulting in lower activity in comparison to Ni based catalyst. Furthermore they also reported that unmodified Al_2O_3 supported catalyst exhibited lower catalytic activity in comparison to Ce and La modified Al_2O_3.

In the case of Pt catalysts, addition of La_2O_3 in the support formulation had a positive effect on the reforming activity was reported as a result of participation/ assistance of La_2O_3 in the reaction rather than a modification of metal dispersion or decrease in coke formation derived from the presence of La_2O_3. While in the case of Ni based catalyst, metal–support interactions were reported to have strong catalytic behavior with addition of Ce and/or La to the Al_2O_3 support. Similarly, the same authors (Galvan et al., 2008 [52]) examined the performance of these catalyst on model compounds of diesel i.e. decalin, hexadecane, and tetralin. The order of activity on both the catalysts was reported to be decalin >hexadecane> tetralin. The greater activity towards decalin was attributed to the more labile tertiary carbons of the molecule, and the lower activity for oxidative reforming of tetralin was reported due to the higher bond dissociation energy of the aromatic C–C and C–H bonds.

Qi et al., 2005[53] examined the use of 0.3 wt. % Ru/3%-K_2O-2.5%-CeO_2/γ-Al_2O_3 catalysts in ATR of n-octane with H_2O/C 1.6 to 2.2, O_2/C 0.35 to 0.45 in the temperature of 750 to 800 °C for 1200 h. Initial high conversion followed by a slow deactivation over the catalyst was reported as a result of increased reverse WGS reaction initially and devastated SR reaction eventually. Chekatamarla and Lane [54] examined the use of noble metal based bimetallic catalyst supported on Al_2O_3. Authors examined the use of 0.26 wt% Pt–0.95%-Pd/Al_2O_3 and 0.22 wt%-Pd-0.90%-Pt/Al_2O_3 based catalysts in ATR of synthetic diesel, with S/C of 3 and O_2/C of 0.5 at 400^{o}C in adiabatic reactor. Bimetallic based catalysts were shown to exhibit higher activity in comparison to monometallic based catalyst. Further the order of

impregnation had no impact on the performance of the catalysts. Higher H_2 yield of the bimetallic catalysts was reported as a result of significant decrease in the lower hydrocarbon concentration coupled with improved CO oxidation activity resulting in lower concentration of undesired CO.

In comparison to noble metals supported on Al_2O_3, Ni supported Al_2O_3 based catalysts were investigated in ATR of gasoline by Wang et al., 2006 [55]. Authors examined the use of N/Al_2O_3 and $Ni\text{-}Re/Al_2O_3$ based catalyst in ATR of gasoline with S/C of 1.5 and O_2/C of 0.8 at 680^{o}C. Authors reported high activity over the bimetallic 10 wt% Ni−2%-Re/Al_2O_3 catalyst in comparison to the monometallic 10 wt%-Ni/Al_2O_3 catalyst with high coke and sulfur resistance. A possible formation of new bimetallic active phase of Ni with Re was reported to be the possible reason for high catalytic activity.

Similar to ATR of hydrocarbons like diesel, gasoline and JP-8 fuels, various catalyst supported on Al_2O_3 have been investigated for ATR of oxygenated hydrocarbons like methanol, ethanol. ATR reforming of methanol is relatively simpler and is carried out at lower temperatures. Sa et al., 2010[56] reviewed various catalyst used in SR of methanol (SRM). Authors reviewed the various Cu and group 8-10 metals. Several factors like high copper surface area, high dispersion and small particle sizes, were reported to affect the activity of the catalyst. Further methods of preparation along with addition to promoters and microstrain and structural disorder were also reported to affect the catalyst performance. The effects of operating conditions on ATR of methanol was reviewed by Wu and Lesmana [57]. Similarly Ghenciu [45] reviewed Al_2O_3 supported Cu catalyst for ATR of methanol. Author reported that most of the formulations reviewed were sensitive to oxidation.

ATR of methanol over $Cu\text{-}CeO_2/Al_2O_3$ was performed by Patel and Pant [58] in the temperature rage 200 to 300^{o}C using S/C of1.5 and varying O_2/C from 0 to 0.5. Authors reported that a catalyst having composition of 30/20/50 wt % Cu-Ce-Al exhibited the best performance at 280^{o}C with S/C of 1.5 and O_2/C of 0.15. The high activity of the catalyst was attributed to addition of CeO_2 to Cu/Al_2O_3 resulting in increase in dispersion and surface area of Cu. Further incorporation of CeO_2 enhanced coke gasification high thermal stability. Similarly authors also reported positive of adding CeO_2 to $Cu\text{-}ZnO/Al_2O_3$ catalyst under similar S/C and O_2/C conditions [59]. Addition of CeO_2 improved the copper dispersion by reducing the particle size of copper, and also facilitating catalyst reduction at lower temperature. Further the presence of CeO_2 inhibited coke formation as a result of oxygen vacancies, imparting high stability to the catalyst. Formation of CuO in $Cu\text{-}ZnO/Al_2O_3$ was reported as a reason for catalyst deactivation [60]. Likewise addition of Zr to $Cu\text{-}ZnO/Al_2O_3$ catalyst was reported by Velu et al., 2001[61]. Authors examined the performance of the catalyst in the temperature range of 180 to 290^{o}C using S/C of 1.3 with varying O_2/C of 0 to 0.4. Addition of Zr was reported to enhance copper reducibility, surface area and dispersion, which in turn influenced the activity of the catalyst. Similar effect of Zr addition to the catalyst was reported Chang et al., 2010 [62]. Authors examined ATR of methanol using S/C of 1.1 and O_2/C of 0.1 in the temperature range of 200 to 300^{o}C. The ratio of CuO/ZnO plays an important role in the promoting effect of ZrO_2. A CuO/ZnO ratio from 0.7 to 0.8 was sufficient to provide greater promoting effect of ZrO_2. The $CuO\text{-}Zn\text{-}ZrO_2/Al_2O_3$ (30/40/20/10) and $CuO\text{-}ZnO\text{-}ZrO_2/Al_2O_3$ (20/50/20/10) exhibited the best performance. The

higher loading of Cu i.e. 40 wt % inhibited the promotion effect of ZrO_2 and affected the activity of the catalyst

Smaller amount of Fe was reported to improve the stability of $Cu/ZnO/Al_2O_3$. Kawamura et al, 2008 [63] investigated ATR of methanol over Fe promoted catalyst, with varying Fe content from 0 to 2 wt% using S/C of 2 and O_2/C 0.14 at 300^{o}C over 6 wt % Cu-3 % -ZnO-Al_2O_3. Authors reported that addition of Fe in comparison to Ce and Zr, exhibited the best effect on the catalyst performance in terms of activity and durability. Addition of Fe resulted in formation of finer ZnO and Cu particles resulting in increase in activity of the catalyst. Further Fe helped in the prevention of reduction of Cu surface area and inhibited the sintering of Cu at high temperatures. The Fe content of 1 wt % was reported to optimum value, with further increase in Fe content resulted in decrease in activity as a result of less active $CuFe_2O_4$ spinel. Most of the evaluations mentioned above prepared the catalyst using co-precipitation method. In comparison Shishido et al., 2007 [64] compared the performance of CuO/ZnO and $CuO/ZnO/Al_2O_3$ catalysts in both co-precipitation (cp) and homogenous precipitation (hp) methods using S/C of 1.2 and O_2/C of 0.5 in the temperature range of 150 to 300^{o}C. Better performance of hp-catalysts was reported as a result of higher dispersion of Cu over the hp catalyst and the high accessibility of Cu to the reactants in comparison to cp catalysts.

Fierro et al., 2005 [65] examined ATR of ethanol over Ni/Al_2O_3 based catalyst with S/C of 1.6 and O_2/C 0f 0.68. The authors examined the effect of loading and doping of metals like Cu, Cr Fe, and Zn on the catalyst performance. A 20 wt % Ni/ Al_2O_3 catalyst was reported to exhibit higher activity in comparison to 11 wt % Ni/Al_2O_3 based catalyst. Addition of small amount of Cu (1%) was reported to improve the H_2 selectivity by promoting the SR of methane, produced during reforming reactions. Addition of Cu in more than 5 % deactivated the catalyst. Addition of Cr, Zn and Fe were reported to decrease H_2 production in comparison to Ni based catalyst at 700^{o}C. In comparison at higher temperature the addition of these metals were reported to have a positive effect on H_2 production (Ni–Zn > Ni–Fe > Ni–Cr >Ni > Ni–Cu).

In a different investigation compared to Fierro et al., 2005[65], Huang et al., 2009 [66] reported positive effect of Fe addition to Ni/Al_2O_3 catalyst in on ATR of ethanol. Authors prepared a 15 wt % Ni based catalyst doped with 5 to 15 wt % Fe_2O_3. The results suggested that iron free Ni catalyst promoted ethanol dehydration reaction to C_2H_4 instead of ethanol dehydration to C_2H_4O at low temperatures i.e. 500^{o}C. The improved activity of Fe promoted catalyst was attributed to the ability of the catalyst to restrict dehydration and promote dehydrogenation products which further undergo SR, PO, and WGS reaction, increasing H_2 selectivity. A 10 wt % Fe_2O_3 doping was reported to be the optimum iron loading. Further the synergistic effect of the $NiAl_2O_4$–$FeAl_2O_4$ mixed crystal formed in Ni-Fe/Al_2O_3 was reported to increase the resistance to both sintering and oxidation in the oxidative atmosphere of ATR, resulting in high durability under these conditions [67].

Youn et al., 2006 [68] examined the use of Ni/γ-Al_2O_3 catalysts containing a second metal (Ce, Co, Cu, Mg and Zn) in ATR of ethanol. Like Fierro et al., 2005 [65] authors

reported a positive effect of addition of Cu to Ni/Al_2O_3 based catalyst. A 20 wt % Ni/Al_2O_3 doped with 3 wt % metals were examined in the ATR of ethanol with S/C of 1 and O_2/C of 0.4 in the temperature range 427 to 827^oC. Addition Co along with Cu was shown to exhibit a positive effect on the conversion of ethanol. But the addition of Co was reported to increase dehydration reaction in comparison to Cu. The higher activity in terms of H_2 production of Cu based catalyst was reported as a result of Cu's ability to catalyze WGS reaction, decreasing CO content of the reformate gas and thereby increasing H_2 content. Addition of Zn was reported to have a negative effect on H_2 yield. Addition of Fe to Co/Al_2O_3 catalyst was shown to improve the suppression of C_2H_4 in ATR of ethanol with S/C of 1.5 and O_2/C of 0.25 in the temperature range of 400 to 600^oC, with complete inhibition at 600^oC. Like the $Ni\text{-}Fe/Al_2O_3$ investigated by Huang et al.,2009[66], addition of Fe to Co/Al_2O_3 was reported to inhibit dehydration reaction and promote dehydrogenation of ethanol and transformation of C_2H_4O increasing H_2 production. Authors reported that $Co\text{-}Fe/Al_2O_3$ catalyst had higher capacity of acetaldehyde transformation by inhibition of dehydration, hydrogenation of C_2H_4 in comparison to $Ni\text{-}Fe/Al_2O_3$ catalyst. But a slight drop in WGS activity was reported over the Co promoted catalyst at 600^oC.

Youn et al., 2007 [69] examined the use of addition of Mo to Al_2O_3 in ATR of ethanol. The Mo loading was varied from 0 to 9 wt % in ATR performed using S/C of 1 and O_2/C of 0.4 at 550^oC. All the bimetallic catalysts were reported to exhibit high activity except the 9 wt % doped Mo catalyst. The addition of Mo to the catalyst was reported to increase the active surface area and reducibility of the catalyst. Modification of electronic structure of Ni was reported to provide the ability to transfer electron from MoO_X to active Ni species resulting in improved the catalytic activity. The descending catalytic activity reported was Ni20Mo5 > Ni20Mo7 > Ni20Mo3 > Ni20 > Ni20Mo9.

Like Huang et al., 2009 [66] who reported a suppression of C_2H_4 by addition of Fe to Ni/Al_2O_3 catalyst in ATR of ethanol, complete inhibition of C_2H_4 was reported by the same authors (Huang et al.,2010 [70]) over a trimetallic $Ni\text{-}Fe\text{-}Zr/Al_2O_3$ catalyst with $NiO/ZrO_2/Fe_2O_3$ content of 15/8/8 wt% of the composite. Formation of a spinel $FeAl_2O_4$ in the catalyst was reported, resulting in more crystal defect sites which caused an increase in reducibility and activity of the catalyst. Furthermore, the acidity was significantly decreased via enveloping or damaging of the acid sites by the mixture spinel phase on the Al_2O_3 surface. This resulted in high H_2 selectivity and thermal stability over $Ni–Zr–Fe/Al_2O_3$ catalyst in ATR of ethanol.

Promotion effect of Ce and Zr on Ni/Al_2O_3 was investigated by Srisiriwat et al., 2009 [71] in ATR of ethanol with S/C of 1.5 and O_2/C of 0.13 in the temperature range of 550 to 700^oC. The unprompted catalyst exhibited lower H_2 selectivity in comparison to the promoted catalyst. A lower H_2 yield was reported over Ni/Al_2O_3 catalyst. Lower Ni dispersion on unsupported catalyst in comparison to the supported catalyst resulted in inefficient reforming of the intermediates formed in the process. Further oxidation of H_2 with O_2 to form H_2O was another reason for lower H_2 yield on unsupported catalyst as compared to the promoted ones. Authors reported that addition of Ce and Zr to Al_2O_3 resulted in the formation of a solid solution with Ce/Zr =1 resulting in oxidation of the carbon-containing

species adsorbed on the catalyst surface, such as acetate species from ethanol decomposition, or CO and CH_4 on the oxide surface. The remarkable oxygen storage capacity of NiCeZrAl was reported to provide both high reforming activity and efficient oxidation of carbon-containing species, such as CH_4 and C_2H_4 to affect the production of H_2 and CO_2 via the oxidation of CO. The O_2 intermediates formed during the reaction were reported to effectively affect the oxygen storage capacity (OSC) of the promoters, especially CeO_2–ZrO_2, by replenishing the O_2 vacancies in the CeO_2-containing support, and in turn helping to reduce coke formation.

Similarly La_2O_3, Ce_2O_3, and ZrO_2 doped Al_2O_3 catalyst was patented by Inui et al., 2010 [72]. Ni, Pt, Rh and Re were used as the active metals for reforming. The composition of the catalyst was 0.5 to 15% Ni, 0.5 to 10% Ce_2O_3, 0.5 to 5% La_2O_3, 0.1 to 2% Pt, 0.5 to 3% ZrO_2, 0.1 to 2% Rh, and 0.1 to 2% Re. The catalyst was capable of complete oxidation of the fuel by consuming all the O_2 supplied, and generating a high heat of combustion. The catalyst was active in endothermic SR, consuming the heat generated by the exothermic oxidation reaction over the catalyst surface leading to ultra-rapid ATR reforming process. The catalyst was reported to be active for reforming liquid hydrocarbons ranging from isooctane and diesel with very long active life. It was operable between 750° C and 1000° C, with pressures from about 0 to 50 psig, S/C ratios from 0 to 3.5, and O_2/C from 0.35 to 0.6. The authors reported that addition of very small amount of platinum group metal(s) can enhance the activity in ATR by providing H_2-spillover onto the catalyst surface. Further the H_2 spillover was beneficial in preventing carbon deposition retarding catalyst deactivation. The use of multi component formulation catalyst was reported to avoid sulfur poisoning.

While Ni free catalyst using similar oxides and noble metals was patented by Shi and Chintawar [73]. The catalyst was supported on Al_2O_3 doped Ce, La, and Zr with wt ratio of Ce: La: Zr: Al of about 2:1:2:6 prepared by sequential impregnation. When ZrO_2, CeO_2 and/or La_2O_3 are used, the ZrO_2 may comprise 0 to 67% of the total loading of promoters, while CeO_2 comprised from 15 to 67% and La_2O_3 from 8 to 25%. Three noble metals i.e. Pt, Pd, and Rh in the wt ratio of 2:6:1 respectively, were used as source of active metals. Authors reported that Pt exhibited higher activity for oxidation of saturated hydrocarbons and good poison tolerance. Further Pd was reported to be active for the oxidation of both olefins and aromatic hydrocarbons, along with good CO oxidation activity. Finally Rh was used because of its high SR activity along with excellent activity in catalyzing the reaction of NH_3 with NO_x to form N_2, which may help in preventing the formation of NH_3. Like Pd, Rh also exhibited good CO oxidation activity. In addition, Pt, Pd and Rh together were found to display a Pt-Pd-Rh synergism useful in fuel reforming. The catalyst was tested for ATR of gasoline with 35 ppm with S/C of 2.3 and O_2/C of 3.7 in the temperature range of 700 to 820^{o}C. It was active for hundreds of hours without the presence of sulfur. Slight loss in activity was reported when the gasoline contained sulfur. Table 2 summarizes the performance of various Al_2O_3 supported catalyst in ATR of various hydrocarbons.

Table 2: Performance of Al_2O_3 supported catalyst for ATR reforming of hydrocarbons and oxygenated hydrocarbons.

	Table 2											
		Conditions				Definition				Reported values		
References	Fuel	Catalyst	S/C	O_2/C	Temp (^oC)	Yield Y (%)	Selectivity S (%)	Molar comp M_p (%)	Y (%)	Conversion (%)	Selectivity S (%)	Molar comp Mp (%)
Chekatamarla and Lane [54]	Synthetic diesel	Pt (0.26)–Pd (0.95)/Al_2O_3 Pd (0.22)–Pt (0.90)/Al_2O_3	3	0.5	450	20	NA	17	>75 ~79-80	NA	NA	NA
Fierro et al., 2005 [65]	Ethanol	20 wt%- Ni/Al_2O_3	1.6	0.68	650-800	-	12	NA	NA	>90@800	~90@800	NA
Ferrandon et al.,2006 [47]	Gasoline with 34 ppm S	2 wt. %-Rh/La–Al_2O_3	1.5-3	0.45	700-800	21	NA	17	1900[a]	NA	NA	60.56
Galvan et al., 2008 [52]	Model diesel prepared from surrogates doped with 50 S	0.8 wt%- Pt/ CeO_2–Al_2O_3 0.7 wt% -Pt/ La_2O_3–Al_2O_3 0.8 wt%- Pt/ CeO_2–La_2O_3-Al_2O	3	0.2-0.5	800	NA	NA	17	NA	70[b] 90[b] 70[b]	NA	>26[b] ~29[b] >25[b]

Huang et al., 2008 [67]	Ethanol	15 wt %-Ni/Al_2O_3 15 wt %-Ni-10 wt %-Fe/Al_2O_3	3	2-3	600	23	14	NA	41.80[c] 111.54[c]	31.32[c] ~100[c]	85.10[d] 115[d]	NA
Huang et al., 2010 [70]	Ethanol	15 wt %Ni/Al_2O_3 15 wt %-Ni–8 %-Zr/Al_2O_3, 15 wt %-Ni–8 %-Fe/Al_2O_3 15 wt %-Ni–8 %-Fe-8%-Zr/Al_2O_3	3	0.5	600	24	15	NA	NA	100[e] 100[f] 99[g] 100[h]	75.82[i] ~86[j] >86.22[k] 85.79[l]	NA
Kawamura et al.,2008 [63]		6 wt %-Cu/(3)ZnO/Al_2O	2	0.14	300	NA	NA		NA	>90	NA	NA
Navarro et al., 2006 [51]	Hexadecane	7 wt% -Pt/ (8.8) CeO_2–Al_2O_3 8.2 wt% Ni/ (8.1) CeO_2–Al_2O_3	3	0.5		NA	NA	17	NA	~100 ~100	NA	~40[m] ~85

Patel and Pant, 2007[58]	Methanol	30 wt %-Cu/(20)CeO_2/Al_2O_3	1.5	0-0.5	280	NA	NA	NA	NA	99.5	179[n]	NA
Patel and Pant, 2007[59]	Methanol	30wt%-Cu/(30)ZnO/Al_2O_3 30wt%-Cu/(20)ZnO/Al_2O_3	1.5	0.15	260	NA	NA	NA	NA	60 77	132[n] 180[n]	NA
Qi et al., 2005 [74]	n-Octane	3 wt. % -Ru/3 wt%-K_2O-2.5 wt% CeO_2/γ-Al_2O_3	1.2-3	0.3-0.45	450-850	NA		17	NA	NA	NA	~40[o]
Srisiriw -at et al., 2009 [71]	Ethanol	15wt%Ni/Al_2O_3, 15wt%Ni/8wt%CeO_2/Al_2O_3, 15wt%Ni/8wt%ZrO_2/Al_2O_3 15wt%Ni/4wt%CeO_2-4wt%ZrO2/Al_2O_3,	1.5	0.13	700		NA	17	NA	100	NA	62.19 64.84 63.87 63.44
Velu et al.,2001[61]		36 wt.%-45-Zn-14.3 Zr/Al_2O_3	1.3		230	NA	NA	NA	NA	>65	>155[n]	
Wang et al., 2006 [55]	Gasoline with 3.8 ppm S	10 wt% Ni /Al_2O_3 10 wt% Ni−2%-Re/Al_2O_3	1.7	0.8	547-747	NA	NA	17	NA	~98[p] ~100	NA	**>60** **~60**

Xue et al., 2009 [49]	Gasoline with 158 ppm S	1.2 wt. %-Pt/15wt.%-Gd_2O_3-1.6 wt.% CeO_2–Al_2O_3	2-5	0.15-0.35	700-800	NA	NA	17	NA	75[q]	NA	56.9
Youn et al., 2006 [68]	Ethanol	20 wt %-Ni/Al_2O_3 20 wt%-Ni-3wt %Cu/Al_2O_3 20 wt%-Ni-3wt %Co/Al_2O_3 20 wt%-Ni-3wt %Zn/Al_2O_3 20 wt%-Ni-3wt %Ce/Al_2O_3 20 wt%-Ni-3wt % Mg/Al_2O_3	1	0.4	550	NA	NA	17	NA	100 100 100 100 100 100	NA	~45[r] ~55[r] >45[r] 40[r] >40[r] ~25[r]
Youn et al., 2007 [69]	Ethanol	20 wt %-Ni/Al_2O_3 20 wt%-Ni-3wt %Mo/Al_2O_3 20 wt%-Ni-5wt %Mo/Al_2O_3 20 wt%-Ni-7 wt % Mo/Al_2O_3 20 wt%-Ni-9 wt % Mo/Al_2O_3	1	0.4	550	NA	NA	17		100 100 100 100 100	NA	50[s] ~55[t] >55[u] ~ 60[v] 5[w]

a- H_2 selectivity in ATR of ethanol with S/C of 3 and O_2/C of 0.5 which decreases to 26.07% after 30 h
b- H_2 yield at S/C of 1.5 with O_2/C of 0.45 at 700^{o}C for 75 h.
c- H_2 yield in ATR of ethanol with S/C of 3 and O_2/C of 2 at 600^{o}C.
d- H_2 selectivity in ATR of ethanol with S/C of 3 and O_2/C of 0.5 for 30 h.
e- Ethanol conversion in ATR of ethanol with S/C of 3 and O_2/C of 0.5 remains constant for 30 h
f- Ethanol conversion in ATR of ethanol with S/C of 3 and O_2/C of 0.5 decreases to 85 % in 30 h
g- Ethanol conversion in ATR of ethanol with S/C of 3 and O_2/C of 0.5 remains constant for 30 h
h- Ethanol conversion in ATR of ethanol with S/C of 3 and O_2/C of 0.5 remains constant for 30 h
i- H_2 selectivity in ATR of ethanol with S/C of 3 and O_2/C of 0.5 which decreases to 26.07% after 30 h
j- H_2 selectivity in ATR of ethanol with S/C of 3 and O_2/C of 0.5 which decreases to 82.13 after 30 h
k- H_2 selectivity in ATR of ethanol with S/C of 3 and O_2/C of 0.5 remains constant at 86.22% for 30 h
l- H_2 selectivity in ATR of ethanol with S/C of 3 and O_2/C of 0.5 remains constant 30 h
m- H_2 molar composition in ATR of gasoline with 34 ppm sulfur using S/C of 2 and O_2/C at 700^{o}C.
n- Rate of H_2 production in mmol/s kg cat.
o- H_2 molar composition in ATR of n-octane with S/C of 2 and O_2/C of 0.38 at 800^{o}C stable for more than 60 h.
p- Gasoline conversion in ATR stable for 30 h.
q- Stable for 1000 h.
r- The dry composition was measured on dry basis.
s- Dry H_2 molar composition was stable for first 100 min and decreased to 15 % after 600 min in ATR of ethanol with S/C of 1 and O_2/C of 0.4.
t- Dry H_2 composition was stable for 500 min and decreased slightly after 500 min.
u- Dry H_2 molar composition stable for 600 min.
v- Dry H_2 molar composition slightly decreases after first 200 min and is fairly stable for the last 400 min.
w- Dry H_2 molar composition decreases with time and ends at ~1 % at 600 min.

2.4.2 Oxides:

Oxides like CeO_2, ZrO_2 of Ce-ZrO_2 have been widely investigated in H_2 production via SR, ATR and PO processes. ZrO_2 is a hard, thermally stable material with monoclinic phase stable up to working up to 1200 ^oC and tetragonal phase stable from 1200 up to 1900^oC [75]. ZrO_2 is inert in comparison to other support materials like Al_2O_3 or SiO_2. ZrO_2 is used to prevent sintering of metals like Ni in presence of steam under reforming conditions [76]. Further ZrO_2 has high resistance for coke formation and preventing by products and promoting CO oxidation reactions [77]. ATR reforming of hydrocarbons like diesel, gasoline, ethanol have been investigated by various authors (Kaila et al., 2006[78], 2008[79], Mawdsley and Krause.,2006 [47], Youn et al.,2010 [80].

Kaila et al., 2006 [78] examined the use of ZrO_2 supported noble metals in ATR of simulated gasoline and diesel fuels. Authors examined the performance of 0.5 wt % Pt; Rh supported on ZrO_2 and compared them with Ni/Al_2O_3 catalyst. ATR of mixture containing n-dodecane, methylcyclohexane, n-heptane, and toluene with S/C of 3 and O_2/C of 0.34 was examined in the temperature range 400 to 900^oC. Authors reported that the Rh supported catalyst was active under SR conditions, while it exhibited lower activity under PO conditions in comparison to Pt. Further, the Pt catalyst showed higher carbon deposition in comparison to Rh ones. But both the metals were more stable as compared to Ni based catalyst. Deactivation under simulated gasoline fuel was higher as compared to simulated diesel. The Rh and Ni catalyst were prone to deactivation whereas Pt based catalyst maintained it stability.

Same authors (Kaila et al., 2008[79]) also examined the use of Rh, Pt supported on ZrO_2 support as an ATR catalyst for simulated and commercial diesel. The simulated diesel mixture was doped with 10 ppm 4, 6-DMDBT a heterocyclic sulfur compound. Authors reported stable activity over the bimetallic catalyst $PtRh/ZrO_2$ (Rh/Pt =2), with very little effect of the heterocyclic sulfur on the activity of the catalyst. But addition of H_2S as a sulfur source affected both monometallic and bimetallic catalyst. Carbon deposition was reported to increase with Pt loading while sulfur deposition was strongest on the Rh catalyst. The carbon deposition was reported to decrease in the presence of sulfur, either due to the blockage of active sites, thereby preventing the deposition, or to enhancement of the coke removal reactions. The bimetallic catalyst was reported to have higher WGS activity.

Mawdsley and Krause, 2006 [81] examined the use of 2 wt% Rh /Y-ZrO_2 in ATR of gasoline and gasoline surrogates with S/C of 1.5 and O/C of 0.45 in the temperature range of 700 to 800^oC. High activity of the catalyst was reported to be based mainly on the dispersion of Rh, and not on the nature of the support. Hydrothermal treatment of the catalyst was performed by exposing it to a flowing gas mixture of 33% H_2, 17% steam and, 50% He at 900 C for 24 h was shown to increase PO activity of the catalyst in comparison to SR.

Similarly Gutierrez et al., 2011[82] examined the use of ZrO_2 supported monometallic Pt, Ph, and bimetallic Pt Rh catalyst in ATR of ethanol with 0.5 wt % metal loading using S/C of 2 and O_2/C of 0.2 along with temperatures between 300 to 900^oC. Similar to ATR of hydrocarbons Rh supported catalyst exhibited higher activity compared to Pt based ones.

Further the addition of Pt to Rh in bimetallic catalyst improved the stability of the catalyst. Further formation of coke was higher over Pt based catalyst in comparison to bimetallic and monometallic Rh ones.

Similarly to Mawdsley and Krause, 2006 [81] addition of Y_2O_3 to ZrO_2 was shown to exhibit high catalyst activity in ATR of ethanol. ATR of ethanol over Zr, Y, La, Ca, and Mg doped 20 wt% Ni/ZrO_2 was examined by Youn et al.,2010 [76]. The ATR experiments were performed using S/C of 1.5 and O_2/C of 0.25. Introduction of lower valent cation (Y^{3+}, La^{3+}, Ca^{2+}, and Mg^{2+}) into mesoporous ZrO_2 was reported to improve the textural stability of mesoporous ZrO_2, leading to high surface area and large pore volume. Further metal oxide stabilizer (M) enhanced the structural stability of metastable ZrO_2 via formation of cubic fluorite structural solid solution, resulting in an enhancement in oxygen vacancy concentration. It was reported that the enhancement of oxygen vacancy of support was closely related to the reducibility of NiO species in the Ni/M–ZrO_2 catalysts resulting in high catalytic activity. The addition of metal oxide also improved the resistance to carbon formation during the process.

Although ZrO_2 supported catalyst have shown high activity in ATR of various hydrocarbons and oxygenated hydrocarbons, it is susceptible to coke formation during the ATR process [79]. It has low surface area and mechanical strength at high temperatures [80]. In comparison CeO_2 based materials have received a lot of attention in a wide range of applications. CeO_2 plays an important role in two of the most important commercial catalytic processes: three-way catalysis (TWC) and fluid catalytic cracking (FCC) [83]. Other applications include diesel soot oxidation [84], oxidation of volatile organic wastes [85] and fuel cell technology [86, 87]. In all these applications the unique features responsible for making CeO_2 a promising material for use either as a support or as an active catalyst are stated below.

1. CeO_2 based materials ($Ce^{3+/}Ce^{4+}$) redox couple, with its ability to shift between CeO_2 and Ce_2O_3 under oxidizing and reducing conditions, respectively.
2. The ease of formation of labile oxygen vacancies (OSC).
3. Promoting noble-metal activity and dispersion.

Chekatamarla and Lane [54] examined the use of Pt, Pd, Ni, bimetallic catalyst for the ATR of diesel at S/C ratio = 3, O_2/C ratio = 0.5 at 400^{o}C over CeO_2 supported catalysts. The authors reported that incorporation of Ni or Pd in Pt/CeO_2 increased the sulfur tolerance and improved catalytic activity in comparison to mono metallic catalyst due to a strong metal-metal and metal–support interaction in the catalyst. The improved performance of the bimetallic catalysts was reported due to structural and electronic effects rather than the degree of metal dispersion. Apart from the above investigations most of the investigation of ATR of hydrocarbons and oxygenated hydrocarbons was conducted over CeO_2 and modified CeO_2 supported catalyst.

ATR of methanol Cu/CeO_2 was investigated by Perez Hernandez et al.,2007 [88] using O_2/C of 0.83 and S/C of 0.15 in the temperature range 200 to 260^{o}C. Loading of Cu was varied from 2 to 10 wt %. A highly dispersed Cu species was reported as the reason for the high activity of the catalyst. A 2 wt% Cu loading exhibited the best performance in the 210 to 230^{o}C, while 6 wt % loading was effective over 230^{o}C. Catalyst with higher loading

i.e. 10 wt % exhibited lower activity due to Cu crystallite sintering. At higher temperature over 230^{o}C oxidation of Cu during the reaction was reported as the reason for H_2 depletion. Similar effect of Au loading on the activity of Au/CeO_2 was reported by Pojanavaraphan et al., 2012 [89]. Authors examined ATR of methanol using S/C of 2 and O_2/C of 1.25 in the temperature range of 200 to 450^{o}C with varying Au loading from 1 to 5 wt %. At lower loading the Au crystallites were well dispersed and the sizes were smaller exhibiting higher catalytic activity. Increasing metal loading was reported to decrease the metal support interaction and increasing the ease of reduction of Au particles, thus imparting high catalytic activity over 5 wt % Au/CeO_2 at 300^{o}C. Ni supported catalyst were also reported to exhibit high catalytic activity for ATR of methanol at similar temperature i.e. 250^{o}C [90].

Cai et al., 2008 [91] reported very high catalytic activity of Rh/CeO_2 catalyst in ATR of ethanol with S/C of 0.9 and O_2/C of 0.3 in the temperature range of 700 to 900^{o}C. Authors reported that Rh oxide clusters diffused into the CeO_2 fluorite structure, acting as privileged pathway for oxygen diffusion and storage. Further, CeO_2 prevented the sintering of smaller Rh particles resulting into high catalytic activity. The CeO_2 particles within the size range of 7 to 20 nm provided sufficient Rh–CeO_2 interfacial perimeter, i.e. facilitated the activation of water and/or oxygen for a continuous removal of carbonaceous compounds on Rh particles leading to cleaner Rh surface. Cai et al., 2007[92] also examined the use of Ir/CeO_2 in ATR of ethanol under same S/C, O_2/C, and temperature conditions. Similar effects of inhibition of sintering of metal through the strong interaction between Ir and CeO_2 and high resistance to coke deposition due to the higher oxygen storage-release capacity of CeO_2 were observed.

One of the major limitations of CeO_2 is deactivation due to sintering rate at high temperatures [93, 94]. It also has very low surface area. When exposed to high temperatures i.e. at 800^{o}C, the specific surface area of CeO_2 decreases drastically which in turn shrinks, it's crucial redox properties and oxygen storage/release capacity [95]. The OSC of pure CeO_2 is unsatisfactory for some practical uses. CeO_2 crystallizes in the fluorite structure in which each cerium ion is coordinated to eight O_2 neighbors', making CeO_2 more stable and reduction of Ce (IV) to Ce (III) unfavorable. Metal decoration has been observed for metal catalysts supported on reducible oxides [96]. Degradation of catalytic activity is caused by decreases in metal surface area in supported metal catalysts [97].

Improvement of the thermal properties of CeO_2 and retention of active surface area at high temperature are thus necessary to exploit the redox property of CeO_2 for various applications. One of the best approaches to tackle this problem is by substituting another metal/metal oxide into the CeO_2 lattice thereby facilitating the formation of composite oxides. CeO_2 easily forms solid solutions with other rare earth elements and with elements belonging to the transition-metal series. Replacement of cerium ions by cations of different size and/or charge modifies ionic mobility inside the lattice resulting in the formation of a defective fluorite structured solid solution. Such modifications in the structure of CeO_2 confer new properties to the catalysts, such as better resistance to sintering and high catalytic activity [83, 95, 98].

The addition of Zr positively affects the sintering ability of the catalyst. Further addition of ZrO_2 to CeO_2 improved the coke removal ability of CeO_2 [99]. Presence of ZrO_2 increases the O_2 mobility in the CeO_2 lattice and increases the process of vacancy formation,

making the material more reducible [100-102] and reduction is no longer confined to the surface but extends deep into the bulk [103, 104]. The composition of the binary oxide impacts the OSC. It is observed that the percentage of reducible Ce^{4+} and the thermal stability increased with Zr/Ce ratio.

Co-precipitated Ce–ZrO_2 supported catalyst have been reported to exhibit high oxygen storage capacity of CeO_2 in Ce–ZrO_2 solid solution, strong interaction between Ni and Ce–ZrO_2, basic property, and high capability for H_2 uptake [105-107]. The ability of the catalyst to provide mobile O_2 species from the support to Ni plays an important role in preventing carbon deposition. The activity of the catalyst was reported as a result of higher surface area along with smaller nano-crystallite sizes of both $Ce_{0.8}Zr_{0.2}O_2$ support and NiO. Further authors suggest that these advantages results in the better dispersion of Ni, higher Ni surface area and enhanced O_2 transfer. The catalyst also showed higher thermal resistance. The high surface area was maintained due to agglomeration of primary particles during digestion and strengthening of network structure giving a porous matrix, capable of withstanding thermal treatment at high temperatures.

Karatzas et al., 2011 [108] examined ATR of diesel over RhPt supported on CeO_2–ZrO_2, Al_2O_3, SiO_2, and TiO_2 based catalyst with S/C of 2.5 and O_2/C of 0.49. Complete conversion of diesel with 40% H_2 content in the reformate gas with lowest ethylene content was reported. The higher activity on RhPt/CeO_2–ZrO_2 was ascribed to the higher reducibility of Rh_iOx species as well as to the superior Rh and Pt dispersion. Further, the presence of CeO_2 was beneficial in promoting WGS activity and reduced coke deposits compared to the Al_2O_3 supported catalyst.

Unlike the above authors ATR of model diesel components i.e. dodecane and tetralin was examined by Gould et al., 2007 [109] using Ni based catalyst, supported on $Ce_{0.75}Zr_{0.25}O_2$ using S/C of 2 and O_2/C of 0.6 and 1.2. The catalyst exhibited high conversion for ATR of all the three components. Performance of the catalyst in terms of carbon deposition in ATR of isooctane was examined by the same research group[Chen et al.,2007[110]). The experiments were performed with increasing the temperature of the catalyst bed to 300^{o}C with S/C of 1.8 and O_2/C of 0.5, followed by increasing the temperature at the rate of 2^{o}C/min to 650^{o}C at the same S/C and O_2/C ratios for 175 min. In the final stage of experiment, O_2/C was reduced to 0.8 with same S/C and temperature. Filamentous and coating type of carbon species were reported to form on the catalyst. The authors reported that 1 wt % Ni loading showed formation of only coating type carbon. While increasing the Ni loading to 2 wt % showed the presence of both the types of carbon species. Finally 15 wt % Ni catalyst showed the formation of graphite carbon on the catalyst. The rate of coating type carbon formation was reported to be low and independent of Ni loading and particle size, while the formation of filamentous carbon formation increased with Ni particle size. The onset of filamentous carbon growth would require a certain minimum number of Ni particles per unit support area. The group also examined the effect of Ni particle size on the sulfur tolerance of CeO_2-ZrO_2 catalyst (Mayne et al., 2011[111]). Highly dispersed small Ni particles (<5 nm) exhibited unfavorable reaction characteristics, suggested by increased olefin production. The authors reported that on smaller Ni particles the adsorption and reaction of larger diameter isooctane was difficult, resulting in lower reforming activity. Further, the authors reported those smaller Ni particles can be easily

oxidized to NiO having lower reforming activity. Catalysts having larger Ni particles were prone to deactivation by addition of the sulfur containing thiophene. A significant increase in the catalyst temperature was reported by small amount of thiophene in ATR of isooctane by Mayne et al., 2010 [112]. The addition of sulfur was reported to block Ni sites responsible for endothermic SR, while the exothermic PO sites were not affected. According to the authors the reactivity of thiophene depends strongly on the reaction conditions. Based on the feed conditions thiophene completely converted to H_2S or a combination of both H_2S and unreacted thiophene was observed. A complete conversion of thiophene to H_2S resulted in small decrease in activity followed by a stable reforming performance thereafter. But the latter case of combination presence of both H_2S and thiophene results in continuous decline in reforming activity.

Biswas and Kunzru, 2007 [113] examined the use of 30 wt % $Ni/Ce_{0.74}Zr_{0.26}O_2$ catalyst in ATR of ethanol with S/C of 4 and O_2/C of 0.25 in the temperature range of 400 to 650^{o}C. Measurable coke formation over the catalyst with stable operation for 15 h of operation was reported. Filamentous and agglomerated carbon formations were reported on the catalyst surface. ATR of complex oxygenated hydrocarbons like palm oil free fatty acids (PEAFD) over 5 wt % $Ni/Ce_{0.75}Zr_{0.25}O_2$ with S/C of 3 and O_2/C of 0.8 at 900^{o}C was examined by Shotipruk at al.,2009 [114]. Addition of O_2 during ATR was favorable for reducing the degree of carbon deposition on the catalyst surface. Along with SR, PO of fatty acids to H_2 and CO takes place. This resulted in reducing the rate of fatty acid decomposition resulting in lower formation of C_2H_6, C_2H_4, and C_3H_6 consequently lowering the degree of carbon deposition on the catalyst. Further under ATR conditions, oxidation of carbon forming hydrocarbons species to other form of carbon containing species is promoted. Table 3 provides a summary of performance of various mix oxide supported catalyst in ATR of various fuels.

Table 3: Performance of mix oxide supported catalyst for ATR reforming of hydrocarbons and oxygenated hydrocarbons.

		Conditions				Definition				Reported values		
References	Fuel	Catalyst	S/C	O_2/C	Temp (^oC)	Yield Y (%)	Selectivity S (%)	Molar comp M_p (%)	Conversion (%)	Y (%)	S (%)	Mp (%)
Biswas and Kunzru, 2007[113]	Ethanol	30wt.%-Ni/$Ce_{0.74}Zr_{0.26}O_2$	4	0.75	400-650	19	11	NA	›90[a] ~100	4.23@600 4.34@650	›85 ~ 85	NA
Cai et al., 2007[92]	Ethanol	2 wt. %-Ir–CeO_2	1.4	0.3	427-627	NA	NA	17	100	NA	NA	~41@427[a] ~50 @627[a]
Cai et al., 2008 [91]	Ethanol	1 wt. %-Rh–CeO_2	0.9	0.3	427-627	NA	NA	17	100	NA	NA	A 51@550 A 70@650
Chekatamarla and Lane [54]	Diesel	Pt/CeO_2 Pd/CeO_2 $Pd\text{-}Pt/CeO_2$ $Pt\text{-}Pd/CeO_2$	3	0.5	400[b]	20	NA	NA	NA	>65 >70 ~75 ~80 ~72	NA	NA

		Pt-Ni/CeO_2 Ni-Pt/CeO_2									~78		
Kaila and Krause, 2006 [78]	Simulated gasoline	0.5 wt % Rh/ZrO_2 0.5 wt % Pt/ZrO_2	3	0.34	750-900	NA	17	NA	95[c] 52.3[c]	95.5[d] 59.6[d]	95.9[e] 28.7[e]	7.2 55.1	NA
Kaila et al., 2008 [108]	Simulated gasoline	0.5-RhPt/ZrO_2[g] 1- RhPt/ZrO_2[g] 2-RhPt/ZrO_2[g]	3	0.34	750-900	NA	17	1.4	98 97 99		NA	NA	61 62 63
Karatzas et al., 2011[108]	Low sulfur diesel	RhPt/CeO_2–ZrO_2[h]	2.5	0.49	650	NA	17	15	97.6		NA	NA	40
Gould et al., 2007[109]	Dodecane Tetralin 50/50	10 wt%-Ni/$Ce_{0.75}Zr_{0.25}O_2$	2	0.6	\ 500-	22	NA	NA	NA		~1[i] ~1[i] ~1[i]	~1 ~1 ~1	NA

	mixture				1100							
Gutierrez et al., 2011 [82]	Ethanol	0.5wt%-Rh/ZrO_2 0.5 wt %-Pt/ZrO_2 0.5-RhPt/ZrO_2[g]	2	0.2	500-900	19	NA	17	100 >60 100	>3.5 >3.0 1		
Perez Hernandez et al.,2007 [88]	Methanol	2 wt%-Cu/CeO_2	0.15	0.83	>275	NA	NA	17	>275	>90	~70	NA
Pojanavaraphan et al., 2012 [89]	Methanol	5 wt%-Au/CeO_2	2	1.25	400	NA	NA	17	NA	>90		>50
Mayne et al., 2011[111]	isooctane	0.7 wt%-Ni/$Ce_{0.75}Zr_{0.25}O_2$ 3 wt%-Ni/$Ce_{0.75}Zr_{0.25}O_2$ 5 wt%-Ni/$Ce_{0.75}Zr_{0.25}O_2$ 10 wt%-Ni/$Ce_{0.75}Zr_{0.25}O_2$	3	0.75	500	27	NA	NA	64 76 81 87	>1.2 >1.2 ~1.1 >0.8	NA	NA

a- Ethanol conversion was ~98% above 427^{o}C.
b- The reactor was operated under adiabatic conditions with inlet temperature of 400^{o}C.
c- Conversion of n-heptane under ATR conditions at 700^{o}C.
d- Conversion of methyl cyclohexane under ATR conditions at 700^{o}C.
e- Conversion of toluene under ATR conditions at 700^{o}C.
f- ,6-dimethyldibenzothiophene

g- Molar ratio of Pt/Rh
h- Weight ratio of Rh/Pt of 1
i- The conversion refers to conversion of the fuel to CH_4 and CO_X

2.4.3 Perovskites:

Recently perovskites have received attention as fuel processing catalysts. Perovskite are complex oxides having general formula ABO_3 where A is usually a rare earth cation (La, Gd, Pr, Nd, or Er) and B is a transition metal cation (Cr, Mn, Fe, Ni, Al, or Co). A-site replacement affects mainly the amount of sorbed oxygen, whereas B-site replacement influences the nature of the sorbed oxygen [115]. They have exhibited effective catalytic applications for combustion [116], natural gas PO [117], SR [118] and electrochemical reactions for SOFCs [119-122]. They have also shown great promise for ATR of hydrocarbons due to their well-known thermal stability in a broad range of temperature as well as high oxygen storage capacity (OSC) and oxygen ion conductivity [74].

Mawdsley and Krause,2008 [123] examined the use of first row transition metal rare earth perovskites as catalysts for the ATR of hydrocarbon fuels. Five different type of oxides $LaCrO_3$, $LaMnO_3$, $LaFeO_3$, $LaCoO_3$, and $LaNiO_3$ were examined in the ATR of isooctane with S/C of 1.1 and O_2/C of 0.4 with screening temperature of 700^{o}C. Oxides like $LaCrO_3$, $LaFeO_3$, and $LaMnO_3$ were reported to be structurally stable but were significantly less active than $LaNiO_3$ and $LaCoO_3$. The structural stability of Ni based perovskites was improved by partial substitution of Cr, Al, Fe Ga, and Mn without significantly decreasing H_2 yield. Cr was reported to be the best element for B site substitution in terms of maintaining H_2 yield and having some degree of sulfur tolerance. Further the A site of substitution of Cr stabilized Ni Perovskites while La increased the coke tolerance. Sulfur tolerance of this perovskite was examined for 144 h by doping the fuel with 5 ppm sulfur source with 33 % decrease in H_2 yield. The decrease in activity was reported as a result of formation of carbon fibers rather than sulfur poisoning.

Effect of substitution of $LaNiO_3$ with Ce to form a monolithic $La_{0.8}Ce_{0.2}NiO_3$, for utilization in ATR of gasoline or its model compounds was investigated by Qi et al., 2005[74]. The catalytic performance was examined with S/C of 2 and O_2/C of 0.38 between 600 and 800^{o}C. The catalysts were prepared in two forms: as a pellet and on a cordierite substrate exhibiting similar activities. The monolithic based catalyst was compared with 0.3 wt % Rh/CeO_2-ZrO_2/cordierite, with monolith based catalyst exhibiting better performance. To increase the mechanical strength of monolithic catalyst, oxide binders such as Al_2O_3 or ZrO_2 had to be added. Addition of Al_2O_3 was reported to have a positive impact on the mechanical strength of the monolithic catalyst. As the interaction of Al_2O_3 with the active phase was not strong enough to form other complex oxides resulted in higher mechanical strength of the catalyst. But it was strong enough to help prevent the catalyst pealing. Long term performance of the pellet catalyst exhibited high thermal stability and H_2 yield without CH_4 slipping, and fairly good sulfur tolerance (5 ppm) for 220 h. The good performances of $La_{0.8}Ce_{0.2}NiO_3$, better thermal stability, coke and sulfur resistance in comparison to $LaNiO_3$ was ascribed to the increased oxygen mobility as a result of redox ability of CeO_2.

Villioria et al., 2011[124] examined the use of $LaCoO_3$ perovskite synthesized by co-precipitation (COP), sol–gel (PEC) and combustion (SCS) methods in ATR of diesel. The perovskite prepared by the SCS method was reported to achieve a higher development of the

porous network as well as higher homogeneity in bulk and surface in comparison to COP and PEC. Formation of some secondary phases such as Co_3O_4 and La $(OH)_3$ were observed in PEC and COP methods of preparation. The catalytic activity was examined at S/C of 3 with O_2/C of 0.5 at 800^{o}C. The short time activity of the samples was reported as PEC > SCS > COP. While for long term stability test for 15 to 24 h revealed the order of activity as SCS > PEC > COP. The lower catalytic activity of COP was reported as a result of presence of La_2O_3 while the higher activity of the other two catalysts was as a result of presence of the La_2CoO_4 phase. The precipitation of Co surface concentration was the major reason for catalyst deactivation. The stability of the catalyst in terms of carbonaceous deposits was COP > SCS > PEC. The decrease in carbonaceous species was associated with the increase in $La_2O_2CO_3$ phase concentration in the perovskites. Further, the catalyst surface area increased with the presence of the $La_2O_2CO_3$ phase, lowering coke production: improving the catalyst stability.

To increase the stability of the $LaCoO_3$ addition of Ru to the perovskite was investigated by Navarro et al., 2007 [125] and Mota et al., 2011-12[126-128]. A partially substituted $LaCoO_3$ with Ru to $LaCo_{1-x}Ru_xO_3$ by varying Ru content from 0.2 to 0.4 wt % was examined in ATR of diesel using the same conditions as above. The perovskite with higher degree of Co substitution (x = 0.4) showed the higher activity and stability. It was reported that a higher proportion of perovskite phase in $Ru/LaCoO_3$ that is produced during the partial decomposition reaction, greater metallic Co and La_2O_3 surface proportion is produced favoring the increase in catalyst stability. Further, the greater exposition of Ru in this catalyst was reported to be responsible for the increase in stability of the catalyst. This resulted in lower tendency to form carbonaceous deposits on the Ru particles. The better catalytic activity of the Ru-containing sample could be also related to the participation of bulk oxygen during the reaction, favoring adsorption of the reactants. The participation of La through an enhanced adsorption of CO_2 by formation of lanthanum carbonates, which participate in coke gasification, was also one of the reasons for improved stability of the catalyst.

Ru-doped lanthanum chromite and aluminite were examined as catalyst for ATR reforming of dodecane by Liu et al., 2006 [129]. The catalytic performance was examined using S/C of 0 to 3 and O_2/C of 0.25 and 0.55. Both the catalyst exhibited high catalytic activity and sulfur tolerance. The recovery of the catalyst was high after switching the sulfur containing fuel with sulfur free fuel.

A different kind of La based perovskite was examined by Kondakindi et al., 2010 [130] in ATR of dodecane a diesel model component with S/C of 3 and O_2/C of 0.3 in the temperature range of 650 to 900^{o}C. The modification of the perovskite at the A-site with Ce and at the B-site with Co and Pd was examined. Among the catalyst investigated, $La_{0.95}Ce_{0.05}Fe_{0.77}Co_{0.17}Pd_{0.06}O_3$ exhibited the highest activity. Although the catalyst exhibited high activity, carbon depositions were observed on spent samples of the $LaFe_{0.77}Co_{0.17}Pd_{0.06}O_3$ and $La_{0.95}Ce_{0.05}Fe_{0.77}Co_{0.17}Pd_{0.06}O_3$ catalysts in comparison to the

$LaFe_{0.8}Co_{0.2}O_3$ catalyst. They also reported lower catalytic activity and higher carbon deposition over $Pd/LaFe_{0.8}Co_{0.2}O_3$ in comparison to the perovskites.

In contrast to Kondakindi et al., 2010 [130], Erri et al., 2006 [131] examined A site substitution of $LaFeO_3$ perovskites with Ce and B site substitution with Ni in ATR of JP-8 fuel. The activity of the catalyst was examined using H_2O/C of 3.0 and O_2/C of 0.364 between 500 and 775^oC. Phase segregation of the catalyst with Ce exhibiting limited solubility, and Ni separation was observed during the reduction of the catalyst, but these changes did not affect the catalyst's activity and stability. The extent of Ni substitution was reported to have no effect on the conversion of fuel, but the Ni rich catalyst exhibited high carbon resistance. The addition of Ce, however, greatly enhanced coking resistance due to improved ion conductivity within the crystal structure, promoting the oxidation of deposited carbon.

Like ATR of diesel and JP-8, $LaFeO_3$ and $LaNiO_3$ along with $LaCoO_3$ and $LaMnO_3$, was examined in ATR of ethanol by Chen et al. 2010 [132] using S/C of 2 and O_2/C of 0.98 in the temperature range of 500 to 700^oC. $LaNiO_3$ was reported to be highly active for H_2 production. The performance of the perovskite catalyst was compared to impregnated Ni/La_2O_3. The analysis of the catalyst showed that Ni is well dispersed over $La_2O_2CO_3$ support in the perovskite catalyst, improving H_2 selectivity and the activity of catalyst for the reactions involving C–C bond cleavage. Further, the catalyst favored the dehydrogenation and decomposition of ethanol/acetaldehydes. The impregnated catalyst exhibited lower catalytic activity and lower coke resistance in comparison to the perovskites. ATR of ethanol over Ni doped $LaNiO_3$ was examined by Huang et al., 2012 [133]. The doping of Ni retained the perovskite structure in the form of solid solution La (Ni, Fe) O_3, with formation of metal Ni and formation of Ni-Fe alloy after the reduction. The Ni metal was active in the conversion of ethanol, acetaldehyde, and methane while the Ni-Fe improved the WGS activity, increasing the catalytic activity of the perovskite.

Table 4 provides a summary of performance of various perovskite based catalyst in ATR of various fuels.

Table 4: Performance of perovskite based catalyst for ATR reforming of hydrocarbons and oxygenated hydrocarbons.

	Table 4											
		Conditions				Definition				Reported values		
References	Fuel	Catalyst	S/C	O_2/C	Temp (^oC)	Yield Y (%)	Selectivity S (%)	Molar comp M_p (%)	Conversion (%)	Y (%)	Selectivity S (%)	Molar comp Mp (%)
Chen et al. 2010 [132]	Ethanol	$LaNiO_3$reduced $LaNiO_3$unreduced $LaCoO_3$ $LaFeO_3$ $LaMnO_3$	1	0.25 -1	500-700	NA	16	NA	60 ~100 ~100 ~100 ~100	NA	~80[1] ~50[2] ~58[3] ~50[2] 30[2]	
Erri et al., 2006 [131]	JP-8	$LaFe_{0.8}Ni_{0.2}O_3$ $LaFe_{0.6}Ni_{0.4}O_3$ $LaFe_{0.4}Ni_{0.6}O_3$ $La_{0.6}Ce_{0.4}Fe_{0.8}Ni_{0.2}O_3$ $La_{0.6}Ce_{0.4}Fe_{0.6}Ni_{0.4}O_3$ $La_{0.6}Ce_{0.4}Fe_{0.4}Ni_{0.6}O_3$	3	0.36	500-775	NA	NA	17	98.5 97 95.2 91.8 91 94.5	NA	NA	39.4 39.1 40.5 38.9 42.8 42.3

Huang et al.,2012 [133]	Ethanol	$LaNiO_3$ $LaNi_{0.95}Fe_{0.05}O_3$ $LaNi_{0.90}Fe_{0.10}O_3$ $LaNi_{0.80}Fe_{0.20}O_3$	1.5	0.25	600	22	prov	NA	100^4 100^4 100^4 75.5^4	2.6^4 3^5 3.3^4 1.3^6	NA	NA
Kondakindi et al., 2010 [130]	Dodecane	$LaFeO_3$ $LaFe_{0.8}Co_{0.2}O_3$ $LaFe_{0.77}Co_{0.17}Pd_{0.06}O_3$ $La_{0.95}Ce_{0.05}Fe_{0.77}Co_{0.17}Pd_{0.06}O_3$ 2.6 wt%-Pd/$LaFe_{0.8}Co_{0.2}O_3$	3	0.3	650-900	25	NA	NA	$>95^7$ $>80^7$ $>80^7$ $\sim95^7$ $\sim91^7$	$>15^7$ $>5^7$ $\sim11^7$ $>15^7$ $>10^7$	NA	NA
Mawdsley and Krause, 2006[123]	Isooctane	$LaNiO_3$ $LaMn_{0.9}Ni_{0.1}O_3$ $LaFe_{0.9}Ni_{0.1}O_3$ $LaGa_{0.9}N_{i0.1}O_3$ $LaAl_{0.9}Ni_{0.1}O_3$ $LaCr_{0.9}Ni_{0.1}O_3$ $PrCr_{0.9}Ni_{0.1}$ O3	1.1	0.5	700	26	NA	NA	100 82.9 ±0.6 90.5 ±0.9 89.8±0.1 87.8 ±1.3 87.8± 1.3 87.6 ± 1.9	14.5± 0.3 10.1± 0.1 11.6± 0.1 11.5 ±0.1 10.9 ±0.1 13.3± 0.1 11.3 ± 0.2	NA	NA

		$NdCr_{0.9}Ni_{0.1}O_3$ $GdCr_{0.9}Ni_{0.1}O_3$ $ErCr_{0.9}Ni_{0.1}O_3$							87.6 ±1.9 99.0 ±0.2 97.7± 0.4	11.3 ± 0.2 11.3 ±0.1 13.9 ±0.1		
Mota et al., 2011-12[126, 127]	Diesel	LaCo $LaCoRu_{0.01}$ $LaCoRu_{0.5}$ $LaCoRu_{0.1}$ $LaCoRu_{0.2}$ $LaCoRu_{0.4}$	3	0.5		NA	18	NA	~95 ~90 ~98 ~100 ~92 100	NA	~70[8] ~68[9] ~60[10] ~63[11] ~60[12] 50[13]	-
Navarro et al.,2007[125]	Diesel	$LaCoO_3$ Ru/La_2O_3 $Ru/LaCoO_3$ Ru/Co_3O_4	3	0.5	850	27	NA	-	100 100 100 100	~1.5 >1.3 ~1.4 ~1.1		NA
Villioria et al., 2008[134]	Diesel	$ZrO_2/LaCoO_3$-A[16] $ZrO_2/LaCoO_3$-A[16] $ZrO_2/LaCoO_3$-N[17] $ZrO_2/LaCoO_3$-N[17]	3	0.5	600 800 600 800	28	NA	17	100[k] 100[k] 100[k] 100[k]	>65[14] 65[14] ~62.5[15] ~65[15]	NA	30[14] >30[14] ~28[15] ~29[15]
Villioria et al., 2011[124]	Diesel	$LaCoO_3$-COP $LaCoO_3$-Sol gel $LaCoO_3$-SCS	3	0.5	800	28	NA	NA	Not provided	30[18] ~42[18] 40[18]	0.95[18] 0.45[18] 0.53[18]	NA

1. The selectivity reported was achieved at O_2/C of 0.5.
2. The selectivity was reported at O_2/C of 0.25.
3. The selectivity was reported at O_2/C of 0.55
4. The conversions and yields reported were stable for 300 h.

5. Conversion increased to 92% at 9 h.
6. Conversion remains constant but yield decreases to 2.6 at end of 300 h.
7. H_2 yield increased to 2.4 at 9 h.
8. The selectivity reported at 750^{o}C.
9. The selectivity decreased to 40 % after 24 h.
10. The selectivity decreased to 50 % after 24 h.
11. The selectivity decreased to ~45% after 24 h.
12. The selectivity decreased to 50 % after 24 h.
13. H_2 yield was stable for 24 h.
14. For the first 1.5 h yield was high as 80% further decreasing to 50 %.
15. The conversion was stable for the first 24 h and decreased by 5 % after 24 h.
16. The catalyst was prepared using acetate salts and the yield was recorded in first 5 h of 80h evaluation.
17. The catalyst was prepared using nitrate salts and the yield was recorded in first 5 h of 80h evaluation.
18. The yield and selectivity are reported for the first 5 h of operation.

3. Conclusion:

As concern of green house gas mitigation and providing energy security for the growing population grows, development renewable energy sources like H_2 energy have become greatly important. This review investigates the recent developments in the field of autothermal H_2 production (i.e. ATR) for propulsion and distributed power generation. ATR is one of the promising processes for H_2 production because of its high thermal efficiency and low energy requirement. In spite of the advantages of the process, few problems like heat management, reformer start up, and catalyst improvements have to be addressed.

From the patent survey undertaken various designs have been patented to improve the short comings and the problems associated with traditional ATR reformers. Designs to improve the heat management and the efficiency of the reformer have been patented. Designs incorporating the modifications of the oxidant source are successfully invented. Uses of various kinds of catalyst structures for heat mitigation have shown promise for commercial scale applications. For the application of ATR reformers for propulsion and distributed power generation the reformer start up is a key issue to be resolved. Various innovative methods for reformer start up are also patented.

From the comprehensive catalyst survey performed, it can be seen that noble like Rh and Ru are the promising active metals for ATR catalyst. Non noble metals like Ni have also shown to be another promising metal for use in ATR catalyst. In order to reduce the cost of noble metal based ATR catalyst, a combination of Ni and elements like Co, Mo exhibiting high activity, coke, and sulfur tolerance are reported.

Catalyst supports like Al_2O_3 which has shown to be a promising SR catalyst, but has to be modified for application as ATR catalyst. Doping of Al_2O_3 with CeO_2, La_2O_3, and ZrO_2 have shown to improve the stability of catalyst support. Further the uses of other supports like ZrO_2, Ce-ZrO_2 are also investigated. In addition to these supported catalyst the use of perovskites as catalyst has been investigated. The use of Ni, La and Fe based Perovskites are patented and researched for reforming of fuels like gasoline, diesel and ethanol.

4. Future perspective:

ATR has shown promise for fuelling fuel cells. H_2 production from fossil fuels like gasoline or diesel could be an answer to the immediate problem of H_2 supply for fuel cells utilization. But for long term applicability the use of renewable fuels like ethanol, butanol, biodiesel, biodiesel by-product glycerol and bio-oils show potential. Use of ethanol as a renewable fuel has been developed in countries like Brazil and USA making use of resources like sugar cane, corn, and lignocellulosic sources offering more sustainability in the future. However the problems like energy density, tolerance for contamination, and high vapour pressure are one of the few concerns affecting the effective utilization of ethanol.

To mitigate these problems associated with use of ethanol, butanol has been developed as an alternative fuel. Butanol has high energy content i.e. 31.2 higher than 24.7 MJ/kg for ethanol, but closer to gasoline (35.3 MJ/kg). It exhibits higher tolerance to water contaminants due to lower hygroscopic nature of the fuel; further lower vapour pressure makes distribution in the existing systems easier. Further research in production of butanol has been undertaken to develop butanol manufacturing process. Efforts in genetically engineered strain, butanol recovery processes for the production of butanol have been widely explored to avoid competition with food sources [135, 136]. Use of biodiesel has received attention due to the advantages of lower viscosity, no engine modifications, low sulfur (<0.001%), natural lubricant properties compared to petrodiesel resulting in less engine wear. Further biodiesel has high H_2 content and it can be utilized as a H_2 carrier. However since biodiesel is prepared by transesterification of triglycerides (TG). The major concern with the use of biodiesel as H_2 carrier would be the supply of TG. Development of microalgae for the supply of TG for biodiesel production has been investigated. These microalgae's can supply renewable TG, with biodiesel yield potential of 50–100 times greater than biodiesel from soybeans [137]. Microalgae can utilize waste CO_2 from fossil-fueled power plants and other high carbon emitting facilities and help in mitigating green house gases.

The current biodiesel production process produces by-product i.e. glycerol. Glycerol has H_2 carrier has also been investigated. The future availability of glycerol is uncertain. As new glycerol free process of manufacturing next generation biodiesel are been developed and implemented [138-141]. Likewise uses of fuels like bio-oils derived from pyrolysis of biomass have received importance as a result of diversity of feedstock including agricultural and industrial wastes along with simplicity of fast pyrolysis process for production. But the stability of these bio-oils is greatly affected by various factors like storage, Ph, chemical reactions and water content. Bio-oils has water content of 15 to 35 wt % [142] which would result in energy consumption during vaporization of the bio oils for vapour phase ATR. The presences of organic compounds like acetic acid affect the performance of the reforming of catalyst as result of coke formations. Further these oils are susceptible to chemical reactions like condensation and polymerization reactions of phenol and sugar molecules during storage increasing viscosity of the bio oils. The formation of these complex compounds may result in the formation of coke during ATR of the bio oils. The supply of the complex bio oil is undetermined based on devolvement of processes of manufacturing of bio-oils and the other problems associated with storage and usage. Use of fuel like biodiesel or next generation biodiesel, butanol can be effective future H_2 carriers based on availability. But still there is long way to go in terms ATR catalyst development, design and construction of effective ATR reformers.

Recently implementation of micro reactor technology for H_2 production has been evaluated and commercial reformers have been designed and commercialized [143-145]. Micro reactors would be one of the key factors in success full implementation of fuel cells as they are miniature devices with high throughout compared to conventional reactors, exhibit high heat and mass transfer rates, operation in mass and heat transfer-limited regimes. Large numbers of these micro reactors can be stacked to obtain the desired output with smaller space and weight.

5. Acknowledgement:

The authors wish to acknowledge the Research Councils UK for continuing funding in sustainable H_2 production (GR/R50677, EP/D078199/1, EP/F027389/1, EP/G01244X/1), and Dr Martyn V. Twigg and Johnson Matthey plc for expert advice and catalyst materials and financial support over the years.

References:

[1] Asif M, Muneer T, Energy supply, its demand and security issues for developed and emerging economies. Renew and Sust Energy Rev 2007; 11: 1388-413.

[2] Muneer T, Asif M, Kubie J, Generation and transmission prospects for solar electricity: UK and global markets. Energy Convers Manage 2003; 44: 35-52.

[3] Veziroglu TN, Hydrogen movement and the next action: Fossil fuels industry and sustainability economics. Int Journal of Hydrogen 1997; 22: 551-6.

[4] Hurtak JJ, Energy technologies for the 21st century: Substitutes for fossil fuel. Fuel and Energy Abstracts 1996; 37: 202.

[5] Kapur IC, Role of renewable energy for the 21st Century. Renewable Energy. Renewable Energy Energy Efficiency, Policy and the Environment 1999; 16: 1245-50.

[6] Midilli A, Dincer I, Ay M, Green energy strategies for sustainable development. Energ Policy 2006; 34: 3623-33.

[7] Martin S, Wörner A, On-board reforming of biodiesel and bioethanol for high temperature PEM fuel cells: Comparison of autothermal reforming and steam reforming. J Power Sources 2011; 196: 3163-71.

[8] Jurado F, Valverde M, Cano A, Effect of a SOFC plant on distribution system stability. J Power Sources 2004; 129: 170-9.

[9] Rostrup-Nielsen J.Steam reforming of hydrocarbons. A historical perspective. 2004:121-6.

[10] J.R R-N, Production of synthesis gas. Catal Today 1993; 18: 305-24.

[11] Pen˜a MA, Gómez JP, Fierro JLG, New catalytic routes for syngas and hydrogen production. Appl Catal A Gen 1996; 144: 7-57.

[12] Cheekatamarla PK, Lane AM, Catalytic autothermal reforming of diesel fuel for hydrogen generation in fuel cells: I. Activity tests and sulfur poisoning. J Power Sources 2005; 152: 256-63.

[13] Kang I, Bae J, Autothermal reforming study of diesel for fuel cell application. J Power Sources 2006; 159: 1283-90.

[14] Freni S, Calogero G, Cavallaro S, Hydrogen production from methane through catalytic partial oxidation reactions. J Power Sources 2000; 87: 28-38.

[15] Docter A, Lamm A, Gasoline fuel cell systems. J Power Sources 1999; 84: 194-200.

[16] Ahmed S, Krumpelt M, Hydrogen from hydrocarbon fuels for fuel cells. Int Journal of Hydrogen 2001; 26: 291-301.

[17] Krumpelt M, Krause TR, Carter JD, Kopasz JP, Ahmed S, Fuel processing for fuel cell systems in transportation and portable power applications. Catal Today 2002; 77: 3-16.

[18] Liu D-J, Kaun TD, Liao HKH-K, Ahmed S, Characterization of kilowatt-scale autothermal reformer for production of hydrogen from heavy hydrocarbons. Int Journal of Hydrogen 2004; 29: 1035-46.

[19] Aasberg-Petersen K, Christensen TS, Stub Nielsen C, Dybkjær I, Recent developments in autothermal reforming and pre-reforming for synthesis gas production in GTL applications. Fuel Process Technol 2003; 83: 253-61.

[20] Roychoudhury S, Castaldi M, Lyubovsky M, LaPierre R, Ahmed S, Microlith catalytic reactors for reforming iso-octane-based fuels into hydrogen. J Power Sources 2005; 152: 75-86.

[21] Liu D-J, Kaun TD, Liao H-K, Ahmed S, Characterization of kilowatt-scale autothermal reformer for production of hydrogen from heavy hydrocarbons. Int Journal of Hydrogen 2004; 29: 1035-46.

[22] Lee SHD, Applegate DV, Ahmed S, Calderone SG, Harvey TL, Hydrogen from natural gas: part I—autothermal reforming in an integrated fuel processor. Int Journal of Hydrogen 2005; 30: 829-42.

[23] Ahmed S, Papadias DD, Lee SHD, Ahluwalia RK. AUTOTHERMAL AND PARTIAL OXIDATION REFORMER-BASED FUEL PROCESSOR, METHOD FOR IMPROVING CATALYST FUNCTION IN AUTOTHERMAL AND PARTIAL OXIDATION REFORMER-BASED PROCESSORS. United States patent 20100095590, 2010.

[24] Bae JM, Ahmed S, Kumar R, Doss E, Microchennel development for autothermal reforming of hydrocarbon fuels. J Power Sources 2005; 139: 91-5.

[25] Robb GM. Staged air autothermal reformer for improved startup and operation. United States patent 7172638, 2007.

[26] Kaeding S, Guenther, N. Reformer and method for reacting fuel and oxidant to reformate. United States patent 20070084118, 2007.

[27] Yamazaki Y, Maruko S, Komori S. Oxidative autothermal reformer and oxidative autothermal reforming method using the same. United States patent 7981372, 2011.

[28] Docter A, Vogel B, Oliver S. Reactor for autothermal reforming of hydrocarbons. United States patent 7481856, 2009.

[29] Lesieur RR. Compact light weight autothermal reformer assembly. United States patent 6969411, 2005.

[30] Lesieur RR, Szydlowski DF, Barber TJ, Chiappetta LM, Peschke WO. Autothermal fuel gas reformer assemblage. United States patent 20020088179, 2002.

[31] Papavassiliou V, Shah MM, Bergman J, John T. Autothermal reactor and method for production of synthesis gas. United States patent 7255840, 2007.

[32] Peters R, Tschauder A, Pasel J, Stolten D. Autothermic Reformer. United States patent 20090136798, 2009.

[33] Retallick WB, Whittenberger WA. Regenerative autothermal catalytic steam reformer. United States patent 7179313, 2007.

[34] Filippi E. Process for obtaining a heating fluid as indirect heat source for carrying out reforming reactions. United States patent 7465324 2008.

[35] Pettit WH, Voecks G, Borup RL. Combined autothermal/steam reforming fuel processor mechanization. United States patent 7270901, 2007.

[36] Malhotra ASL, TX, US), Gosnell, James Hanlan (Houston, TX, US). Autothermal reformer-reforming exchanger arrangement for hydrogen production. United States patent 7550215, 2009.

[37] Kumar RV, Kastanas GN. Fuel processor apparatus and method based on autothermal cyclic reforming. United States patent 6878362, 2005.

[38] Kumar RV, Lyon RK, Cole JA.Unmixed Reforming: A Novel Autothermal Cyclic Steam Reforming Process Advances in Hydrogen Energy 2002:pp31-45.

[39] Ahmed S, Lee SHD, Carter JD, Krumpelt M, Myers DJ. Fuel processor and method for generating hydrogen for fuel cells. United States patent 7563292, 2009.

[40] Yukihiro S, Mizuno Y. Method for Starting Autothermal Reformer. United States patent 20090223861, 2009.

[41] Arcuri K, Schimelpfenig, Kurt Leahy J, Morgan M. Autothermal reformer reactor processes patent 7351751, 2008.

[42] Wheat SW, Mirkovic VR, Nguyen KH, K, Curtis L. , Stevens JF, Casey DG. Autothermal reforming in a fuel processor patent 7081144, 2006.

[43] Pettit WH, Sennoun MEH, Voecks GE. Multi-port autothermal reformer. United States patent 7261749, 2007.

[44] Shi Y, Zhao JL. Fast startup in autothermal reformers. United States patent 20050245620, 2005.

[45] Faur Ghenciu A, Review of fuel processing catalysts for hydrogen production in PEM fuel cell systems. Curr Opin Solid State Mater Sci 2002; 6: 389-99.

[46] Cimino S, Lisi L, Russo G, Torbati R, Effect of partial substitution of Rh catalysts with Pt or Pd during the partial oxidation of methane in the presence of sulphur. Catal Today 2010; 154: 283-92.

[47] Ferrandon M, Mawdsley J, Krause T, Effect of temperature, steam-to-carbon ratio, and alkali metal additives on improving the sulfur tolerance of a Rh/La–Al_2O_3 catalyst reforming gasoline for fuel cell applications. Appl Catal A Gen 2008; 342: 69-77.

[48] Shamsi A, Baltrus JP, Spivey JJ, Characterization of coke deposited on Pt/alumina catalyst during reforming of liquid hydrocarbons. Appl Catal A Gen 2005; 293: 145-52.

[49] Xue Q, Gao L, Lu Y, Sulfur-tolerant Pt/Gd_2O_3–CeO_2–Al_2O_3 catalyst for high efficiency H2 production from autothermal reforming of retail gasoline. Catal Today 2009; 146: 103-9.

[50] Alvarez-Galvan MC, Navarro RM, Rosa F, Briceño Y, Ridao MA, Fierro JLG, Hydrogen production for fuel cell by oxidative reforming of diesel surrogate: Influence of ceria and/or lanthana over the activity of Pt/Al2O3 catalysts. Fuel 2008; 87: 2502-11.

[51] Navarro RM, Álvarez-Galván MC, Rosa F, Fierro JLG, Hydrogen production by oxidative reforming of hexadecane over Ni and Pt catalysts supported on Ce/La-doped Al_2O_3. Appl Catal A Gen 2006; 297: 60-72.

[52] Alvarez-Galvan MC, Navarro RM, Rosa F, Briceño Y, Gordillo Alvarez F, Fierro JLG, Performance of La,Ce-modified alumina-supported Pt and Ni catalysts for the oxidative reforming of diesel hydrocarbons. Int Journal of Hydrogen 2008; 33: 652-63.

[53] Qi A, Wang S, Fu G, Wu D, Autothermal reforming of n-octane on Ru-based catalysts. Appl Catal A Gen 2005; 293: 71-82.

[54] Cheekatamarla PK, Lane AM, Efficient bimetallic catalysts for hydrogen generation from diesel fuel. Int Journal of Hydrogen 2005; 30: 1277-85.

[55] Wang L, Murata K, Matsumura Y, Inaba M, Lower-Temperature Catalytic Performance of Bimetallic Ni−Re/Al2O3 Catalyst for Gasoline Reforming to Produce Hydrogen with the Inhibition of Methane Formation. Energy Fuels 2006; 20: 1377-81.

[56] Sá S, Silva H, Brandão L, Sousa JM, Mendes A, Catalysts for methanol steam reforming—A review. Appl Catal B 2010; 99: 43-57.

[57] H.S. Wu aDL, Short Review: Cu Catalyst for Autothermal Reforming Methanol for Hydrogen Production. Bulletin of Chemical Reaction Engineering & Catalysis 2012; 7: 27-42.

[58] Patel S, Pant KK, Hydrogen production by oxidative steam reforming of methanol using ceria promoted copper–alumina catalysts. Fuel Process Technol 2007; 88: 825-32.

[59] Patel S, Pant KK, Selective production of hydrogen via oxidative steam reforming of methanol using Cu–Zn–Ce–Al oxide catalysts. Chem Eng Sci 2007; 62: 5436-43.

[60] Murcia-Mascarós S, Navarro RM, Gómez-Sainero L, Costantino U, Nocchetti M, Fierro JLG, Oxidative Methanol Reforming Reactions on CuZnAl Catalysts Derived from Hydrotalcite-like Precursors. J Catal 2001; 198: 338-47.

[61] Velu S, Suzuki K, Kapoor MP, Ohashi F, Osaki T, Selective production of hydrogen for fuel cells via oxidative steam reforming of methanol over CuZnAl(Zr)-oxide catalysts. Appl Catal A Gen 2001; 213: 47-63.

[62] Chang C-C, Chang C-T, Chiang S-J, Liaw B-J, Chen Y-Z, Oxidative steam reforming of methanol over CuO/ZnO/CeO_2/ZrO_2/Al_2O_3 catalysts. Int Journal of Hydrogen 2010; 35: 7675-83.

[63] Kawamura Y, Ishida T, Tezuka W, Igarashi A, Hydrogen production by oxidative methanol reforming with various oxidants over Cu-based catalysts. Chem Eng Sci 2008; 63: 5042-7.

[64] Shishido T, Yamamoto Y, Morioka H, Takehira K, Production of hydrogen from methanol over Cu/ZnO and Cu/ZnO/Al2O3 catalysts prepared by homogeneous precipitation: Steam reforming and oxidative steam reforming. J Mol Catal A Chem 2007; 268: 185-94.

[65] Fierro V, Akdim O, Provendier H, Mirodatos C, Ethanol oxidative steam reforming over Ni-based catalysts. J Power Sources 2005; 145: 659-66.

[66] Huang L, Xie J, Chu W, Chen R, Chu D, Hsu AT, Iron-promoted nickel-based catalysts for hydrogen generation via auto-thermal reforming of ethanol. Catal Commun 2009; 10: 502-8.

[67] Huang L, Xie J, Chen R, Chu D, Chu W, Hsu AT, Effect of iron on durability of nickel-based catalysts in auto-thermal reforming of ethanol for hydrogen production. Int Journal of Hydrogen 2008; 33: 7448-56.

[68] Youn MH, Seo JG, Kim P, Kim JJ, Lee H-I, Song IK, Hydrogen production by auto-thermal reforming of ethanol over Ni/γ-Al2O3 catalysts: Effect of second metal addition. J Power Sources 2006; 162: 1270-4.

[69] Youn MH, Seo JG, Kim P, Song IK, Role and effect of molybdenum on the performance of Ni-Mo/γ-Al2O3 catalysts in the hydrogen production by auto-thermal reforming of ethanol. J Mol Catal A Chem 2007; 261: 276-81.

[70] Huang L, Xie J, Chen R, Chu D, Hsu AT, Nanorod alumina-supported Ni–Zr–Fe/Al_2O_3 catalysts for hydrogen production in auto-thermal reforming of ethanol. Mater Res Bull 2010; 45: 92-6.

[71] Srisiriwat N, Therdthianwong S, Therdthianwong A, Oxidative steam reforming of ethanol over Ni/Al2O3 catalysts promoted by CeO_2, ZrO_2 and CeO_2–ZrO_2. Int Journal of Hydrogen 2009; 34: 2224-34.

[72] Inui T, Dabbousi BO, Ahmed S, Al-muhaish FI, Siddiqui MAB. Oil- based thermo-neutral reforming with a multi-component catalyst United States patent 20100216633, 2010.

[73] Shi Y, Chintawar P. A catalyst and methods of production and use are provided. The catalyst may be used to reform fuels to hydrogen for use in fuel cells. The fuels may include sulfur. United States patent 20060013760, 2006.

[74] Qi A, Wang S, Fu G, Ni C, Wu D, La–Ce–Ni–O monolithic perovskite catalysts potential for gasoline autothermal reforming system. Appl Catal A Gen 2005; 281: 233-46.

[75] Teterycz H, Klimkiewicz R, Łaniecki M, The role of Lewis acidic centers in stabilized zirconium dioxide. Appl Catal A Gen 2003; 249: 313-26.

[76] Youn MH, Seo JG, Song IK, Hydrogen production by auto-thermal reforming of ethanol over nickel catalyst supported on metal oxide-stabilized zirconia. Int Journal of Hydrogen 2010; 35: 3490-8.

[77] Chary KVR, Ramesh K, Naresh D, Rao PVR, Rao AR, Rao VV, The effect of zirconia polymorphs on the structure and catalytic properties of V_2O_5/ZrO_2 catalysts. Catal Today 2009; 141: 187-94.

[78] Kaila RK, Krause AOI, Autothermal reforming of simulated gasoline and diesel fuels. Int Journal of Hydrogen 2006; 31: 1934-41.

[79] Kaila RK, Gutiérrez A, Krause AOI, Autothermal reforming of simulated and commercial diesel: The performance of zirconia-supported RhPt catalyst in the presence of sulfur. Appl Catal B 2008; 84: 324-31.

[80] Youn MH, Seo JG, Cho KM, Park S, Park DR, Jung JC, et al., Hydrogen production by auto-thermal reforming of ethanol over nickel catalysts supported on Ce-modified mesoporous zirconia: Effect of Ce/Zr molar ratio. Int Journal of Hydrogen 2008; 33: 5052-9.

[81] Ferrandon M, Krause T, Role of the oxide support on the performance of Rh catalysts for the autothermal reforming of gasoline and gasoline surrogates to hydrogen. Appl Catal A Gen 2006; 311: 135-45.

[82] Gutierrez A, Karinen R, Airaksinen S, Kaila R, Krause AOI, Autothermal reforming of ethanol on noble metal catalysts. Int Journal of Hydrogen 2011; 36: 8967-77.

[83] Trovarelli A, de Leitenburg C, Boaro M, Dolcetti G, The utilization of ceria in industrial catalysis. Catal Today 1999; 50: 353-67.

[84] Lahaye J, Boehm S, Chambrion P, Ehrburger P, Influence of cerium oxide on the formation and oxidation of soot. Combust Flame 1996; 104: 199-207.

[85] Matatov-Meytal YI, Sheintuch M, Catalytic Abatement of Water Pollutants. Ind Eng Chem Res 1998; 37: 309-26.

[86] Murray EP, Tsai T, Barnett SA, A direct-methane fuel cell with a ceria-based anode. Nature 1999; 400: 649-51.

[87] Scott L. Swartz D, M. Seabaugh M, T. Holt C, J. Dawson W, Fuel processing catalysts based on nanoscale ceria. Fuel Cells Bull 2001; 4: 7-10.

[88] Pérez-Hernández R, Gutiérrez-Martínez A, Gutiérrez-Wing CE, Effect of Cu loading on for hydrogen production by oxidative steam reforming of methanol. Int Journal of Hydrogen 2007; 32: 2888-94.

[89] Pojanavaraphan C, Luengnaruemitchai A, Gulari E, Hydrogen production by oxidative steam reforming of methanol over Au/CeO2 catalysts. Chem Eng J 2012; 192: 105-13.

[90] Pérez-Hernández R, Gutiérrez-Martínez A, Palacios J, Vega-Hernández M, Rodríguez-Lugo V, Hydrogen production by oxidative steam reforming of methanol over $Ni/CeO_2–ZrO_2$ catalysts. Int Journal of Hydrogen 2011; 36: 6601-8.

[91] Cai W, Wang F, Van Veen AC, Provendier H, Mirodatos C, Shen W, Autothermal reforming of ethanol for hydrogen production over an Rh/CeO_2 catalyst. Catal Today 2008; 138: 152-6.

[92] Cai W, Zhang B, Li Y, Xu Y, Shen W, Hydrogen production by oxidative steam reforming of ethanol over an Ir/CeO_2 catalyst. Catal Commun 2007; 8: 1588-94.

[93] Laosiripojana N, Assabumrungrat S, Methane steam reforming over Ni/Ce-ZrO2 catalyst: Influences of Ce-ZrO2 support on reactivity, resistance toward carbon formation, and intrinsic reaction kinetics. Appl Catal A Gen 2005; 290: 200-11.

[94] Laosiripojana N, Chadwick D, Assabumrungrat S, Effect of high surface area CeO_2 and $Ce-ZrO_2$ supports over Ni catalyst on CH4 reforming with H_2O in the presence of O_2, H_2, and CO_2. Chem Eng J 2008; 138: 264-73.

[95] Aneggi E, Boaro M, Leitenburg Cd, Dolcetti G, Trovarelli A, Insights into the redox properties of ceria-based oxides and their implications in catalysis. J Alloys Compd 2006; 408-412: 1096-102.

[96] Bernal S, Calvino JJ, Cauqui MA, Gatica JM, Larese C, Pérez Omil JA, et al., Some recent results on metal/support interaction effects in NM/CeO2 (NM: noble metal) catalysts. Catal Today 1999; 50: 175-206.

[97] Nagai Y, Dohmae K, Ikeda Y, Takagi N, Hara N, Tanabe T, et al., In situ observation of platinum sintering on ceria-based oxide for autoexhaust catalysts using Turbo-XAS. Catal Today; In Press, Corrected Proof.

[98] Reddy BM, Khan A, Lakshmanan P, Aouine M, Loridant S, Volta J-C, Structural Characterization of Nanosized CeO_2−SiO_2, CeO_2−TiO_2, and CeO_2−ZrO_2 Catalysts by XRD, Raman, and HREM Techniques. J Phys Chem B 2005; 109: 3355-63.

[99] Aneggi E, de Leitenburg C, Dolcetti G, Trovarelli A, Promotional effect of rare earths and transition metals in the combustion of diesel soot over CeO_2 and CeO_2-ZrO_2. Catal Today 2006; 114: 40-7.

[100] Lemaux S, Bensaddik A, van der Eerden AMJ, Bitter JH, Koningsberger DC, Understanding of Enhanced Oxygen Storage Capacity in Ce0.5Zr0.5O2: The Presence of an Anharmonic Pair Distribution Function in the Zr−O_2 Subshell as Analyzed by XAFS Spectroscopy. J Phys Chem B 2001; 105: 4810-5.

[101] Fornasiero P, Fonda E, Di Monte R, Vlaic G, Kaspar J, Graziani M, Relationships between Structural/Textural Properties and Redox Behavior in $Ce_{0.6}Zr_{0.4}O_2$ Mixed Oxides. J Catal 1999; 187: 177-85.

[102] Vlaic G, Fornasiero P, Geremia S, Kaspar J, Graziani M, Relationship between the Zirconia-Promoted Reduction in the Rh-Loaded $Ce_{0.5}Zr_{0.5}O_2$Mixed Oxide and the Zr-O Local Structure. J Catal 1997; 168: 386-92.

[103] Fornasiero P, Balducci G, Di Monte R, Kaspar J, Sergo V, Gubitosa G, et al., Modification of the Redox Behaviour of CeO_2 Induced by Structural Doping with ZrO_2. J Catal 1996; 164: 173-83.

[104] Trovarelli A, Zamar F, Llorca J, Leitenburg Cd, Dolcetti G, Kiss JT, Nanophase Fluorite-Structured CeO_2-ZrO_2Catalysts Prepared by High-Energy Mechanical Milling. J Catal 1997; 169: 490-502.

[105] Dong W-S, Roh H-S, Jun K-W, Park S-E, Oh Y-S, Methane reforming over Ni/Ce-ZrO_2 catalysts: effect of nickel content. Appl Catal A Gen 2002; 226: 63-72.

[106] Roh H-S, Jun K-W, Dong W-S, Chang J-S, Park S-E, Joe Y-I, Highly active and stable Ni/Ce–ZrO_2 catalyst for H_2 production from methane. J Mol Catal A Chem 2002; 181: 137-42.

[107] Roh H-S, Potdar HS, Jun K-W, Kim J-W, Oh Y-S, Carbon dioxide reforming of methane over Ni incorporated into Ce–ZrO_2 catalysts. Appl Catal A Gen 2004; 276: 231-9.

[108] Karatzas X, Jansson K, González A, Dawody J, Pettersson LJ, Autothermal reforming of low-sulfur diesel over bimetallic RhPt supported on Al2O3, CeO_2–ZrO_2, SiO_2 and TiO_2. Appl Catal B 2011; 106: 476-87.

[109] Gould BD, Tadd AR, Schwank JW, Nickel-catalyzed autothermal reforming of jet fuel surrogates: n-Dodecane, tetralin, and their mixture. J Power Sources 2007; 164: 344-50.

[110] Chen X, Tadd AR, Schwank JW, Carbon deposited on Ni/CeZrO isooctane autothermal reforming catalysts. J Catal 2007; 251: 374-87.

[111] Mayne JM, Dahlberg KA, Westrich TA, Tadd AR, Schwank JW, Effect of metal particle size on sulfur tolerance of Ni catalysts during autothermal reforming of isooctane. Appl Catal A Gen 2011; 400: 203-14.

[112] Mayne JM, Tadd AR, Dahlberg KA, Schwank JW, Influence of thiophene on the isooctane reforming activity of Ni-based catalysts. J Catal 2010; 271: 140-52.

[113] Biswas P, Kunzru D, Oxidative steam reforming of ethanol over Ni/CeO_2-ZrO_2 catalyst. Chem Eng J 2008; 136: 41-9.

[114] Shotipruk A, Assabumrungrat S, Pavasant P, Laosiripojana N, Reactivity of and toward steam reforming of palm fatty acid distilled (PFAD) with co-fed oxygen and hydrogen. Chem Eng Sci 2009; 64: 459-66.

[115] Lim S-S, Lee H-J, Moon D-J, Kim J-H, Park N-C, Shin J-S, et al., Autothermal reforming of propane over Ce modified $Ni/LaAlO_3$ perovskite-type catalysts. Chem Eng J 2009; 152: 220-6.

[116] Zhai Y, Xiong J, Li C, Xu X, Luo G, Influence of preparation method on performance of a metal supported perovskite catalyst for combustion of methane. J Rare Earths 2010; 28: 54-8.

[117] Dai X, Yu C, Wu Q, Comparison of $LaFeO_3$, $La_{0.8}Sr_{0.2}FeO_3$, and $La_{0.8}Sr_{0.2}Fe_{0.9}Co_{0.1}O_3$ perovskite oxides as oxygen carrier for partial oxidation of methane. J Nat Gas Chem 2008; 17: 415-8.

[118] Zeppieri M, Villa PL, Verdone N, Scarsella M, De Filippis P, Kinetic of methane steam reforming reaction over nickel- and rhodium-based catalysts. Appl Catal A Gen 2010; 387: 147-54.

[119] Escudero MJ, Irvine JTS, Daza L, Development of anode material based on La-substituted SrTiO3 perovskites doped with manganese and/or gallium for SOFC. J Power Sources 2009; 192: 43-50.

[120] Sengodan S, Yeo HJ, Shin JY, Kim G, Assessment of perovskite-type La0.8Sr0.2ScxMn1−xO3–δ oxides as anodes for intermediate-temperature solid oxide fuel cells using hydrocarbon fuels. J Power Sources 2011; 196: 3083-8.

[121] Fu C, Sun K, Zhang N, Chen X, Zhou D, Electrochemical characteristics of LSCF–SDC composite cathode for intermediate temperature SOFC. Electrochim Acta 2007; 52: 4589-94.

[122] Liu Z, Cheng L-z, Han M-F, A-site deficient $Ba_{1-x}Co_{0.7}Fe_{0.2}Ni_{0.1}O_{3-\delta}$ cathode for intermediate temperature SOFC. J Power Sources 2011; 196: 868-71.

[123] Mawdsley JR, Krause TR, Rare earth-first-row transition metal perovskites as catalysts for the autothermal reforming of hydrocarbon fuels to generate hydrogen. Appl Catal A Gen 2008; 334: 311-20.

[124] Villoria JA, Alvarez-Galvan MC, Al-Zahrani SM, Palmisano P, Specchia S, Specchia V, et al., Oxidative reforming of diesel fuel over LaCoO3 perovskite derived catalysts: Influence of perovskite synthesis method on catalyst properties and performance. Appl Catal B 2011; 105: 276-88.

[125] Navarro RM, Alvarez-Galvan MC, Villoria JA, González-Jiménez ID, Rosa F, Fierro JLG, Effect of Ru on $LaCoO_3$ perovskite-derived catalyst properties tested in oxidative reforming of diesel. Appl Catal B 2007; 73: 247-58.

[126] Mota N, Álvarez-Galván MC, Al-Zahrani SM, Navarro RM, Fierro JLG, Diesel fuel reforming over catalysts derived from LaCo1−xRuxO3 perovskites with high Ru loading. Int Journal of Hydrogen 2012; 37: 7056-66.

[127] Mota N, Navarro RM, Alvarez-Galvan MC, Al-Zahrani SM, Fierro JLG, Hydrogen production by reforming of diesel fuel over catalysts derived from LaCo1−xRuxO3 perovskites: Effect of the partial substitution of Co by Ru (x = 0.01–0.1). J Power Sources 2011; 196: 9087-95.

[128] Mota N, Alvarez-Galván MC, Navarro RM, Al-Zahrani SM, Goguet A, Daly H, et al., Insights on the role of Ru substitution in the properties of $LaCoO_3$-based oxides as catalysts precursors for the oxidative reforming of diesel fuel. Appl Catal B 2012; 113–114: 271-80.

[129] Liu D-J, Krumpelt M, Chien H-T, Sheen S-H, Critical issues in catalytic diesel reforming for solid oxide fuel cells. J Mater Eng Perform 2006; 15: 442-4.

[130] Kondakindi RR, Kundu A, Karan K, Peppley BA, Qi A, Thurgood C, et al., Characterization and activity of perovskite catalysts for autothermal reforming of dodecane. Appl Catal A Gen 2010; 390: 271-80.

[131] Erri P, Dinka P, Varma A, Novel perovskite-based catalysts for autothermal JP-8 fuel reforming. Chem Eng Sci 2006; 61: 5328-33.

[132] Chen H, Yu H, Peng F, Yang G, Wang H, Yang J, et al., Autothermal reforming of ethanol for hydrogen production over perovskite $LaNiO_3$. Chem Eng J 2010; 160: 333-9.

[133] Huang L, Zhang F, Wang N, Chen R, Hsu AT, Nickel-based perovskite catalysts with iron-doping via self-combustion for hydrogen production in auto-thermal reforming of Ethanol. Int Journal of Hydrogen 2012; 37: 1272-9.

[134] Villoria JA, Alvarez-Galvan MC, Navarro RM, Briceño Y, Gordillo Alvarez F, Rosa F, et al., Zirconia-supported $LaCoO_3$ catalysts for hydrogen production by oxidative reforming of diesel: Optimization of preparation conditions. Catal Today 2008; 138: 135-40.

[135] García V, Päkkilä J, Ojamo H, Muurinen E, Keiski RL, Challenges in biobutanol production: How to improve the efficiency? Renew and Sust Energy Rev 2011; 15: 964-80.

[136] Huang H, Liu H, Gan Y-R, Genetic modification of critical enzymes and involved genes in butanol biosynthesis from biomass. Biotechnol Adv; 28: 651-7.

[137] Brian J G, The economics of producing biodiesel from algae. Renewable Energy 2011; 36: 158-62.

[138] Biodiesel plant planned for Singapore. Pump Indus Anal 2008; 2008: 3.

[139] Jacobs to support Neste's renewable diesel plant in Singapore. Pump Indus Anal 2008; 2008: 4.

[140] Arvidsson R, Persson S, Fröling M, Svanström M, Life cycle assessment of hydrotreated vegetable oil from rape, oil palm and Jatropha. J Clean Prod; 19: 129-37.

[141] Neste Oil cleans up in biofuels. Focus Catal 2006; 2006: 6.

[142] Zheng J-L, Wei Q, Improving the quality of fast pyrolysis bio-oil by reduced pressure distillation. Biomass Bioenergy 2011; 35: 1804-10.

[143] InnovaTek uses biodiesel in microchannel steam reformer. Fuel Cells Bull 2006; 2006: 2.

[144] US Army funding for InnovaTek to develop mini fuel processors. Fuel Cells Bull 2011; 2011: 8.

[145] InnovaTek, Chevron to develop bio-diesel processing technology. Fuel Cells Bull 2007; 2007: 4.

6. Definitions:

Biswas and Kunzru, 2007 defined H_2 selectivity in ATR of ethanol by EQ- 9.

$$\frac{\text{moles of hydrogen produced}}{\text{(total moles of hydrogen in product)}})\times 100 \quad [11]$$

Fierro et al., 2005 [65] defined hydrogen selectivity in ATR of ethanol as below by EQ-12

$$S_{H_2}(\%) = \frac{F_{H_{2out}}}{3\times[(F_{ETOH})_{in} - (F_{ETOH})_{out} CF]] - [(F_{H_2O})_{in} - (F_{H_2O})_{out} CF]} \times 100 \quad [12]$$

Where F_{EtOH} is the molar flow rate of ethanol F_{H2out} is the molar flow rate of H_2 at outlet. While (F_{H20}) is molar flowrate of water and CF is the correction factor defined as below.

$$CF = \frac{[H_e]_{in}}{[H_e]_{out}} = \frac{[V]_{in}}{[V]_{out}} \quad [13]$$

In the above definition $[He]_{in}$ and $[He]_{out}$ represent the helium concentration at inlet and outlet of the reactor.

Huang et al., 2008[67] defined H_2 selectivity in ATR reforming of ethanol is given by EQ-12.

$$S_{H_2} = (\frac{F_{H_{2out}}}{3[(F_{ETOH})_{in} - (F_{ETOH})_{out}]}) \times 100 \quad [14]$$

Where F_{EtOH} is the molar flow rate of ethanol and ($F_{H2}o$) is the molar flowrate of water and F_{H2out} is the molar flow rate of H_2 at outlet. They also defined H_2 selectivity in a different examination i.e. Huang et al., 2010[70] as shown below.

$$S_{H_2} = \left(\frac{2\left(F_{H_2}\right)}{2\left(F_{H_2}\right) + \sum y.F(C_xH_yO_z)}\right)\times 100 \quad [15]$$

.

Cai et al., 2007-8 [91, 92], Navarro et al., 2006) [51] defined molar composition of H_2 in ATR reforming of ethanol and diesel by EQ-16. Chen et al., 2010 defined H_2 selectivity in the following manner. In the equation below F_{EtOH} represents flowrate of ethanol and X is conversion of ethanol.

$$S_{H_2} = \left(\frac{F_{H_{2out}}}{[(6-2\delta)F_{ETOH\,in}X_{ETOH}]}\right) \quad [16]$$

Erri et al., 2006, Gutierrez et al., 2011 [82], Karatzas et al., 2011 [108], Perez-Hernandez et al.,2007[88], Qi et al., 2005[53], Srisiriwat et al., 2009 [71], Villioria et al., 2008, Wang et al., 2006 [55], Xue et al., 2009 [49], and Youn et al., 2007 [69] defined molar composition of H_2 in ATR of JP-8, ethanol, low sulfur diesel, n-octane, methanol, ethanol, diesel, sulfur containing gasoline, sulfur doped gasoline, and ethanol respectively.

Also Kaila and Krause, 2006 [78], Krause., 2008 [79] defined selectivity by the same equation as below

$$M_p(\%) = \frac{mol_p}{\sum mol_{sp}}\times 100 \quad [17]$$

Where mol_p represents the moles of each product, and mol_{sp} represents the of sum moles of products.

Mota et al., 2011 defined selectivity towards H_2 in ATR of diesel using following equation.

$$S_{H_2} = \left(\frac{\left(molei\right)_{out}}{\left[\left(moleC_mH_n\right)_{in} - \left(moleC_mH_n\right)_{out}\right]}\right)\times 100 \quad [18]$$

Biswas and Kunzru, 2007 defined H_2 yield in ATR of ethanol by EQ- 18.

$$Y_{H_2} = \frac{\text{moles of hydrogen produced}}{\text{moles of EtOH fed}} \quad [19]$$

Chekatamarla and Lane [54] defined H_2 yield in ATR of gasoline as below.

$$\mathrm{Y_{H_2}(\%)} = \left(\frac{(\mathrm{R})_{\text{products}}}{\left(\mathrm{R_{water}} + \mathrm{R_{diesel}}\right)}\right)\times 100 \quad [20]$$

In the above equation of R represents the ratio of H_2.

Ferrandon et al., 2008 [47] defined H_2 yield in ATR of gasoline as below.

$$\mathrm{Y_{H_2}(\%)} = \frac{\mathrm{F_{H_{2out}}}}{\left(\mathrm{F_{gasoline}}\right)} \quad [21]$$

In the above equations flow rates of H_2 and gasoline are in ml/min

Gould et al., 2007 [109] defined H_2 yield in ATR of surrogates of jet fuel.

$$Y_{H_2} = \frac{\text{moles of hydrogen produced}}{\text{atomic molar flowrate H in fuel}} \quad [22]$$

Gutierrez defined H_2 yield same as Biswas and Kunzru provided as per EQ-18.

Huang et al., 2008-12 [67] defined H_2 yield in ATR reforming of ethanol by equation EQ-20.

$$Y_{H_2}(\%) = \frac{F_{H_{2out}}}{\left(3 \times F_{ETOH_{in}}\right)} \times 100 \quad [23]$$

$$Y_{H_2} = \frac{F_{H_{2out}}}{\left(7 \times F_{fuelin}\right)} \times 100 \quad [24]$$

Kondakindi et al., 2010 [130] defined H_2 yield as follows

$$Y_{H_2} = (\frac{\text{moles of hydrogen produced}}{(\text{moles of fuel converted})} \quad [25]$$

Mawdsley and Krause [123] defined H_2 yield by EQ-26

$$Y_{H_2} = (\frac{\text{moles of hydrogen produced}}{(\text{moles of fuel })} \quad [26]$$

Mayne defined H_2 yield in ATR of isooctane using the following equation.

$$Y_{H_2}(\%) = \frac{F_{H_{2out}}}{\left(8 \times F_{C_{18}H_{18}}.inlet\right)} \times 100$$

Navarro et al., 2007 defined H_2 yield using the following definition.

$$Y_{H_2} = (\frac{\text{moles of hydrogen produced}}{(\text{moles of C feed})} \quad [27]$$

Villioria et al., 2008-11 defined H_2 yield as

$$Y_{H_2} = (\frac{\text{moles of hydrogen produced}}{(\text{mole ammount } H_2 \text{ in the feed})}) \times 100 \quad [28]$$

Conversion defined by various authors like Biswas and Kunzru, 2007, Cai et al., 2007-8, Chekatamarla and Lane, Fierro et al., 2005, Galvan et al., 2008, Gutierrez et al., 2011, Kaila and Krause, 2006, Kaila et al.,2008, Huang et al., 2008-10, Navarro et al., 2006, Srisiriwat et al., 2009, Wang et al., 2006, Youn et al., 2007 is given below

$$X_{fuel} = (\frac{(mole)_{in} - (mole)_{out}}{[(mole)_{in}]}) \times 100 \quad [29]$$

Gould et al., 2007 defined conversion in ATR of diesel surrogates as below

$$X_{\text{fuel}}(\%) = (\frac{F_{\text{totalout}}(F_{CO} + F_{CO_2} + F_{CH_4})}{(\text{nFuel}_{\text{in}})}) \times 100 \quad [30]$$

Navarro et al., 2007 [125] and Qi et al, 2005[53] defined conversion by the following equation.

$$X_{fuel} = \left(\frac{\text{mole ammount of C in reformate}}{\text{(total mole ammount C in the feed)}}\right)\times 100 \quad [31]$$

Mayne et al., 2011 [111] defined conversion using following equations

$$Y_{CO}(\%) = \frac{F_{CO_{out}}}{\left(8\times F_{C_{18}H_{18}}.inlet\right)}\times 100 \quad [32]$$

$$Y_{CO_2}(\%) = \frac{F_{CO_{2out}}}{\left(8\times F_{C_{18}H_{18}}.inlet\right)}\times 100 \quad [33]$$

$$Y_{CH_4}(\%) = \frac{F_{CH_{4out}}}{\left(8\times F_{C_{18}H_{18}}.inlet\right)}\times 100 \quad [34]$$

$$Y_{2-4}(\%) = \frac{(2F_{C_2H_4} + 2F_{C_2H_6} + 3F_{C_3H_6} + 3F_{C_3H_8} + 4F_{C_4H_8})_{exit}}{\left(8\times F_{C_{18}H_{18}}.inlet\right)}\times 100 \quad [35]$$

Conversion was defined as

$$(\mathrm{Y}_{CO} + Y_{CO_2} + \mathrm{Y}_{CH_4} + Y_{2-4} \quad [36]$$